UNIVERSITY OF CALIFORNIA
RIVERSIDE

Investigation of the Effect of In-Situ Catalyst on the Steam Hydrogasification of Biomass

A Dissertation submitted in partial satisfaction
of the requirements for the degree of

Doctor of Philosophy

in

Chemical and Environmental Engineering

by

Xin Fan

December 2012

Dissertation Committee:
Dr. Joseph M. Norbeck, Chairperson
Dr. David Cocker
Dr. Sharon Walker

The Dissertation of Xin Fan is approved:

_____

_____

_____

Committee Chairperson

University of California, Riverside

ACKNOWLEDGMENTS

I owe my sincere gratitude to my advisor, Professor Joseph M. Norbeck, for his support and patient guidance of my Ph.D study to help me achieve my research goals. I would like to express my sincere gratitude to Dr. Chan S. Park, my co-advisor, who gave me important guidance toward my Ph.D research projects.

I wish to express my sincere thanks to my reading committee members, Professor David Cocker, Professor Sharon Walker and my candidacy committee members, Professor Yushan Yan and Professor Yadong Yin, for their valuable advices and comments on my dissertation.

I would like to thank Kevin Street, the wastewater resources analyst from Riverside Water Quality Control Plant who provided me the biosolids samples. I warmly thank our Lab Engineer Junior Castillo, who helped me a lot on setting up reactor system. I also wish to thank my colleagues Xiaoming Lu, Qian Luo, Yang Li, Zhongzhe Liu, Yoothana Thanmongkhon and other graduate students in our group for many help. I owe my loving thanks to my family. My patents gave me endless encouragement and support for my Ph.D life in the United States.

Riverside, CA, USA, December 2012

Xin Fan

ABSTRACT OF THE DISSERTATION

Investigation of the Effect of In-Situ Catalyst on the
Steam Hydrogasification of Biomass

by

Xin Fan

Doctor of Philosophy, Graduate Program in Chemical and Environmental Engineering
University of California, Riverside, December 2012
Dr. Joseph M. Norbeck, Chairperson

The gasification of biomass is potentially an efficient and economically viable technology to assist in reducing the global dependence on fossil fuels and carbon dioxide emission. CE-CERT steam hydrogasification technology combines hydrogen with water to convert carbonaceous matters to a high energetic synthesis gas which offers several advantages for biomass gasification compared to other mainstream gasification technologies. Although steam hydrogasification appears to be an advantageous gasification technology, it still needs to be improved for optimum efficiencies to assess the overall commercial viability. A particular challenge for the scaling-up steam hydrogasification process is the low reactivity of carbon with hydrogen. The gas residence time in the large-scale gasifier needs to be substantially long to account for the slow reaction rate in the presence of hydrogen. The consequence is that much larger size and more expensive gasifier is required to implement the large-scale CE-CERT process which leads to a considerably high initial investment cost. The main objective of this thesis is to investigate the effect of biosolids serving on the steam hydrogasification of

biomass for improving the steam hydrogasification efficiency. The use of biosolids is motivated by its low cost, integrated in the steam gasification as the feedstock and the potential for catalytic effect due to its typically high concentration in iron and calcium. This research will not only contribute to technological analysis for the scaling-up CE-CERT steam hydrogasification process but also provide an alternative pathway for biosolids energy recovery in a cost-efficient manner.

Characteristics and kinetics of steam hydrogasification of biomass was investigated initially in chapter two with the objectives to optimize the reaction conditions and to establish a simplified approach for kinetic measurements in the steam hydrogasification. A newly designed laboratory-scale reactor, referred to as the inverted batch reactor is used in this thesis. This reactor succeeded performing the desired realistic thermal conditions to allow for fundamental laboratory studies of the steam hydrogasification. The heating rate and temperature were found to have significant influence on the steam hydrogasification. Kinetic parameters were obtained by using a first-order kinetic model based on product gas formation.

Steam hydrogasification of the co-mingled biosolids with biomass was investigated in chapter three to determine the effect of biosolids on the steam hydrogasification of biomass. It is experimentally demonstrated that the biosolids integrated in the feed dramatically improved the steam hydrogasification efficiency not only in carbon conversion but also in gasification reaction rate. The steam hydrogasification with 50wt% biosolids in the feed yielded more than 70% carbon conversion at 700℃. There was an approximately 6% increase in the carbon conversion

compared to the steam hydrogasification of biomass. The gasification rates of CH_4 and CO formation were enhanced by 18% and 12%, respectively. The characterization of metal elemental compositions in the biosolids revealed that the biosolids was particular rich in Fe, Ca.

Catalytic steam hydrogasification of biomass with different catalysts based on metal compounds of Fe, Ca, Mg, Na and K is investigated in chapter three. Steam hydrogasification of biomass with non-catalysts, with the in-situ biosolids and with the added catalysts were evaluated to identify the catalytic activity of biosolids. The catalytic activity of catalysts in the steam hydrogasification for CO formation followed the order of iron catalysts > biosolids > other tested catalysts. And the catalytic activity for CH_4 formation was in the sequence of calcined dolomite > biosolids > other tested catalysts. Biosolids in-situ integrated in biomass feedstock was found to be highly active and effective to catalyze the steam hydrogasification and improve the steam hydrogasification efficiency. The catalytic action of biosolids on the steam hydrogasification may be attributed to the synergistic effect of iron, calcium and alkali metals in the biosolids.

Table of Contents

List of Tables

List of Figures

Chapter 1

Introduction and Background

1.1 Biomass Gasification

1.1.1 Energy from biomass

Biomass, referred to organic matters produced during the process of photosynthesis, is a major source of renewable energy [1-2]. The carbon cycle of biomass from its growth absorbing CO_2 toward releasing CO_2 back into the atmosphere leads to a net zero CO_2 emissions [3-4]. Biomass is the only current renewable energy source for liquid transportation fuel [5]. The sustainable use of biomass can contribute to reduce the reliance on fossil fuels and greenhouse gas emission [4-6]. Bioenergy derived from biomass currently represents approximately 10%-14% of the world's primary energy supply [6]. The current goal of the United States is to have at least 20% of petroleum demand replaced with biofuels from biomass by 2020 [7].

Biomass resources contribute to a broad variety of biomass feedstock, such as forestry residues, agricultural residues, herbaceous crops, crops oils and municipal green wastes. The agricultural residues and forestry residues are the primary biomass feedstock resources in the United States [8, 9]. The forestry residues include residues from the logging, wood processing mills, pulping liquors, paper mills and urban woody residues. The wood processing mills, pulping and paper mills are estimated to produce 145 million dry tons of residues annually and the annual residues derived from logging operations and urban wood are about 107 million dry tons [9]. The agricultural residues include

grains used for biofuels production (eg, soybean and corn), crop residues from corn stover, small grain straw and others, perennial grass and corps, animal manures and food residues. The United States can produce 428 million dry tons of annual crop residues, 377 million dry tons of perennial crops, 87 million dry tons of grains used for biofuels [9]. The primary biomass resources in California State are forestry residues, agricultural residues and urban wastes [10]. Biomass resources in California State are estimated to 80 million gross tons of biomass per year. And an annual 32 million dry tons biomass in California is considered feasible to use as the biomass feedstock for renewable electricity generation and biofuels [11]. California's biomass resources offer substantial opportunities in helping to meet the in-state future needs of clean and renewable energy.

There are many ecological and economic benefits of biomass as an energy supply. The residues from biomass resources are abundant, easily accessible and broadly available to national wide regions. The carbon dioxide released to the atmosphere during biomass energy consumption is fixed by the photosynthesis during biomass growth. Thus, a very short life cycle of biomass can realize a zero net carbon dioxide emission [12, 13]. Biomass is the only renewable energy source to create liquid transportation fuels compared to other renewable energy, such as solar, wind and geothermal energy. Biomass to liquid fuels is advantageous in terms of delivery, storage and infrastructural compatibility. Biomass replacing fossil fuels can reduce the dependence on imported energy, particular in petroleum that contributes to enhance the energy security in the United States [14]. The development of biomass energy industry provides direct or indirect employment opportunities.

Despite many benefits of biomass energy, there are technological barriers to overcome. Biofuels are more expensive than fossil fuels due to the cost on biomass feedstock. The biomass feedstock cost includes the cost on growing, harvesting, collection and transportation of biomass. It reduces the competitiveness of biomass energy compared with fossil fuels and other renewable technologies [1-4, 15]. Better understanding of currently available biomass feedstock including biomass distribution and characterization, transport, storage and processing costs is required. Better techniques must be developed for cost-effective growing, harvesting and transportation of biomass feedstock and bioenergy industrial systems require access to biomass resources. The obstacle to the increased utilization of second generation biofuels is that lack of commercial-scale reliable technologies. It is important for the development of large-scale conversion technologies to improve the efficiency and lower the cost [16, 17].

Conversion technologies

Biofuels are types of fuel productions derived from biomass, including biogas, biodiesel, ethanol, methanol, DME, synthetic gasoline, Fischer-Tropsch diesel fuels. First generation biofuels are made from food crops, such as soybean, sugar, corn and vegetable oil. For example, biodiesel can be produced from trans-esterification of vegetable oils. However, the first generation biofuels are limited due to the competition with cropland use for food supply [18]. Therefore, second generation biofuels from nonfood biomass is emphasized on its development currently. The lignocellulosic biomass is comprised of cellulose, hemicellulose and lignin is the main biomass source for second generation biofuels.

The biomass feedstock can be converted into biofuels or energy productions by conversion technologies. Figure 1.1 shows a diagram for a description of biomass conversion processes. These conversion technologies for second generation biofuels from lignocellulosic biomass are divided in two main processing routes: biochemical and thermochemical technologies [19].

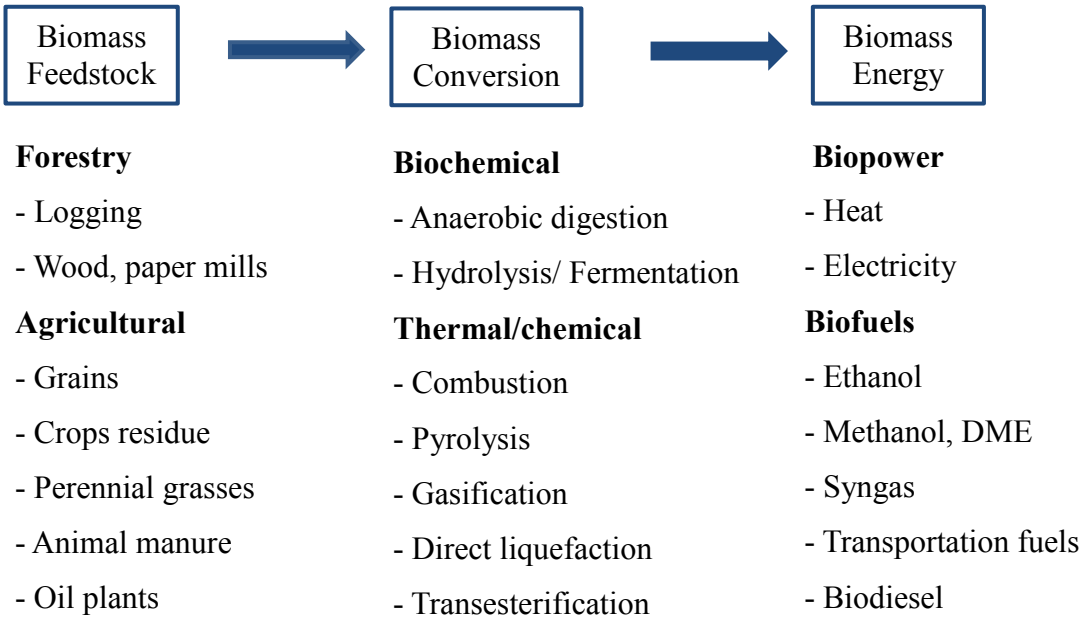

Figure 1.1 Conversion of biomass to a variety of biofuels and energy products

Biochemical technologies can convert the carbohydrate chains of the lignocellulosic biomass into ethanol production. The ethanol production from lignocellulosic biomass is referred to as cellulosic ethanol. The biochemical processes for cellulosic ethanol generally include steps of pretreatment, hydrolysis and fermentation [20]. The pretreatment process is an initial process step to break up lignin and expose the cellulose and hemicellulose fractions for subsequent hydrolysis. The sugars are released in chemical hydrolysis or enzymatic hydrolysis of hemicellulose and cellulose fractions. Following hydrolysis, enzymatic fermentation is the next step to convert the resultant sugars into ethanol. And then the concentration and purification of ethanol production are achieved by distillation and dehydration. The lignin component in lingo-cellulosic biomass is difficult to be hydrolyzed and residual lignin solids are separated, dried and combusted to generate heat and electricity power in bio-refinery plant. Cellulosic ethanol from biochemical technologies has not been in commercialization. Much remains to be done to reduce the final ethanol production cost, such as improving the sugar yields, reducing the cost for the pre-treatment process and reducing the cost of enzymes [21, 22].

Thermochemical conversion technologies for biofuels are chemical reforming processes under the appreciated pressure and temperature levels to convert biomass feedstock into synthetic gas fuels or liquid fuels. Thermochemical conversion processes can produce the energy products in a very short residence time of seconds to minutes compared to biochemical processes. Three main thermochemical technologies are pyrolysis, gasification and direct liquefaction [23]. Direct liquefaction technologies are based on hydrogenation of carbonaceous feedstock into liquid hydrocarbons [24]. Direct

liquefaction proceeds under very high pressure levels in the range of 5-20 bars compared to pyrolysis and gasification. The direct liquefaction of coal has been a reliable technology while direct liquefaction is considered as little attractiveness for the development of biofuels [25]. Pyrolysis is a thermochemical process to decompose biomass in the absence of oxygen into bio-oils, volatile gases and chars. The product yields and distributions are dependent on the reaction parameters such as temperature, heating rate and residence time. Bio-oil, the main product in pyrolysis can be refined into liquid biofuels in the downstream process and can be utilized as a fuel source for power generation. The unreacted, solid residual referred as to chars with ash are combustible qualities for heat generation. The volatile gases include a mixture of H_2, CO, CO_2, hydrocarbon gases and tars. Conventional pyrolysis has a very low gas product yield due to the normally lower temperature range of around 300-500℃ [26] and tars in the gas phase are corrosion to downstream equipment. Pyrolysis is not considered as a good approach for syngas or gas fuels compared with gasification technologies although fast or flash pyrolysis technologies can achieve a relative higher gas yield than slow pyrolysis [27,28]. This thesis will focus on biomass gasification, particular in steam hydrogasification of biomass. The literature reviews of biomass gasification technologies and CE-CERT steam hydrogasification technology are introduced in the following sections.

1.1.2 Gasification technologies

Biomass gasification has been widely researched and applied as a clean, efficient and cost-effective technology for biomass conversion into syngas or synthetic fuels compared to other thermochemical technologies [29-31]. Gasification technologies use reaction agents such as air, oxygen or steam, hydrogen to convert the carbonaceous materials into energetic gaseous products. The product gases are dominantly a mixture of carbon monoxide (CO), hydrogen (H_2) and methane (CH_4) with small quantities of carbon dioxide (CO_2), and steam (H_2O). The yield and chemical composition of product gases are mainly affected by the gasification agent (air, steam, or hydrogen), the gasifier operating conditions, and feed characteristics [30-32]. The other products in gasification include char, tars, inorganic constituents and other higher molecular weight hydrocarbon gases [33]. The gaseous products need to be cleaned up to remove undesirable impurities such as nitrogen and sulfur compounds; unconverted condensable organics (tars) and fine particles in order to improve the gas qualities and protect poisoning of the downstream catalysts. The clean-up product gases can be used for syngas and converted to liquid transportation fuel, gas fuels for heat and electricity generation, hydrogen energy source [3, 29-31].

Gasification is generally classified according to the gasifying agents into partial oxidation, steam gasification, hydrogasification and gasification with other agents like CO_2. The basic overall reaction taking place in the gasifier can be summarized as in the Equation1.1.

Biomass + O_2 or H_2, H_2O, air → CO, H_2, CH_4, CO_2, H_2O,

+ tars + chars + ash Equation (1.1)

Partial oxidation (POX) is a gasification process with pure oxygen or air under high temperature (800 -1600℃) to produce fuel gas production. POX technologies are common known in commercial and large-scale demonstration applications. The relative reactions are presented in the equations 1.2-1.4. The heat in this process can be supplied by the exothermic reactions of partial combustion in the POX gasifies. However, POX provides a low heating value in the produced syngas with large amount of N_2.

Partial oxidation reaction

$C + ½ O_2 \rightarrow CO$ Equation (1.2)

$CO + ½ O_2 \rightarrow CO_2$ Equation (1.3)

$H_2 + ½ O_2 \rightarrow H_2O$ Equation (1.4)

Hydrogasification is a gasification process with hydrogen as the gasifying agent. The predominant reaction in hydrogasification is methanation reaction in the Eqn. 1.5. Hydrogasification can be used for the production of synthetic natural gas (CH_4) from biomass. However, hydrogasification is not attractive for biomass conversion because the reactivity of carbon with hydrogen is much lower than that of carbon with steam and oxygen.

Methanation reaction

$C + H_2 \rightarrow CH_4$ Equation (1.5)

The addition of steam as gasifying agent in gasification process is defined as steam gasification. The steam gasification can yield hydrogen-rich gas product and N_2-

free product gases compared with partial oxidation. For example, the H_2 composition from steam gasification of woody biomass can reach 40% of the output gases [34]. And the reactivity of gasification with steam is higher than gasification with hydrogen. The water-gas reaction in Eqn. 1.6 is the main reaction in steam gasification. Many other chemical reactions involved in the steam gasification are presented in the equation 1.6-1.9. High tars yield in the gas products is a challenge issue for steam gasification. Catalytic steam gasification has been investigated to reduce tars formation. Water gas reaction

$C + H_2O \leftrightarrow CO + H_2$ Equation (1.6)

Boudouard reaction

$C + CO_2 \leftrightarrow 2CO$ Equation (1.7)

Water-gas shift reaction

$CO + H_2O \leftrightarrow CO_2 + H_2$ Equation (1.8)

Steam methane reforming

$CH_4 + H_2O \leftrightarrow 3H_2 + CO$ Equation (1.9)

Type of Gasifiers

The type of gasifiers plays one important role in determining gasification performances [35]. Main commercial gasifiers include primarily downdraft and updraft fixed beds, bubbling and circulating fluidized beds, entrained flow beds [36]. The option of the type of gasifiers is related to with specific features and limitations of the specific application.

Downdraft gasifiers Downdraft fixed beds have co-current flow of feedstock materials and the gasification agent (eg. air, steam, oxygen) moving product gas stream downward. The agent is introduced and reacted with solids at a throat under a high temperature zone. The product gases leave the bottom of bed at high temperature and most of the heat is transferred to the agent added at the throat on the top of bed. This configuration results in a high carbon conversion efficiency and a relatively clean product gas with low content of tar since more tars are cracked when all tars pass through a hot bed of char and. Downdraft gasification is simple and reliable technology for small scale applications of practical capacity up to about 500 kg/h feed rate [37]. So the limitations of downdraft beds are low heating rate, limited scale-up potential [38].

Updraft gasifiers Updraft fixed beds have current-current flow of feedstock materials and the gasification agent moving product gas stream upward. In updraft beds, the solids move down to be gasified and vapors flow up with the hot product gases. The hot ascending gases transfer heat to the incoming feedstock which is dried or preheated before moving to the gasification ozone. For that, the gas exit temperature is low. Some tars in the vapors are carried out by the upward flowing product gases. This configuration features for high carbon conversion and high thermal efficiency. However, updraft gasification has high level of tar in the product gases [39]. So the product gas requires substantial cleanup for further downstream processing. The limited scale- up for updraft beds is about 4t/h feed rate [38]. Although it has little scale-up limitation compared with downdraft beds, it has not been built in practice for large scale power applications due to

high tar content in the fuel gas. Catalytic gasification in updraft beds has been developed for tar cracking and removal recently.

Fluidized bed gasifiers Fluidized beds are classified to bubbling and circulating fluidized beds according to the fluid velocity. Bubbling fluidized beds have relatively low fluid velocities and moderate tar levels in the product gas between the level of the downdraft and updraft beds. Circulating beds have very high gas velocities with recycled solids entrained after passing a cyclone to improve the carbon conversion efficiency [40]. The tar level is relatively low compare with bubbling beds. In fluidized beds, the solid particles are fluidized at high enough velocities of oxygen and steam or air. Silica sands are usual bed materials to avoid sintering and other bed materials such mineral catalysts of olivine, limestone and dolomite are developed to reduce tars [41]. The heating rate of the fluidized beds is much higher than heating rate of the fixed beds. These configurations of fluidized beds provide important features not available in the fixed beds. Fluidized beds have good heat and mass transfer between the gas and solid phase, uniform solid mixing and temperature gradient. And this type of gasifiers can accept various feedstock materials with a wide range of participle sizes and ash contents [42]. Fluidized beds have demonstrated to be reliable with a variety of feedstock for small scale and plant scale applications [43, 44].

Entrained flow gasifiers Entrained gasifiers have co-current flow of the feed and the agent gas. Entrained gasifiers have much higher heating rate and operating temperature compared with fixed beds and fluidized. The heating rate in entrained gasifiers can reach the level of 104 K/s and the operating temperature can be at 1200-

1500℃ [45]. Hence, the product gases have low concentration of tars and methane. The entrained gasifiers have high conversion efficiency and good quality of product gases. And they are viable and suitable for large scale applications above 10t/h with very good scale-up potential. However, this type gasifier has slagging ash due to high temperature above the ash melting.

Commercialization of biomass gasification is still in the development stage as a consequence of both economic and technical challenges [30, 31] although biomass gasification technologies have been widely applied in research and small investment applications. The removal of tars is a key issue for gas production from biomass gasification. Catalytic biomass gasification using inexpensive, disposable catalytic substances are investigated by most researchers to reduce the tar formation and improve the output gas qualities. Biomass feedstock must be dried to remove the moisture content before conversion, which is required by most gasification technologies. The need to drying biomass leads to the cost and energy loss in biomass gasification. There are some barriers to overcome, including: the need for improved conversion efficiency of biomass to reduce reactor size; reliable pretreatment technologies and feeding systems for large-scale gasifiers; improved durability of catalysts for downstream processes; reduction of the cost of facilities [29-32, 46].

Steam hydrogasification technology in CE-CERT process is very advantageous compared to other mainstream gasification technologies for biomass and waste conversion into synthetic liquid or gas fuels.

1.1.3 CE-CERT steam hydrogasification

The College of Engineering Center for Environmental Research and Technology (CE-CERT) at the University of California, Riverside (UCR) has developed a multi-step thermochemical process based on Steam Hydro-gasification to convert carbonaceous matters into synthetic fuels. It is referred to as the CE-CERT process in this thesis. The steam hydrogasification has several advantages that have been demonstrated in our previous studies [47-49]. It is reported by the U.S National Energy Technology Laboratory (NETL) that CE-CERT process has the potential to be 12% higher efficiency with 18% lower capital cost than the most conventional mainstream gasification technologies [50]. This thesis will focus on steam hydrogasification of biomass feedstock, either only or comingled with biosolids. It aims to address the use of inexpensive biosolids from wastewater treatment process as in-situ catalyst to enhance the steam hydrogasification efficiency. A simplified diagram of the CE-CERT process is shown in Figure 1.2.

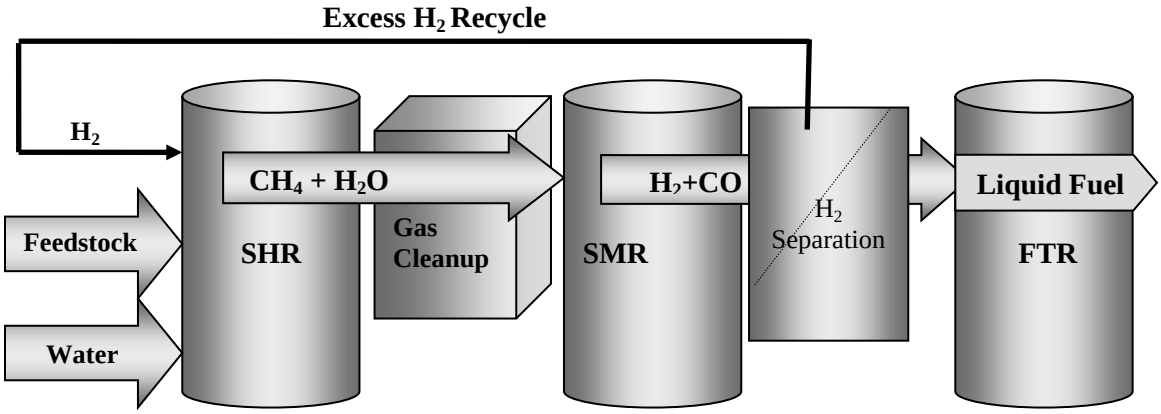

Figure 1.2 A simplified diagram of the CE-CERT Process

Steam hydrogasification combines hydrogen with water to convert carbonaceous materials into the methane rich gases. The output gas stream from the Steam Hydrogasification Reactor is then subjected to a warm gas cleanup unit to primarily remove sulfur species. The cleanup product gases along with steam are then catalytically reformed into syngas (H_2+CO) by the Steam Methane Reforming (SMR). The steam hydrogasification product gases are ideally suited for reforming to produce synthesis gas due to the presence of a significant amount of methane and steam. A H_2/CO ratio of syngas can be controlled by adjusting the input H_2O to feed ratio in the steam hydrogasification. The synthesis gas is fed into a Fischer-Tropsch Reactor (FTR) to be converted into synthetic liquid fuels. It is noted that the CE-CERT process does not require an external H_2 source. The excess H_2 is separated after the SMR and fed back into the Steam Hydrogasification Reactor to make an internal self-sustain source of H_2 in the process.

The basic overall reactions taking place during the CE-CERT process are represented in the equations 1.10-1.12. Cetane ($C_{16}H_{34}$) is used to represent a liquid hydrocarbon production in the Fischer-Tropsch reactions.

Steam Hydrogasification Reaction:

$$C + H_2O + H_2 \rightarrow CH_4 + H_2O + CO + CO_2 \qquad \text{Equation (1.10)}$$

Steam Methane Reforming:

$$CH_4 + H_2O \rightarrow 3H_2 + CO \qquad \text{Equation (1.11)}$$

Fischer-Tropsch Reaction:

$$33H_2 + 16CO \rightarrow C_{16}H_{34} + 16H_2O \qquad \text{Equation (1.12)}$$

The Steam Hydrogasification is a key and innovative step in the CE-CERT process. The features and advantages of the steam hydrogasification compared with other gasification technologies are summarized as follows:

1. One unique feature is the utilization of a slurry feed. It has the ability to handle wet feedstock so that it can reduce the cost of drying feedstock. Thus, this technology provides an attractive option for directly converting feedstock materials with high moisture content into energetic products, such as sewage sludge.
2. It has high carbon conversion efficiency at moderate temperature and pressure and potential for reduced production of tars.
3. No external air or oxygen supply is required as gasifying agent compared to POX and it offers versatility for both small scale and large scale applications.
4. Input H_2O to carbon ratio in the feed can be adjusted to achieve a desired H_2 to CO ratio for efficient downstream production of synthetic fuels.

Although steam hydrogasification in our laboratory has shown to be an advantageous gasification technology, it still needs to be improved for optimum performances to assess the overall commercial viability. Steam hydrogasification is considered as hydrogasification process with the addition of steam. It is known that the reactivity of carbon with different reaction agents at 1073 K is in the order of $r(O_2) >> r(H_2O) > r(CO_2) > r(H_2)$ [51]. The consequence is that the gas residence time in steam hydrogasification gasifier has to be substantially longer to account for the lower reaction rate of carbon with hydrogen. Large size, more expensive gasifier is needed to implement

the large-scale CE-CERT process which leads to a considerable increase in initial investment cost. The relative low reaction rate in the presence of hydrogen is one particular challenge for the development of scaling-up steam hydrogasification. Catalytic gasification with the agent either steam or hydrogen have been developed to enhance the gasification rate and to reduce the tars formation [52-54]. However, it is unknown to us whether the use of catalysts can improve the steam hydrogasification efficiency. Therefore, this thesis will explore catalytic steam hydrogasification by using in-expensive, in-situ catalytic substances in order to improve the steam hydrogasification efficiency. The main objective of this thesis is to find out how active and effective the biosolids is in steam hydrogasification of biomass. The attractiveness of the biosolids is related to its low cost, integrated in the steam gasification as feedstock and its potential for catalytic effect. An introduction to biosolids and literature reviews for the various types of catalysts on biomass gasification will be presented in the following sections.

1.2 Introduction to Biosolids

1.2.1 What are biosolids

Biosolids, historically known as sewage sludge, are solid byproducts from municipal wastewater treatment processes. Biosolids contain approximate 95 percentage water content, as well as nutrient-rich organic matters, inorganic matters and pathogens. The United States has more than 16,500 publicly owned wastewater treatment works (POTWs) that generates over eight million dry tons of biosolids annually [55]. Approximately 60% of annual biosolids is ultimately disposed through land applications and direct landfills [56]. Biosolids disposal to land presents a rising challenge as a consequence of environmental concerns, in particular, excessive accumulation of toxic heavy metals in soil caused by land applications and landfill leachate. The increased quantities of biosolids and more restrictions from legislates on disposal have forced a demand for cost-effective and environmental-friendly biosolids management [57-58]. Energy recovery from biosolids is attracting more and more attention for the beneficial use of biosolids [59].

The quantity and characteristics of the biosolids from municipal wastewater mainly depend on wastewater treatment processes and the type of subsequent treatment for the biosolids [57]. It's necessary to make an understanding of the wastewater treatment processes and processing treatment for biosolids before discussed on biosolids characteristics. A general wastewater treatment process at wastewater treatment plants (WWTP) for municipal biosolids is shown in Figure 1.3.

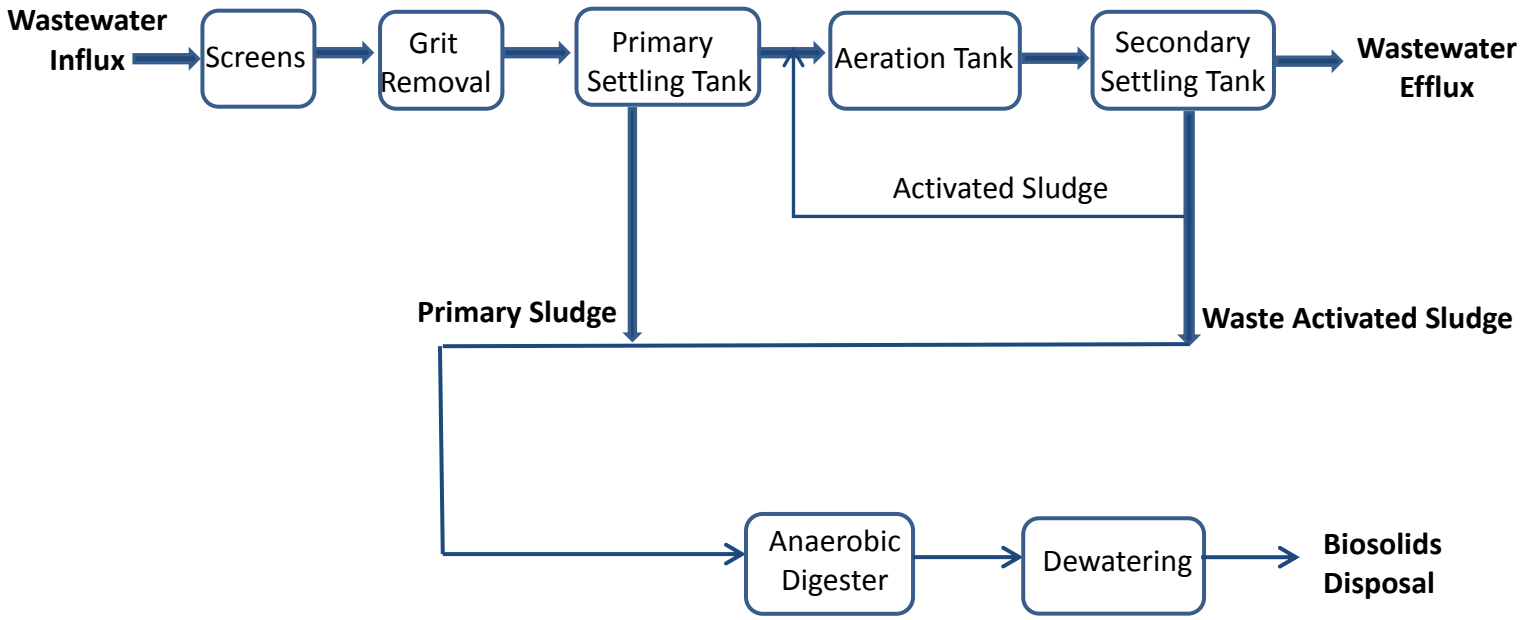

Figure 1.3 A schematic diagram of general wastewater treatment processes at WWTP

Wastewater from the municipal sanitary collection system is firstly pretreated in screening and other facilities to remove coarse solids and grit. After that, the screened wastewater is treated in a primary settling tank for the gravity sedimentation to remove suspended solids prior to a secondary treatment. The secondary treatment is typically a biological treatment process to remove biodegradable organic matters in the wastewater. Microorganisms are used to consume the dissolved and suspended organic matters usually in an aeration tank. Then the wastewater is subsequently clarified in a secondary sedimentation tank to separate the concentrated suspension and microorganisms. Secondary treatment process is required for all municipal plants to reach the minimum treatment level for wastewater efflux. Some municipal WWTP involve a tertiary treatment process (also called advanced treatment) to achieve high effluent quality, such as direct discharge to a drinking water source. For example, biological and chemical precipitation and processes are used in a tertiary treatment for nitrogen or phosphorus removal and chlorinated disinfection.

Biosolids from WWTPs are usually a mixture of sludge from primary and secondary treatment processes [58]. A processed biosolids stream is generated in a specific wastewater treatment process. The biosolids stream produced in a primary treatment process is called primary sludge while the biosolids generated in a secondary sedimentation is called waste activated sludge. Some biosolids produced from the tertiary treatment is referred to as tertiary sludge. The primary sludge is the settled sludge from primary sedimentation tanks, which usually contains 3%-7% solids. Waste activated sludge, the concentrated suspension with excess micro-organisms is settled in secondary

sedimentation tanks but not recycled to the aeration tank as activated sludge. Secondary biosolids contain higher water content than the biosolids from a primary treatment. Biosolids from higher levels of treatment processes also contain increased concentrations of contaminants since the dissolved organic matters and contaminants removed from the wastewater end up in the biosolids [59]. Chemicals such as ferric chloride, aluminum, lime are dosed in wastewater processes to precipitate the suspended solids that lead to the increased concentrations of these chemicals in the biosolids.

Biosolids treatment

POTWs involve additional processing treatments for biosolids to meet regulatory requirements before most use and disposal of biosolids, including thickening, stabilization and dewatering processes. POTWs select the specific processing method for biosolids according to the specific management in biosolids disposal or uses. Major stabilization methods include anaerobic or aerobic digestion, lime stabilization, heat treatment and composting [57]. Physical separation techniques are typically used for dewatering, such as high-speed centrifuges, belt filter press, and air drying.

Stabilization Biosolids are stabilized to reduce the biosolids mass, the pathogens in the biosolids and eliminate offensive odors. Anaerobic digestion is widely used biological technology for biosolids stabilization. Anaerobic digestion uses microorganisms to decompose the biodegradable portion of the volatile compounds in the absence of oxygen environment to produce biogas. The biogas generated from anaerobic digestion of biosolids composes of a primary 60%-65% of methane and about 30-40% of CO_2 [55]. The biogas can be collected and applied as an energy resource for heat or

electricity generation. Anaerobic digestion has been practiced in many large wastewater treatment plants in California and the northeastern U.S. not only to stabilize biosolids but also to recover energy from biosolids to biogas [60].

Dewatering The dewatering treatment significantly reduces the biosolids volume and weight by removing water in the biosolids as much as possible that make biosolids compatible and less expensive for transportation, disposal or beneficial use. The raw biosolids generated in the wastewater treatment process typically have a solids content of approximately 2 to 5%. The dewatering processes can convert biosolids in a liquid form into semi-solids that are approximately 15–50% solids content [59]. For example, belt filter presses produce belt biosolids cakes that achieve 20% to 32% solids content [61]. The dewatered and dry biosolids are required for a number of biosolids management options such as landfills and incineration. Furthermore, many gasification and pyrolysis technologies for energy recovery of biosolids are not compatible for the raw biosolids as feedstock due to the high moisture content in biosolids. An external energy supply is essential to dry and dewatered biosolids that results in a large energy consumption in biosolids management. Therefore, CE-CERT steam hydrogasification technology offers an important advantage in alternative method for biosolids management by directly utilizing the raw biosolids integrated in the feedstock.

Characteristics of biosolids

The typical components of biosolids can be generally classified into six groups as follows [62]:

1. Water, the moisture content varying from a few percentages to more than 95wt%
2. Organic carbon compounds that are approximately 50%-60 wt% on a dry basis
3. Inorganic compounds, such as silicates (Si), iron (Fe), calcium (Ca) and magnesium (Mg), aluminates (Al)
4. Organic and inorganic nitrogen and phosphorous compounds
5. Trace metals and other trace contaminants with concentrations from more than 1000 ppm to less than 1 ppm, such as Zn, Pb, Cu, Cr, Ni, Cd, Hg, As and polychlorinated biphenyls (PCBs), polycyclic aromatic hydrocarbons (PAHs)
6. Pathogens, such as disease-causing organisms of bacteria, parasites and viruses

The influent wastewater and wastewater treatment processes have a large impact on the physical and chemical compositions in biosolids. Biosolids has rich beneficial nutrients such as nitrogen and phosphorous that can be used as fertilizer in soil. The N and P concentrations in a dry basis of biosolids are typically 4wt% and 2 wt%, respectively. Table 1.1 shows metal elemental compositions in biosolids. Some metal elements in biosolids are essential for plant growth, including iron, magnesium, copper and zinc. Solids in biosolids are a combination of organic and inorganic solids. The volatile solids are the organic carbon and nitrogen compounds that compose of approximately 30 to 50% of solids content in biosolids. The energy value of biosolids is

embedded in the volatile solids portion. Energy recovery from biosolids can take advantage of the energy value of biosolids.

Table 1.1 Metal elemental compositions of biosolids and maximum allowable metal concentration in biosolids by the U.S. EPA
(Average value of over 200 biosolids samples from eight states)

Main metal elements	Biosolids[1] (wt%)[2]	Trace metal elements	Biosolids[1] (ppm)[2]	Standard[3] (ppm)[2]
Ca	3.9	Zn	1740	2800
Fe	1.1	Cu	850	1500
Al	0.4	Ni	82	420
K	0.3	Cr	890	1200
Mg	0.4	Mn	260	-
Na	0.2	Pb	500	300

Notes 1. Source from Dowdy et al. [63]
2. All the values are based on a dry basis of biosolids
3. U.S. EPA 1994 [64]

Biosolids disposal and use

Biosolids are managed by POTWs for disposal and beneficial use, including incineration, land applications and landfills, or surface disposal. Figure 1.4 shows practice of biosolids disposal and use in the United States [61].

Landfilling Landfilling is the most common method for biosolid disposal [58]. Biosolids are disposed in landfills with municipal solid waste (MSW). Approximately 30 percent of the biosolids are landfilled or surface land disposed. Landfilling of biosolids usually occurs the quality of the biosolids does not meet the EPA standard for land applications. Biosolids landfilling has been causing secondary pollutions due to leachate

and greenhouse gas emission. The increased land is required for landfilling leads to high cost on landfills [61].

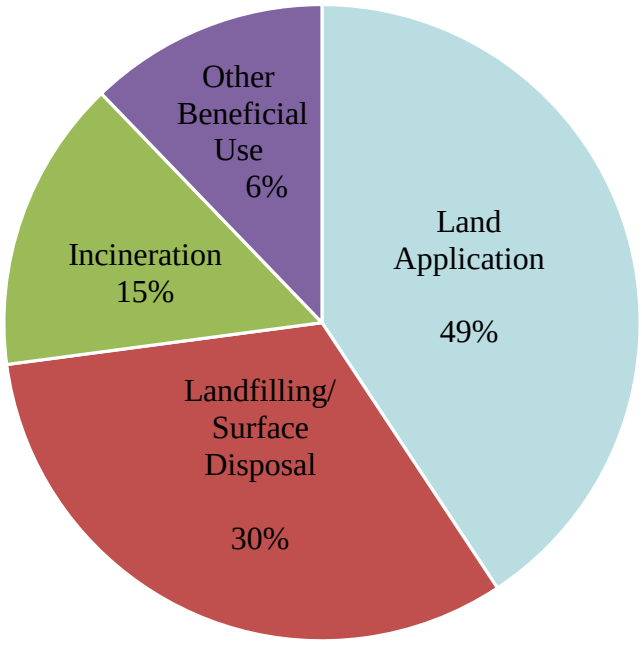

Figure 1.4 U.S. biosolids management practice in 2004

Incineration Incineration is one of conventional methods for biosolids disposal. The process is a complete oxidation of volatile solids in the biosolids at high temperature with excess air to form mainly carbon dioxide and water. About 15% of annual dry tons of biosolids in the United States are disposed by incineration. The only leaving solid residue, the ash is required for disposal in landfills or may be used as construction materials. Environmental problem associated with incineration of biosolids is the release of particulates and pollutants to the atmosphere [58, 59]. Exhausted gases are treated to meet the requirements set by federal and state regulations. The investment cost on the exhaust gas cleanup system is very high so that the cost on incineration disposal is

dramatically increased. Conventional incineration of biosolids generally consumes more energy than the energy recovery from biosolids that cannot be regarded as an energy recovery option for biosolids [59]. Currently, co-incineration of biosolids and coal in coal-fired power plants is applied in practice that is considered as the recovery of energy from the biosolids in the form of heat or electricity [60].

Land Application Land application is the most common method for a beneficial use of biosolids. The biosolids applications to land include agricultural land, forests, mine reclamation and parks. It is estimated that about 50% of biosolids are applied to land. Biosolids can be used as agricultural fertilizer, or serve as soil amendment since nutrients (e.g. nitrogen and phosphorus) and trace metals (e.g. copper, zinc, molybdenum, boron, calcium, iron, magnesium, and manganese) in the biosolids are beneficial for plant growth. Stabilization treatment of biosolids is required before land application. However, the accumulations of the toxic chemicals and heavy metals in the biosolids lead to contaminate the soil. The regulators have been set by the U.S. EPA (1994) for limitations of biosolids to land in order to eliminate secondary environmental pollutions [64].

1.2.2 Biosolids energy recovery technologies

There are two primary energy recovery pathways for biosolids: biodegradation and thermal conversion [65, 66]. Anaerobic digestion is a biodegradation method that has been commonly used to recover energy from biosolids and also is one stabilization type for biosolids treatment. The thermal conversions of biosolids include co-incineration or co-combustion, pyrolysis and gasification technologies. The energy products from digestion and thermal conversions are significantly different. Anaerobic digestion consumes the biodegradable organic matters in the biosolids to produce biogas methane and the byproduct CO_2 and a large fraction of biosolids left for disposal. Thermal conversion can convert the volatile solids in the biosolids into the energy productions and leaves the byproduct only ash fraction. An overview of the thermal conversion of biosolids is presented in Figure 1.5.

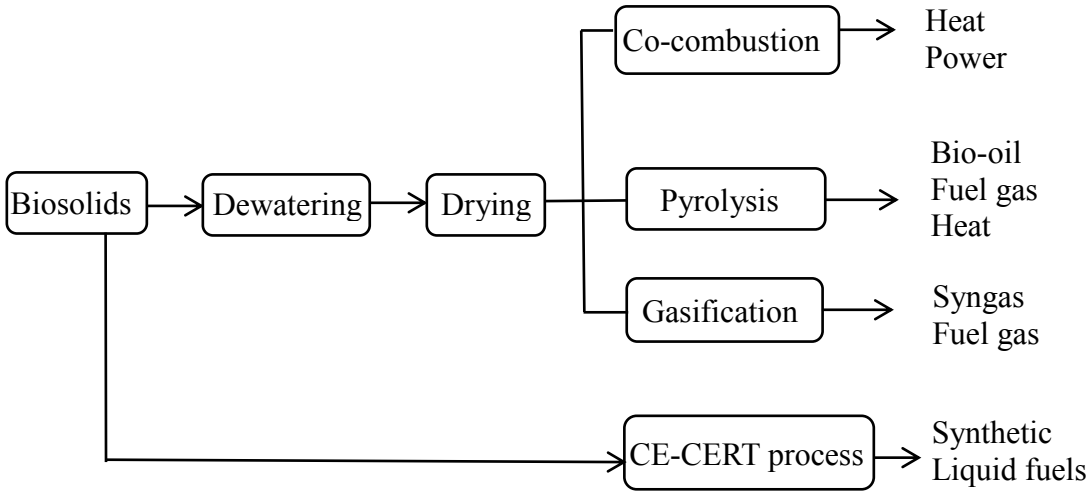

Figure 1.5 Thermal conversion technologies for biosolids energy recovery

Gasification, a relatively new technology can recover the energy value from biosolids with the gasifying agent air, oxygen, steam, hydrogen, or a mixture of these gases at high temperatures. Dry biosolids can be comingled with woody biomass or green waste to meet the required feed characteristics. A thermal drying treatment of biosolids may be included in the gasification upstream that consumes a portion of the energy generated from the gasification process.

The CE-CERT steam hydrogasification process has been developing an alternative option for biosolids energy recovery. The raw biosolids mixed with lignocellulosic biomass can be used as co-mingled feedstock in the steam hydrogasification to be converted into energetic products in a potentially cost-efficient manner compared with other gasification technologies. It should be noted that the raw biosolids contain more than 90% water. Hence, the co-mingled feedstock can achieve a desired carbon to water ratio by directly utilizing the water content in the biosolids as the steam source and the carbon in the biomass as the main carbonaceous matters. Steam hydrogasification offers a significant advantage in biosolids energy recovery by directly utilizing the raw biosolids which eliminates the cost and energy loss on biosolids dewatering and drying treatment.

1.3 Literature Review on Catalysts

There are numerous studies in the literature on biomass gasification using various catalysts. The catalytic gasification of biomass is aimed to improve the quality of the gas product; increase conversion efficiency and reduce tar production [67-69]. There are two approaches in using catalysts for biomass gasification that depends on the position of the catalysts relative to the gasification reactor [67]. Catalysts, called primary catalysts, are added as reactor bed materials or directly mixed with the biomass. The feedstock and primary catalysts can operate within the same gasification reactor and achieve in-situ catalytic gasification. Catalysts, called secondary catalysts, are placed in the downstream reactor to treat the gaseous products from gasifiers.

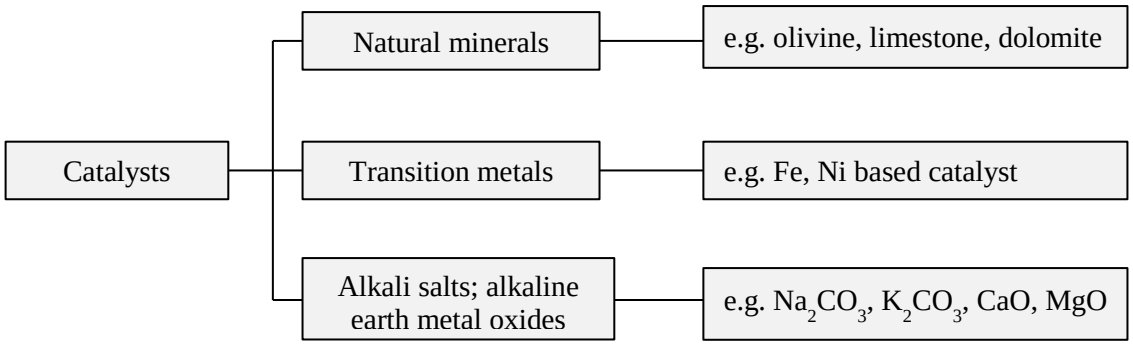

Figure 1.6 A classification of catalysts for biomass gasification

Sutton et al. [67] described three distinct groups of catalyst materials for biomass gasification. They are dolomite, alkali metals and nickel. Bridgwater et al. [68] reviewed dolomites, fluid catalytic cracking catalysts, nickel and metals such as platinum, palladium and rhodium. And the review paper by Abu El-Rub et al. [69] included nine different kinds of catalysts for tar elimination in biomass gasification process. In summary, these catalysts are divided into three kinds of groups and listed in Figure 1.6.

The mineral catalysts are low cost and easy to dispose. Chemical compositions of three mineral catalysts are represented in Table 1.2. The dolomite class has the highest catalytic activity compared with other mineral catalysts [68]. The alkali catalysts can be directly added to biomass by wet impregnation or dry mixing; however, the recovery is difficult and costly and particle agglomeration can occur at high temperature in a fluidized bed reactor [67, 69]. The nickel is an effective, commercially available catalyst but its sensitivity is subject to rapid deactivation and its cost is rather expensive.

Biomass chars are currently reported in biomass gasification to elimination tar yields due to its high alkali metal content [71, 72].

Table 1.2 Chemical composition examples of limestone, olivine and dolomite [68]

Catalyst	CaO	MgO	SiO_2	Fe_2O_3	Al_2O_3	NiO	Cr_2O_3
Limestone	52	1.5	1.5	–	–	–	–
Olivine	0.37	51.8	36.5	9.14	0.88	0.36	0.6
Dolomite	29.06	22.44	0.38	0.2	0.08	_	_

The biosolids samples in this thesis are supplied by the Riverside Regional Water Quality Treatment Plant. The initial research in our lab-scale experiments found that the co-mingled feedstock contributed to actually improve the steam hydrogasification efficiency. The biosolids contain metal species including Fe, Ca, Mg, K, Na as well as some other trace metals. The enhanced conversion efficiency may be the result of a catalytic action in steam hydrogasification as the consequence of the metal species in biosolids. The proposed hypothesis provides motivation to integrate biosolids in-situ in the feedstock to catalyze the steam hydrogasification for a higher reaction rate instead of adding commercial catalysts. The research aims to determine the effect of biosolids on the steam hydrogasification of biomass and investigate the use of biosolids as an in-situ catalytic material to enhance the steam hydrogasification efficiency.

1.4 Objectives

The main objective of this thesis is to investigate the effect of biosolids serving as in-situ catalyst on steam hydrogasification of biomass for improving the steam hydrogasification efficiency. This research will contribute to complement the scaling-up steam hydrogasification process and provide an alternative pathway for beneficial use of biosolids in a cost-efficient manner. The organization of thesis is described as follows.

1. Chapter two will investigate characteristics and kinetics of steam hydrogasification of biomass. The objectives are to optimize the reaction variables achieving a high efficiency and to establish an approach of kinetic measurement for fundamental laboratory studies of steam hydrogasification. A novel batch reactor will be described in this chapter. The experiments are performed under varied reaction conditions to examine effect of major reaction parameters in terms of gas formation rate, carbon conversion. A kinetic study of steam hydrogasification based on the product gas formation will be accomplished to determine the specific reaction rate and activation energies.
2. Chapter three will focus on steam hydrogasification of co-mingled biosolids with biomass as the feedstock. The objective is to investigate how active and effective biosolids affects the steam hydrogasification of biomass. Steam hydrogasification of co-mingled feedstock and biomass feedstock are conducted under the reaction conditions. A comparison of experimental results between the co-mingled feedstock and biomass feedstock will be accomplished to determine effect of biosolids on the steam hydrogasification efficiency including carbon conversion,

the gasification rate. The metal elemental compositions in the biosolids will be characterized by using ICP-AES and SEM- EDS.

3. Chapter four will investigate catalytic steam hydrogasification of biomass using different catalysts aiming to verify the possibility of biosolids serving as in-situ catalyst. This chapter will contribute to understand the catalytic effect of biosolids. The catalysts will be selected based on alkali metals Na and K, alkaline earth metal Ca and Mg, and transition metal iron which are major metal species in the biosolids. Series of experiments with different catalysts are carried out under the same reaction conditions as those in chapter three. The catalytic effect of the tested catalysts will be examined and the catalytic activity of these catalysts will be determined. Finally, steam hydrogasification of biomass with non-catalysts, the in-situ biosolids and the added catalysts will be evaluated to identify the catalytic activity of biosolids as an effective in-situ catalyst.

CHAPTER 2

Characteristics and Kinetics of Steam Hydrogasification of Biomass

This chapter focuses on studying characteristics and kinetics of steam hydrogasification of biomass. It aims to optimize the reaction conditions for high conversion efficiency and to establish an approach for the kinetic measurements in the steam hydrogasification. A newly designed laboratory-scale reactor, referred to as inverted batch reactor is used for the studies of steam hydrogasification in this thesis. The design details, features and operation of the inverted batch reactor are presented in this chapter. Series of experiments were conducted at varied temperatures and different heating rate with the same water to biomass ratio 1.2 g/g. The effect of temperature and heating rate on the steam hydrogasification were examined in terms of char morphology, carbon conversion and gas formation. It is found that heating rate and temperature have a significant influence on the conversion efficiency in the steam hydrogasification. A kinetic study of steam hydrogasification based on the product gas formation was accomplished and kinetic parameters were determined.

2.1 Introduction

The initial reactor in the CE-CERT process is the steam hydrogasification reactor which has been shown to produce the synthetic output gas with a very high percentage of methane. The current types of gasifiers for gasification are introduced in the section 1.1.2. The fluidized bed gasifier is the preferred type for the CE-CERT process demonstration unit (PDU) scale. A fluidized bed for 1 ton/day steam hydrogasification is on-going tested in the lab which can provide best temperature distribution with high heat-up and good mixing of solid-gas phase material to achieve more efficient SHR performances. Further fundamental laboratory studies of SHR kinetics and characteristics are important for optimizing operation conditions in the scaling-up fluidized bed gasifier. Therefore, it's necessary to design a lab-scale reactor system for laboratory experiments which can simulate the similar thermal conditions of a fluidized bed. That's the motivation of a newly designed reactor to be built and used in this thesis as discussed below.

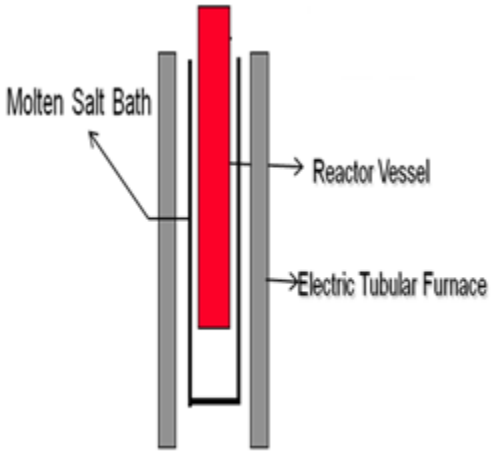

Figure 2.1 A schematic diagram of the micro batch reactor

Two lab-scale batch reactors were used for steam hydrogasification of biomass in the previous experimental work. One is a 12 cc non-stirred batch reactor (S.K.Jeon, 2005) referred to as the micro batch reactor and the other is a 240 cc stirred tank reactor (C.Valkenburg, 2006) referred to as the stirred batch reactor [72, 73].

A simple schematic diagram of the micro batch reactor is shown in Figure 2.1. The reactor vessel is a stainless steel tube of 12 mm I.D. and 100 mm in length. The reactor temperature is controlled by a molten salt bath that is located inside an electric tube furnace. This micro reactor can reach a heating rate up to 600 K/s. It had demonstrated using the micro reactor that steam hydrogasification had higher conversion efficiency in comparison to steam pyrolysis or dry hydrogasification under the same conditions [48]. However, it was far from the working conditions of a scaling-up gasifier due to the non-stirred environment and microgram amount level for the feed. And also it was limited by the maximum pressure capability of 250 psi. Therefore, a stirred batch reactor with a continuous stirred impeller system was built and used in instead of the micro reactor. Figure 2.2 shows a photograph of the stirred batch reactor setup [73]. It not only improved the mass transfer of reactants and but only allowed for a high pressure condition up to 500 psi and gram amount level for the feed. The stirred reactor was previously used to investigate the effect of parameters on SHR such as H_2 to carbon ratio and feedstock variability. But the stirred batch reactor had a limitation of low heating rate which is less than 1 K/s. That hindered its application for kinetic measurements in the SHR.

Figure 2.2 A photograph of the stirred batch reactor setup

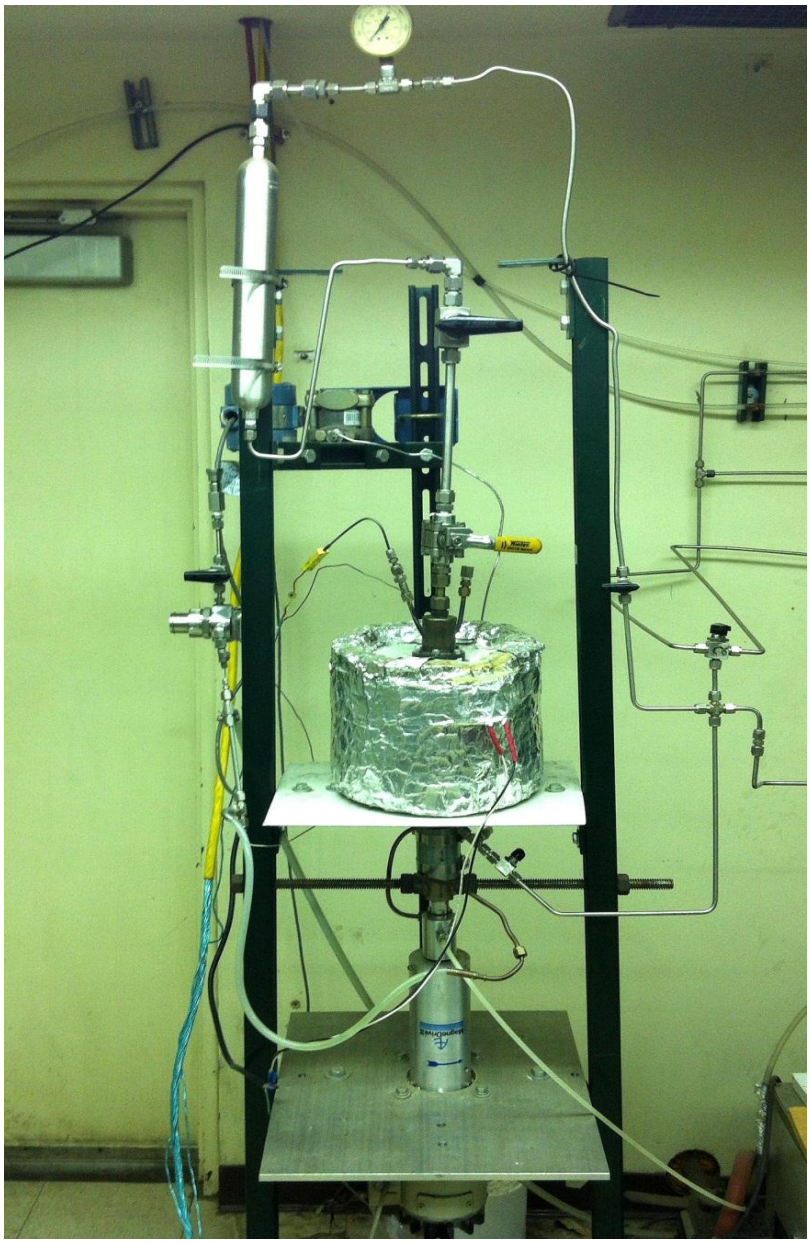

Figure 2.3 A photograph of the inverted batch reactor setup

In process demonstration scale steam hydrogasification, the feedstock will be continuously fed to the fluidized bed gasifier at a constant bed temperature. Therefore, it's necessary to design a new lab-scale reactor which can simulate the similar thermal environment in the fluidized gasifier under rapid heating rate, constant bed temperature. For that, a novel batch reactor system has been developed instead of the stirred batch reactor. The photograph of this reactor system is shown in Figure 2.3. It is referred to as the inverted batch reactor in this thesis.

This inverted batch reactor has an inverted stirred system with a pressure-driven feeding system that can rapidly load the feed materials into the reactor at a desired temperature. This is compared to the stirred batch reactor that required long delays when the reactor was heated up with the feedstock slowly reaching the desired reaction temperature. This unique feature results in rapid heating of the feedstock to a target temperature and more closely represents the thermal conditions in the fluidized bed reactor. That allows for fundamental laboratory studies of steam hydrogasification using a variety of feedstock to complement the development of process demonstration scale CE-CERT process. Additionally, the novel batch reactor is improved with a non-reactive, non-catalytic quartz vessel inserted into the metal reactor vessel to minimize any potential Nickel catalytic effect on the reactions. A comparison of three batch reactors discussed above is summarized in Table 2.1.

Table 2.1 A comparison of current and previous reactors used in the laboratory

Reactor parameters	Micro Batch Reactor (2005)	Stirred Batch Reactor (2006)	Inverted Batch Reactor (2009)
Reactor Volume (cc)	12	240	270
Heating Rate (K/s)	$10\text{-}10^2$	<10	$10^2\text{-}10^3$
Impeller System (Y/N)	No	Yes	Yes
Maximum Pressure (psi)	250	500	400
Feed Amount (g)	$10^{-3}\text{-}10^{-2}$	1-10	1-10

Most of the kinetic measurements of biomass gasification are conducted in the thermogravimetric analyzers (TGA) at low heating rate that are far from those in practical commercial gasifiers [74, 75]. For an accurate kinetics study, the heating period in the gasification should be very rapid to inhibit biomass devolatilization. Therefore, in order to address an experimental approach for an accurate measurement of kinetic parameters, the inverted batch reactor can be applied for analysis of kinetics due to its features.

2.2 Experimental Section

2.2.1 Feedstock Materials

Pinewood sawdust was used as a representative for biomass feedstock and referred to as biomass feedstock in this thesis. The pinewood needs to be prepared before using as feedstock samples in the laboratory experiments. The sawdust particles were first crushed in a laboratory mill (model number: Thomas-Willey model 4, Arthur H. Thomas Company) reducing the size to 1mm and then pulverized in a grinder (model number: Braun KSM-2W) to obtain fine particles size smaller than 500 um. After grounded, the fine particles were sieved to particle size of 150-180 um and then dried in a vacuum oven at 105℃ for 2 hours to vaporize its moisture content. The proximate and ultimate analysis of the pinewood sample is shown in Table 2.2. The data was obtained from Huffman Laboratory Approximate Analysis.

Table 2.2 Proximate and ultimate analysis of pinewood

Proximate Analysis (wt%)	
Moisture	5.65
Volatile Matter	81.52
Fixed Carbon	12.58
Ash	0.25
Ultimate Analysis (wt%, dry basis)	
C	47.56
H	6.31
N	0.05
O	45.81
Balance	0.27

2.2.2 Experimental apparatus

Two lab-scale batch reactors are described in this chapter: the current inverted batch reactor at a high heating rate used for catalytic and kinetic studies and the previous stirred batch reactor used for a comparison at a low heating rate.

Inverted batch reactor

A lab-scale inverted batch reactor is used to study kinetics and characteristics of steam hydrogasification at a high heating rate. A schematic diagram of the inverted bath reactor (Disclosure and Record of Invention, UC Case No. 2012-685-12) is shown in Figure 2.4. This reactor system consists of a pressure-driven feeding system on the top, a reactor vessel in the middle and a magnetically driven impeller system inverted at the bottom.

The feeding system includes a 50 cc stainless steel feeder tube, two high pressure steam ball valves and a 500 cc stainless steel cylinder. One ball valve (Swagelok Company, San Diego, CA) is used for a seal between the feeder tube and the reactor vessel and the other is used for a seal between the feeder tube and the cylinder. The two valves can be operated at the same time for a feed loading. The cylinder is used to provide enough pressurized gas to load the feed in the feeder tube into the reactor. The reactor vessel of 177.8 mm long and 44.5 mm I.D. is made of Inconel 600 (Special Metal Corp., Huntington, WV). It is heated by an irradiative ceramic fiber heater (Watlow Electric Manufacturing Company, St. Louis, MO). The feed samples are held in the feeder tube before they are loaded into the reactor. When the reactor temperature reaches a desire reaction temperature, the feed samples are rapidly introduced into the reactor by

the pressurized carried gas. This reactor configuration results in rapid heating of the feedstock at a constant desired reaction temperature.

A non-reactive, non-catalytic quartz tube is designed and inserted inside the Inconel reactor vessel to minimize any potential Inconel surface effect on the reactions. The quartz tube (G. M. Associates Inc., Oakland, CA) is 115 mm long and 40 mm in I.D. and welded with a quartz fritted porous disc of 4 mm thickness at the bottom. Inconel 600 contains up to 72% of nickel metal. This nickel base alloy Inconel may act as catalytic material at high temperature reported in the literatures [76, 77] and in previous studies (Valkenburg, 2006). Gaseous products can transfer through the fritted disc to flow out while the solid residues are collected in the quartz tube. A magnetically driven impeller system (Autoclave Engineers, Erie, PA) is inverted to install from the bottom of the reactor vessel. A straight-blade type impeller is used to provide continuous stirred environment under pressurized conditions which can improve mass transfer of the reactants. Cooling water using ethylene glycol as the cooling medium is circulated around the impeller system to avoid damage of the magnet above its maximum allowable temperature. The gas flow out of the reactor is filtered by a Swagelok coalescing filter to trap water in the product stream before the product gases are analyzed. K type thermocouples are inserted into the quartz tube and the heater to measure the temperatures. LabView (National Labs, 2006) is used for recording temperature and pressure second by second which is collected by Field-Point modules from the National Instrument.

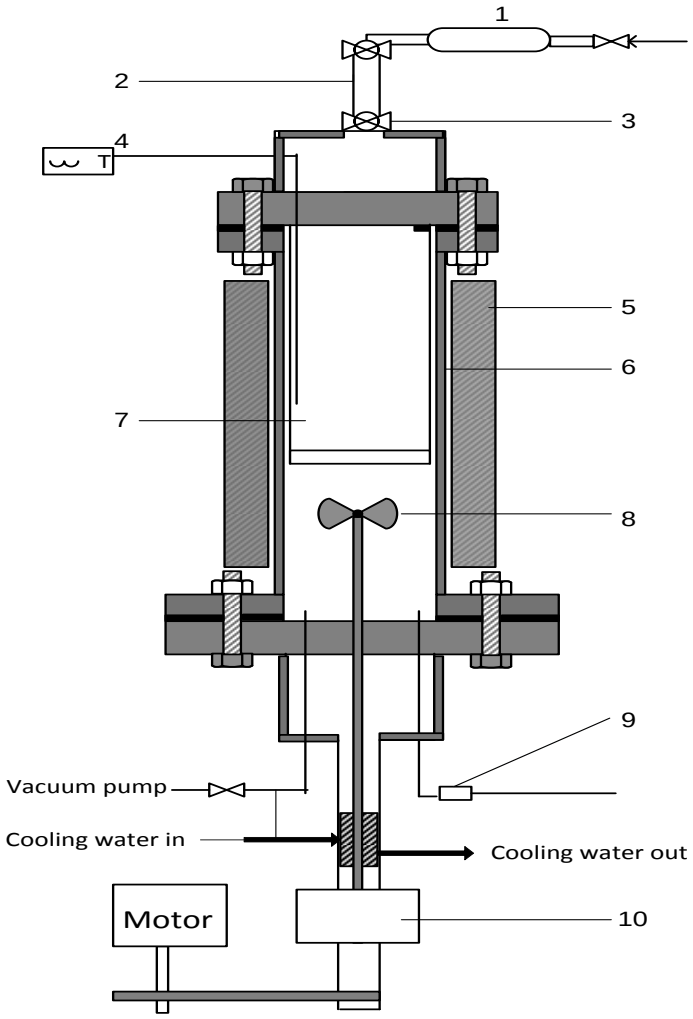

1. Cylinder 2.Feeder tube 3.Ball valve 4.Thermocouple 5.Electronic Heater

6. Reactor vessel 7. Quartz tube 8. Impeller 9. Coalescing filter 10. Magnetic drive

Figure 2.4 A schematic diagram of the inverted batch reactor

Stirred batch reactor

The stirred batch reactor is employed for a low heating rate. A schematic diagram of the inverted bath reactor is shown in Figure 2.5. The reactor consists of an electrical heater, a reactor vessel and a magnetically driven impeller system. The reactor vessel of 40 mm in I.D. and 200 mm in length is made of Inconel 600 and heated by an electrical heater. The reactor allows high temperature and pressure conditions of maximum 500 psi at 800 ℃. This reactor has a special design of magnetic impeller configuration to improve mass transfer of the reactants compared with a TGA system. K type of thermocouples inside the reactor and the heater are used to measure the temperature. The feedstock sample is placed in the reactor initially and then the reactor with the feedstock is heated up to reach the desired reaction temperature. The heating up period takes a long time resulting in a low heating rate. Hence, the stirred batch reactor has a limitation of heating rate due to its configuration.

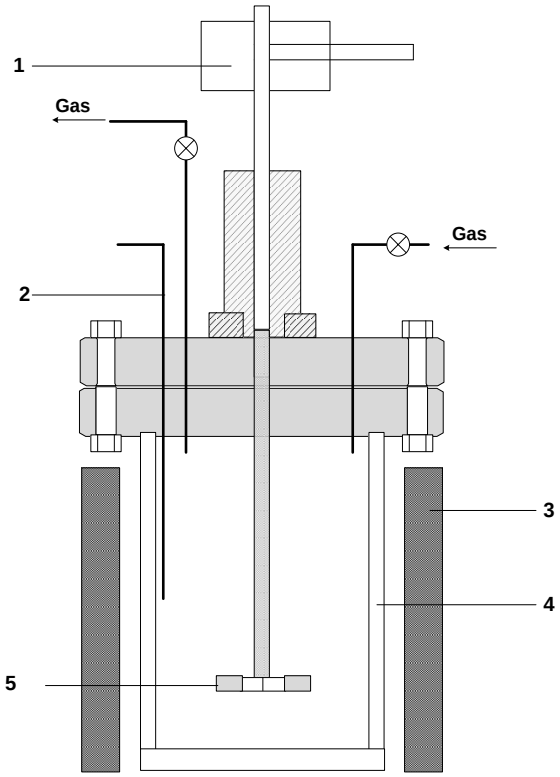

1. Magnetic drive 2. Thermocouple 3. Electronic heater 4. Reactor vessel 5. Impeller

Figure 2.5 A schematic diagram of the stirred batch reactor

2.2.3 Experimental procedure

Series of experiments were performed in the inverted batch reactor to investigate the temperature influence and kinetics in the SHR. The variable reaction conditions were set up at the temperature 600℃, 660℃ and 700℃, respectively with the same H_2O to biomass mass ratio 1:1.2 and hydrogen to H_2O mole ratio 1.5: 1. The procedure for a typical experiment is described as follows.

The prepared feedstock of 1.5g biomass samples mixed with 1.8g water was held in the feeder tube outside the heating zone before each experimental run. Pressurized hydrogen in the cylinder was prepared to use as the gasifying agent as well as the carried gas to facilitate the feedstock loading. The reactor vessel immersed in the heater was tested for leaks and then vacuumed in three times using hydrogen to flush of the air in the reactor. After the reactor system was setup, the reactor vessel in the heating zone was heated from room temperature to a desired reaction temperature. For example, 390 psi hydrogen pressure in the cylinder was ready to provide enough pressure for loading the feedstock into the reactor at 700℃. After the temperature inside the quartz tube reached up to 700℃, the two valves were opened at the same moment and the feedstock was rapidly fed into the quartz tube by the pressurized hydrogen. And the valves must be immediately closed in seconds as soon as the feed was loaded. Each experimental run started from that moment and the impeller system was turned on. Heating of the feedstock samples was considered to be instantaneous at the temperature 700℃ under the hydrogen pressure 270 psi. The heating rate could achieve several hundred K per second. The temperature in the reactor was monitored and adjusted to keep at a constant targeted

temperature during the reaction time. The gaseous products passed through a filter to remove the steam and other condensable components before on-line analysis.

After each experimental run, the heater and impeller system was turned off and the reactor was cooled down to room temperature. The quartz tube was taken out and then dried at 100 ℃ for 20 minutes in order to remove any moisture. The solids residue (char with ash sample) in the quartz tube was weighed to determine the char yield or carbon conversion.

In order to investigate the heating rate influence on SHR, experiments were also conducted in the stirred batch reactor at 700℃ with the same conditions in the inverted batch reactor. The wet feedstock sample was held into the reactor vessel in the heating zone. The reactor was then pressurized with hydrogen to a pressure of 100 psi. The reactor was heated up with the feedstock to reach the targeted temperature. After experiments, the solid residue in the reactor vessel was collected and weighed.

2.2.4 Analysis Methods

Analysis of Gas Products

A Cirrus^{TM} Atmospheric Pressure Residual Gas Analyzer (referred to as RGA and shown in Figure 2.6, MKS Instruments, Inc.) is used for real-time analysis of product gases in this thesis. RGA can identify and analyze gaseous components based on the quadruple mass spectrometer. This quadrupole mass spectrometer RGA has several advantages for on-line analysis of mixture gases [78, 79]. First, RGA can offer a fast on-line monitoring for identification and analysis of a large number of gas mixtures in one signal analyzer including trace contaminants in process gases; solvent vapors; hydrocarbons; atmospheric gas species and so on. Second, RGA can track gas composition over a wide dynamic range from ppb to percentage levels. Third, the operation and maintenance of RGA is convenient due to its bench-top configuration.

Figure 2.6 A photograph of Cirrus Atmospheric Pressure Residual Gas Analyzer

This RGA is an atmospheric pressure system. It means that the inlet gases should be injected into RGA at the atmosphere pressure equal to 1 bar. For that, a PEEK^{TM}

capillary transfer line is used to connect the reactor to RGA system to reduce the product stream pressure acceptable for the RGA. PEEK capillary tubing is widely used in high pressure liquid chromatography and has good chemical resistance and strong structure maintaining dimensional stability. The capillary line (Health & Science, Inc.) used has a dimension of 0.217 mm I.D. and 100 mm long in order to assure a maximum flow rate acceptable for RGA with the minimal gas loss. A T-fitting vent is installed at the inlet of RGA to guarantee a constant 1 atmosphere pressure to RGA. If the inlet gas pressure is lower than 1 bar, RGA will pull the air through the vent to reach 1 atmosphere pressure.

The RGA provides near real-time analysis of the gaseous products by continuous scans of mass spectra every 3-4 seconds. The sensitivity of RGA to a particular gas species is expressed as the peak intensity per unit measure in Eqn. (2.1), which is assumed to be relatively unaffected in a wide range of RGA background.

$$S_C = \frac{I_C}{P_C} \qquad \text{Equation (2.1)}$$

Where Sc is RGA sensitivity to a gas species, Ic (torr) is major intensity of a gas species in mass spectra, Pc (torr) is partial pressure of a gas species in mixture gases.

The RGA records the mass spectra data as intensity in units of torr. The major product gases from the steam hydrogasification are CH_4, CO, CO_2 and less amount of H_2. The relative concentration of a gas species in mixture gases is proportional to the intensity of a gas species according to Eqn. (2.1) based on a constant sensitivity. The sensitivity of a gas species in mixture gases can be obtained by RGA calibration using certified calibration gas.

The evolution of gas products during the steam hydrogasification was analyzed by RGA. The gases evolved were identified by detecting the key fragment ions produced. Hence, analysis for CO and CO_2 are taken for the molecular peak of m/z=28, m/z=44 in the mass spectra pattern while the CH_4 analysis is taken for m/z=15 not m/z=16. This is because both mass spectra patterns of CO and CO_2 have fraction of the fragmental peak in the m/z=16 due to the ionization of oxygen element.

Carbon Conversion

Carbon conversion (*wt %*) in steam hydrogasification is defined as the fraction of carbon in biomass converted to the gaseous products and liquid residue. Before each experimental run, the carbon content of the pinewood feedstock is calculated to be 45% on a wet basis (5.65%). After each experimental run, the carbon content in the solid residue is estimated by assuming that all the char is present as elemental carbon and also that all the ash is retained in the solids residue [73]. The calculation is based on dry, ash free basis of the char weight.

$$\text{Carbon Conversion (wt \%)} = \left(1 - \frac{\text{carbon left over after a test}}{\text{carbon in the feedstock before a test}}\right) \times 100$$

Analysis of Char Products

Scanning Electron Microscopy (SEM) is used to investigate the structural transformations of biomass and char particles. SEM analysis can help to understand the effect of heating rate on char reactivity. Morphological changes of particle surface before

and after SHR are observed. Chars morphology changes at different heating rate from two reactors are analyzed. The SEM analysis in this thesis is performed using a XL30-FEG SEM. The samples are pinewood samples (150-180 um), solid chars (dry, ash basis) from the inverted batch reactor at 700℃ and solid chars from the stirred batch reactor. The sample particles are dispersed on an aluminum plate and platinum-coated in a vacuum electric sputter coater about 30 seconds before SEM analysis.

2.3 Results and Discussion

2.3.1 Effect of heating rate

Temperature profiles

The heating rate has a significant influence on gasification reactivity [80, 81]. Effect of heating rate on the steam hydrogasification was evaluated through the experiments at low heating rate and high heating rate.

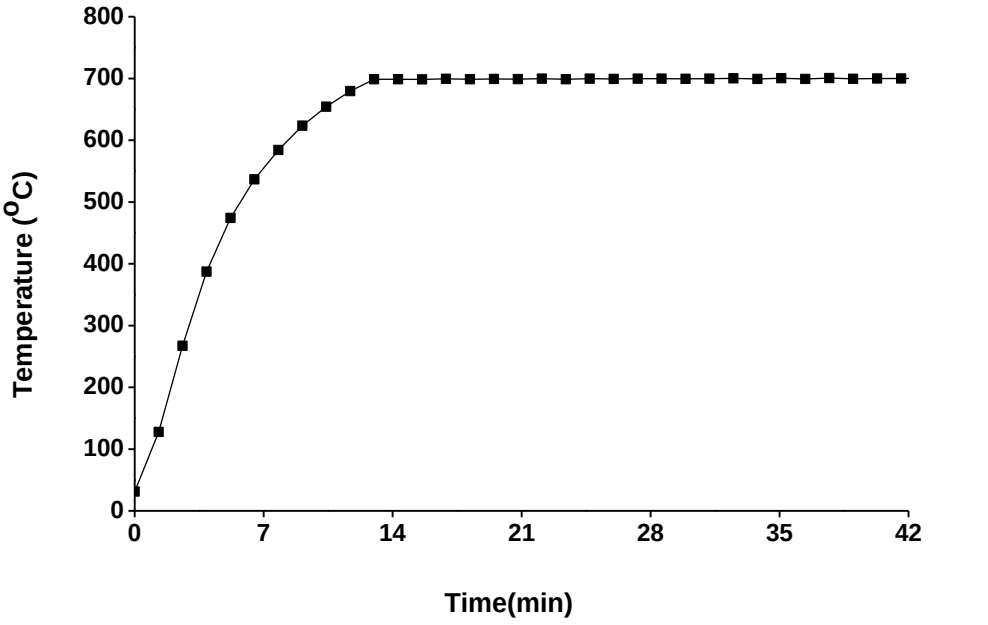

Figure 2.7 A temperature profile from the stirred batch reactor at a 700℃ test

The two reactors provided different thermal conditions due to their different reactor configurations. Figure 2.7 shows the temperature profile in the stirred batch reactor during the steam hydrogasification at 700℃. The feedstock was heated in the reactor from room temperature to 700℃. It is seen that it took at least 12 minutes for the

reactor to reach the desired reaction temperature and then the temperature was stable at 700℃ until the experiment ended. The stirred batch reactor had a long heating up period resulting in a low heating rate. The average heating rate in the stirred batch reactor was defined as,

$$\frac{\Delta T}{\Delta t} \leq 1\,(K/s)$$

The inverted batch reactor made novel designs of a feeding system and a quartz tube in the heating zone in order to improve the heat efficiency compared with the stirred batch reactor. The temperature profile in the inverted batch reactor at 700℃ is shown in Figure 2.8. The temperature profile showed a continuous constant reaction temperature during the whole reaction time. Heating of the feedstock in the inverted reactor was instantaneously completed since the samples were rapidly loaded into the heating zone. It was difficult to calculate the accurate heating rate for the inverted batch reactor based on the definition above. The average heating rate in the inverted batch reactor was estimated in the range level of 10^2-10^3K/s. It was based on the assumption that the instantaneous temperature change was completed within the time change of a response time of K type thermocouple which was measured to be 1-5 seconds. It is considered that the temperature condition is the isothermal reaction condition. Hence, the inverted batch reactor can perform a high heating rate for the steam hydrogasification process.

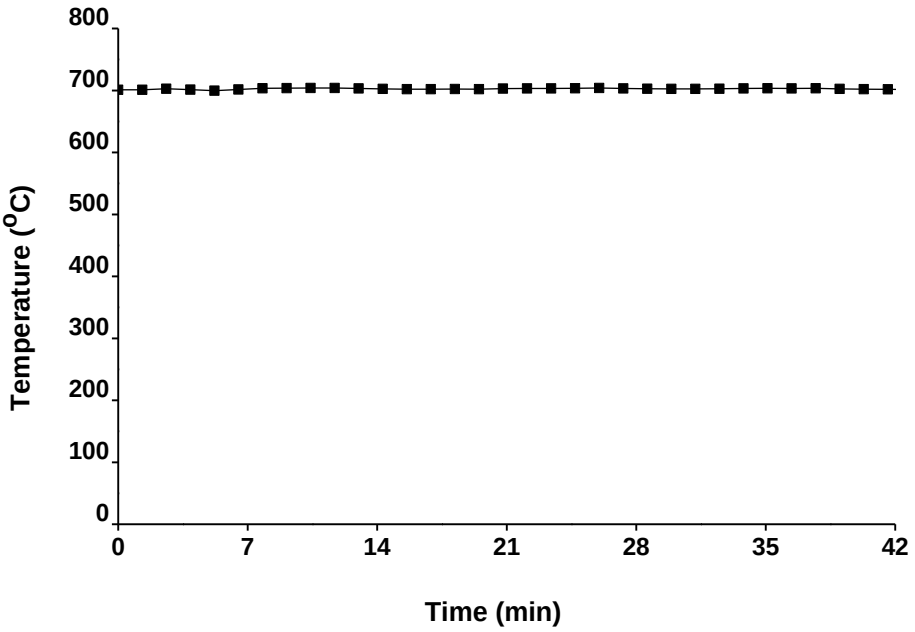

Figure 2.8 A temperature profile from the inverted batch reactor at 700℃

Effect of heating rate on the carbon conversion

Carbon conversion at high heating rate and low heating rate were obtained and effect of heating rate on the steam hydrogasification was determined. The carbon conversions under the prescribed experimental conditions at different heating rate are shown in Figure 2.9. The carbon conversion increased from 50.8% at low heating rate in the stirred batch reactor to 66.4% at high heating rate in the inverted batch reactor. It is found that the heating rate had a strong influence on the carbon conversion in the steam hydrogasification. More chars are converted at high heating rate resulting in less char yield that enhanced the carbon conversion in the steam hydrogasification process. The influence of heating rate demonstrated that a fluidized bed of high heating rate and

constant bed temperature is a preferred type gasifier for scaling-up steam hydrogasification. Besides, the heating rate on pyrolysis or gasification had direct impact on reaction kinetics and high heating rate had a lower activation energy compared with low heating rate [82, 83]. Therefore, high heating rate is essential for kinetic measurement in the gasification system that will be discussed in the section 2.3.3.

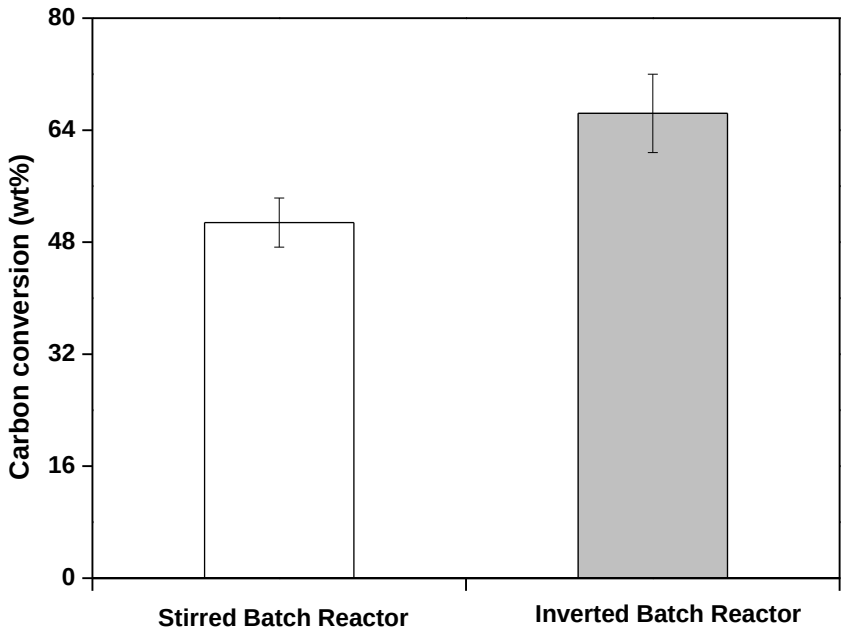

Figure 2.9 Effect of heating rate on carbon conversion in the steam hydrogasification using the inverted batch reactor and the stirred batch reactor

Effect of heating rate on the char morphology

The morphology of chars is affected greatly by gasification temperature and hating rate. Effect of heating rate on char morphology and reactivity in the steam hydrogasification is evaluated through SEM images of chars produced at different heating rate.

Figure 2.10 shows SEM image of a surface state of patent material (pinewood particles). It is observed that a typical patent particle has its original structure of cells strongly bounded with obvious slits and fractures. The grinding process led to the shredded edge in the pinewood particle.

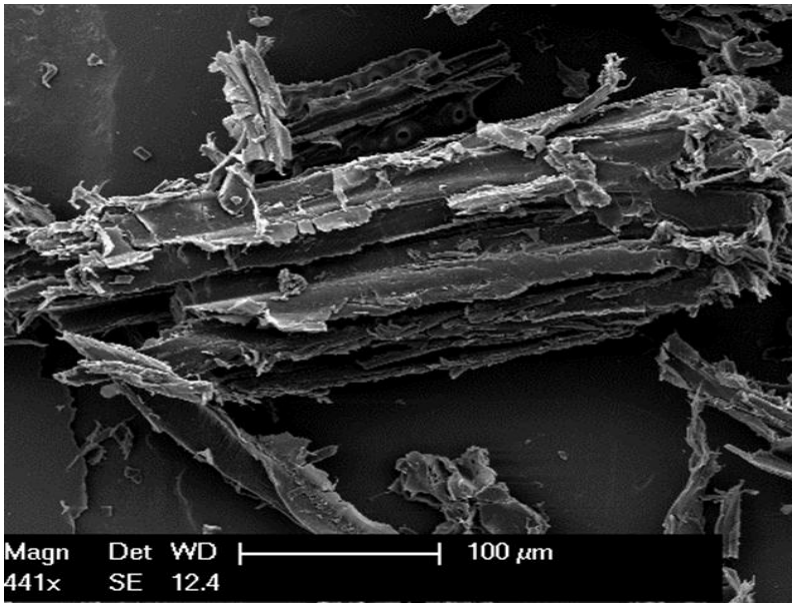

Figure 2.10 SEM image of the patent sample

The chars from the inverted batch reactor were produced at high heating rate while the chars from the stirred batch reactor were produced at low heating rate. The SEM images of chars generated at high heating rate and low heating rate were shown in Figure 2.11 and 2.12, respectively. Effect of heating rate on surface morphologies of chars can be examined by a comparison of SEM images of chars at different heating rate with the patent sample.

At low heating rate, some destruction and deep opening in the char structure were observed compared with the original wood cells structure. The surface state of char maintained uniform rough morphology and presented an obvious porous structure. More remarkable observations can be seen in Figure 2.11(b). The micro pore structure in an arrangement on the char surface was attributed to devolatilization of volatile matters at low temperatures [84].

At high heating rate at 700℃, the char presented a thoroughly deformed structure so that the cell structure did not exist. It was observed that the char had a smooth morphology with signs of melting in Figure 2.12. Besides, the micro pore structure on the char surface was shrinkage and even closed but created larger cavities instead. The similar phenomena on biomass char generated at high heating rate have been reported by Fu et al. [85] and Cetin et al. [86]. High temperature at high heating rate led to the occurrence of plastic transformations of particles which resulted in melting of particles and created a smooth morphology and large cavities [87]. No devolatilization phenomena occurred in the inverted batch reactor due to the high heating rate.

A comparison of biomass char morphology at high and low heating rate was presented above. It is found that heating rate had a remarkable impact on char morphologies. At low heating rate and low temperature, the release of a significant amount of volatile matters occurred resulting in the pore structure. The devolatilization leads to a low char reactivity and conversion efficiency in the gasification process [84,87]. At high heating rate and high temperature, melting of particles occurred resulting in a smooth morphology and shape of cavities. The porous structure would be shrinking or destroyed at direct high temperature due to the plastic deformation (also referred to as melting). It is indicated that no devolatilization happened at high heating rate. It is proven that the inverted batch reactor is able to perform a high heating rate condition in the steam hydrogasification.

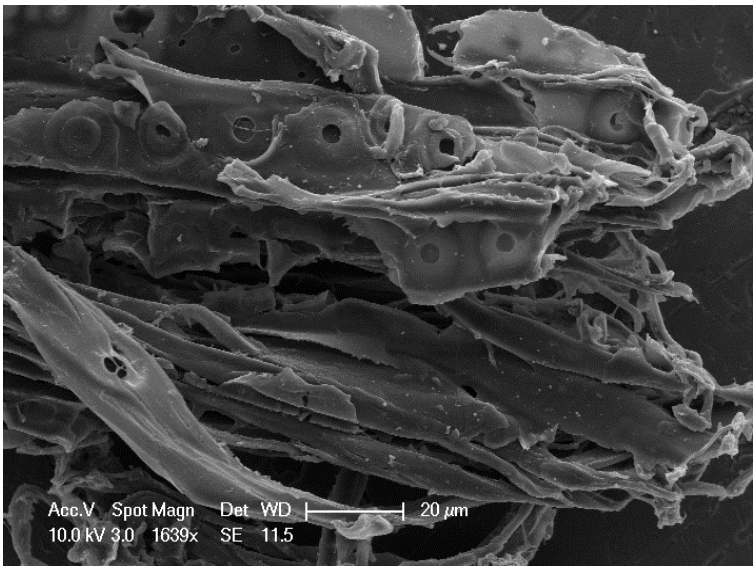

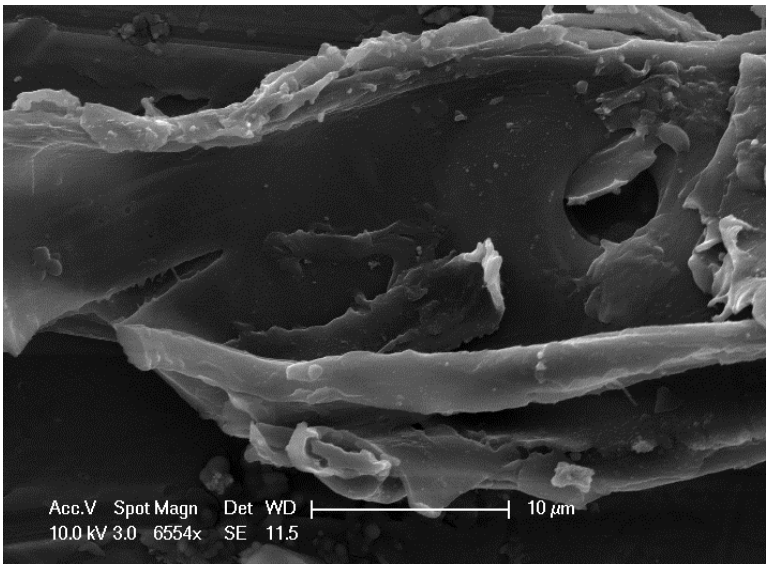

Figure 2.11 SEM images of biomass chars from the stirred batch reactor

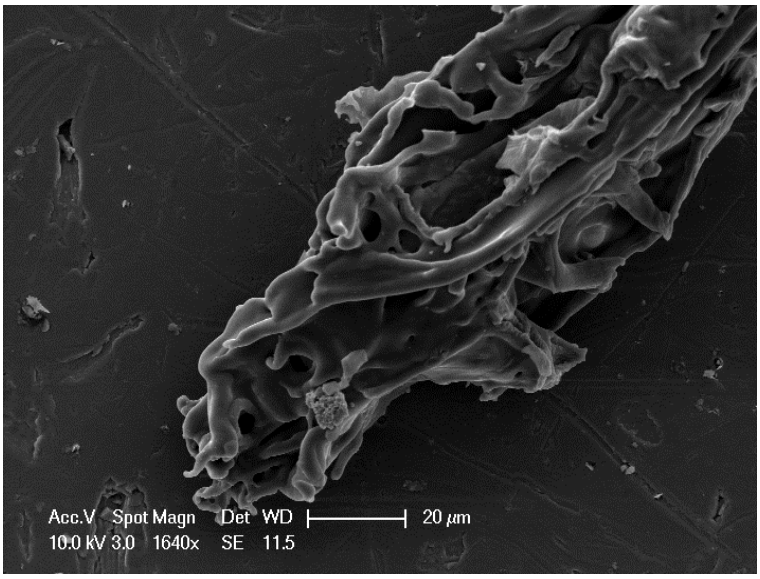

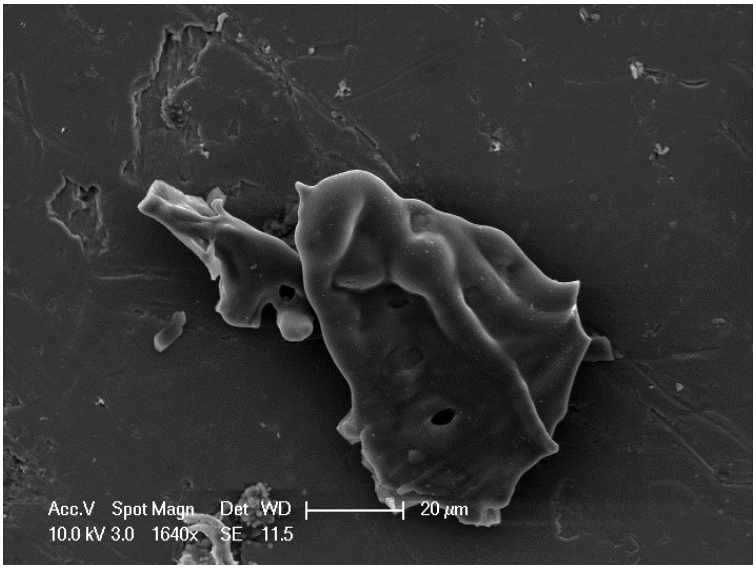

Figure 2.12 SEM images of biomass chars from the inverted batch reactor

2.3.2 Effect of temperature

Effect of temperature on the carbon conversion

Effect of temperature on the steam hydrogasification efficiency was examined at the temperatures range of 600℃ to 700℃ with water to biomass ratio 1.2g/g. The effect of temperature on the carbon conversion efficiency is presented in Figure 2.13.

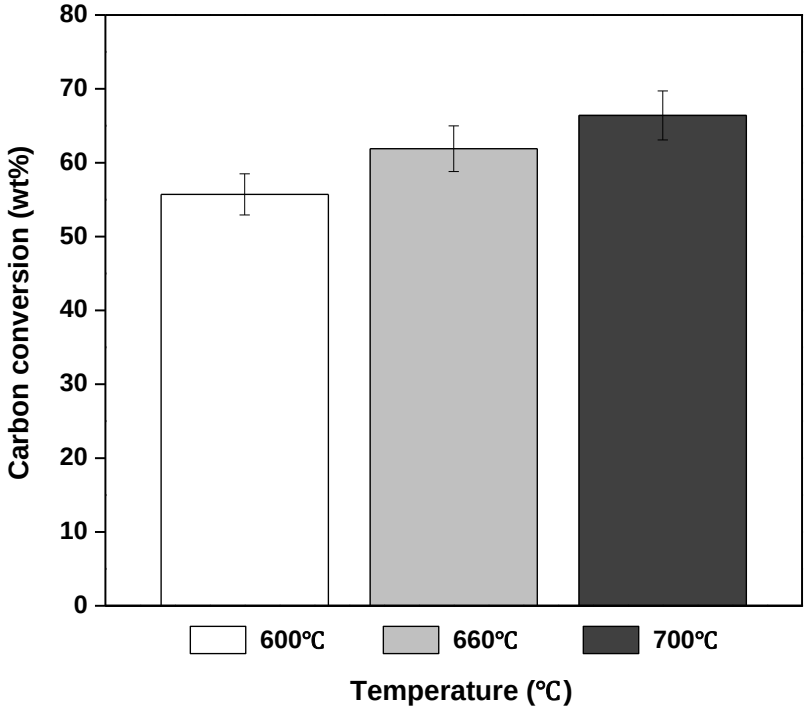

Figure 2.13 Effect of temperature on carbon conversion in the steam hydrogasification

With the temperature increasing from 600℃ to 700℃, the carbon conversion was increased from 55.7% to 66.4%. A higher temperature enhanced the carbon conversion in the steam hydrogasification. The biomass chars decomposed faster at high temperatures than at low temperatures, resulting in a decrease in the char yield and an increase in the

carbon conversion. It is means that high temperatures lead to high reactivity of chars. Reaction temperature in the steam hydrogasification is an important parameter which has strong influence on the carbon conversion. And temperature also affects the gasification rates that will be presented in the followings.

It have been reported that a high reaction temperature promoted biomass decomposition in the steam gasification or in the hydrogasification [88, 89]. In this study, it is demonstrated that the temperature is a favorable reaction parameter for the steam hydrogasification of biomass.

Effect of temperature on the product gas evolution

The main gas products in the steam hydrogasification are CH_4 and CO with small amount of CO_2. Effect of temperature on the formation of the product gases CH_4, CO and CO_2 are presented in Figures 2.14-2.16, respectively. Each product gas had its own variation with the reaction time and temperature, different from others. The intensity value in the gas formation is proportional to the amount of a product gas generated.

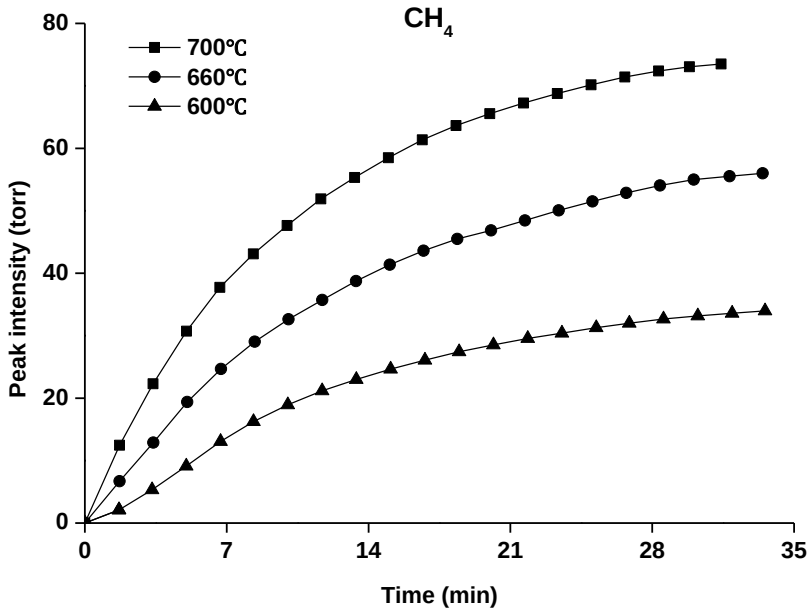

Figure 2.14 Effect of temperature on the CH_4 evolution in the steam hydrogasification

For CH_4 in Figure 2.14, it is found that CH_4 evolution was largely promoted when the temperature was increased from 600℃ to 700℃. The CH_4 amount monotonously increased with reaction time and the maximum amount of CH_4 at 700℃ was achieved at around 25mins while the maximum amount of CH_4 at 600℃ was reached after 30mins. It means that the higher temperature the higher maximum amount of CH_4 generated in the steam hydrogasification and the less reaction time needed to reach the maximum point. Similar to CH_4, the CO and CO_2 amounts were also increased with reaction time and temperature. However, it can be seen that the release of CO_2 at 700℃ took about 10mins to complete while the release of CH_4 and CO took around 25mins and 20mins to complete, respectively.

It is proven that reaction temperature has a remarkable influence on the product gas formation during the steam hydrogasification process. The amount of CH_4, CO and CO_2 generated in the steam hydrogasification was increased with an increase of reaction temperature.

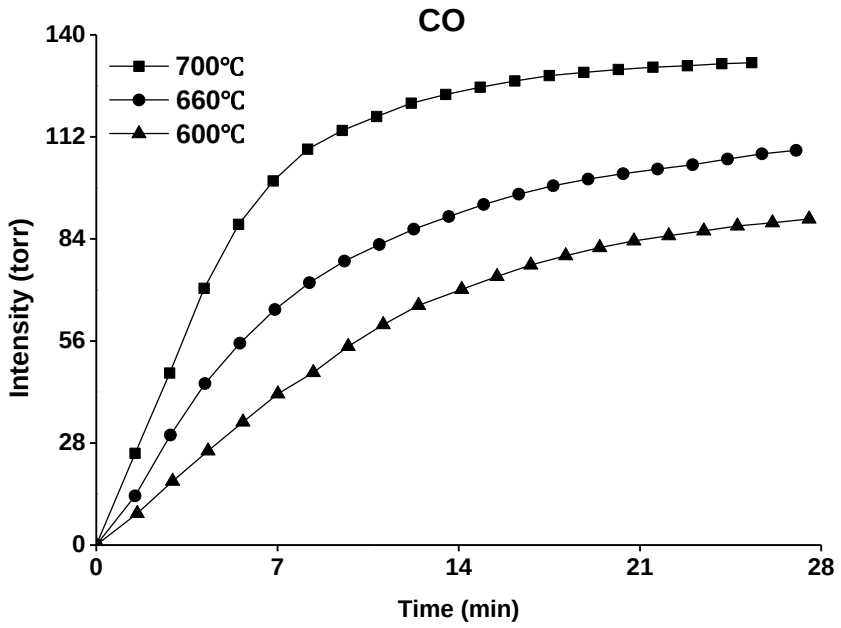

Figure 2.15 Effect of temperature on the CO evolution in the steam hydrogasification

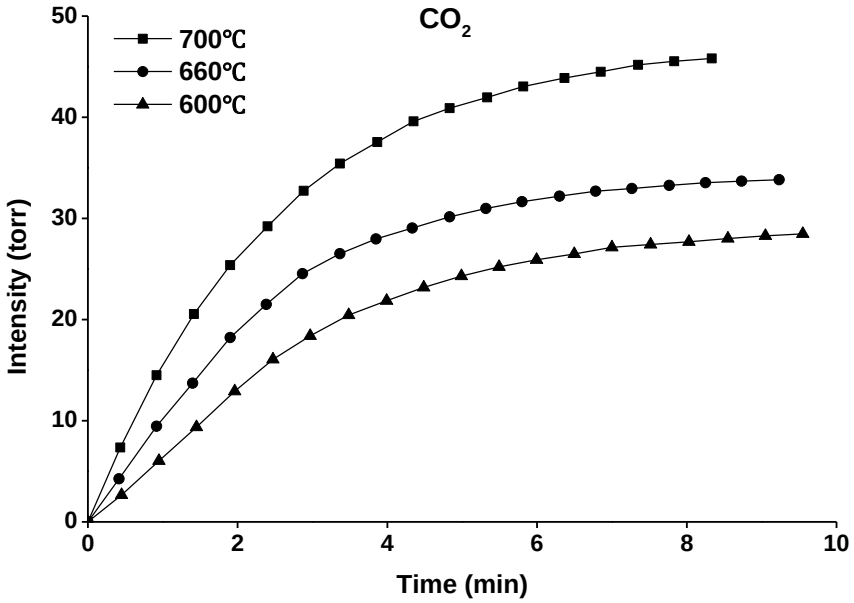

Figure 2.16 Effect of temperature on the CO_2 evolution in the steam hydrogasification

2.3.3 Kinetics Study

Kinetic model

Determination of kinetic parameters in the steam hydrogasification of biomass is one of the major objectives in this chapter. Kinetic parameters are valuable for the design of large-scale gasifiers, process simulation and optimization of process variables [90]. Lignocellulose biomass has the variability of composition, physical properties and the mechanisms of thermal degradation of biomass components are not comprehensive understood since series of consecutive and competitive reactions occur simultaneously during the gasification [91]. Although modeling approaches of biomass pyrolysis or gasification has been proposed by some researchers [90-92], developing a rigorous kinetic model for biomass gasification is a very challenge project. Therefore, the measurement of kinetic parameters in this study aims to derive a simplified kinetic model suitable for the steam hydrogasification.

The main product gases CH_4, CO and CO_2 were generated from series of complex and competitive reactions in the presence of hydrogen and steam. A first-order kinetic model proposed by Encinar et al. [93] is employed for kinetics analysis in the steam hydrogasification process. This model is assumed that the biomass decomposes through series first-order parallel reactions and that each product gas species is generated from a single, independent and molecular reaction, each having different activation energy. We proposed the principles of the kinetic model are suitable for the steam hydrogasification. The experimental data are expected to fit to a first-order kinetic rate expression.

The reaction rate equations in details are presented in the followings. The rate of formation of a product gas species in a batch reactor is expressed as equation (2.2):

$$r = \frac{dm}{dt} \qquad \text{Equation (2.2)}$$

Where, m is moles of a gas species generated at a given time t.

The rate of biomass mass loss in a batch reactor in a first-order kinetic is expressed as the equation (2.3):

$$-\frac{dM}{dt} = kM \qquad \text{Equation (2.3)}$$

Where, M is mass of biomass residue at a given time.

The m moles of a gas species at a given time can be related to M according to the equation (2.4):

$$m = \alpha(M_0 - M) \qquad \text{Equation (2.4)}$$

Where, M_0 is the initial mass of biomass to be gasified

M is mass of biomass residue at a given time

α is an conversion coefficient between a gas species and biomass residue.

Differentiation of equation (2.4) and combination of equation (2.3) are accounted for the equation (2.5):

$$\frac{dm}{dt} = -\alpha\frac{dM}{dt} = \alpha kM = \alpha k\frac{m - \alpha M_0}{-\alpha} = k(m_0 - m) \qquad \text{Equation (2.5)}$$

Where, $m_0 = \alpha M_0$ is the total moles of gas generated when the release of the gas is ended in the gasification process. This value of m_0 can be obtained by extending reaction time until no more product gas is released.

The first-order kinetic expression equation (2.6) is given below after separation of variables and integration of equation (2.2-2.5) in details above:

$$\ln \frac{m_0}{m_0 - m} = kt \qquad \text{Equation (2.6)}$$

Where, m is moles of a gas species generated at a given time t

m_0 is the total moles of a gas species generated in the gasification process

k is the rate constant of a gas species formation

According to equation (2.6), a plot of its left side versus time should yield a straight line with no intercept in the origin, of which the slope is the value of rate constant k or specific reaction rate. A thermal condition under continuous stable temperature during the reaction time is critical for the determination of rate constant k at a defined temperature.

Rate constants

Plots of $ln(m_0/(m-m_0)$ versus time for the individual product gas (CH_4, CO and CO_2) can be obtained from the gas evolutions in Figures 2.14-2.16. For that plot, the generated gas amount m at any given time is determined by the intensity value in the gas evolution while m_0, the value when no more the gas species is released, is obtained from the maximum amount in the gas evolution.

Values of rate constants are obtained from least squares analysis in the plots of $ln(m_0/(m-m_0)$ versus time. Figure 2.17 shows the plots of $ln(m_0/(m-m_0)$ versus time for CH_4 formation in the steam hydrogasification at different temperatures 600℃, 660℃ and 700℃. It is firstly found that the experimental data points fitted a straight line through the

zero point and the correlation coefficients of least squares analysis were up to 0.99. This good linear relationship of $ln(m_0/(m-m_0)$ versus time supports the first-order kinetic rate based on the kinetic model. Secondly, it is also observed that the slopes of the straight lines became larger with an increase of the reaction temperature. The slope of the straight line determined the value of rate constant k_{CH4} at a defined temperature. That means a higher temperature led to an increase of specific reaction rate. The plots for CO and CO_2 formation are shown in Figs 2.18 and 2.19. The CO and CO_2 presented similar results to those for the CH_4.

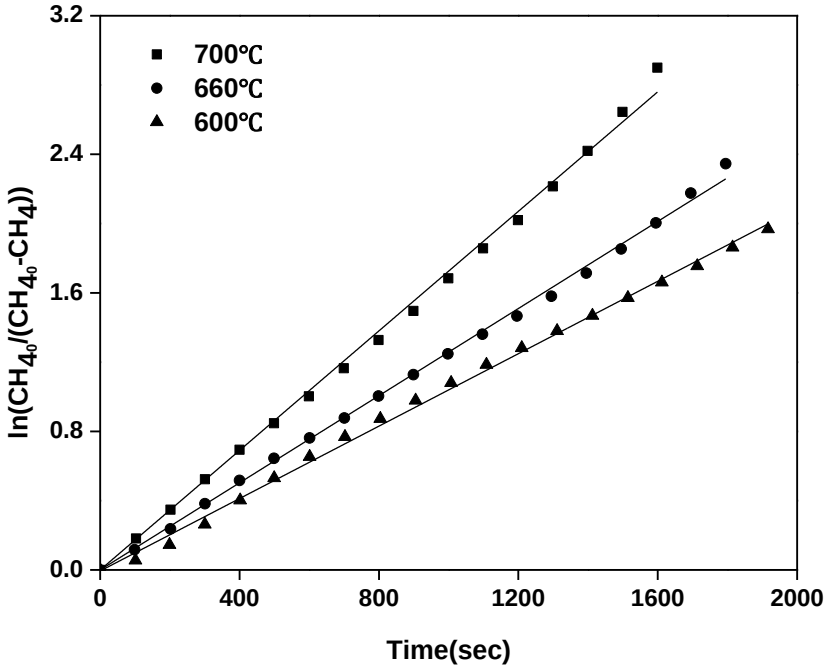

Figure 2.17 Plots of $ln(m_0/(m_0-m)$ versus time for CH_4 formation at different temperatures. The solids lines are least squares analysis results.

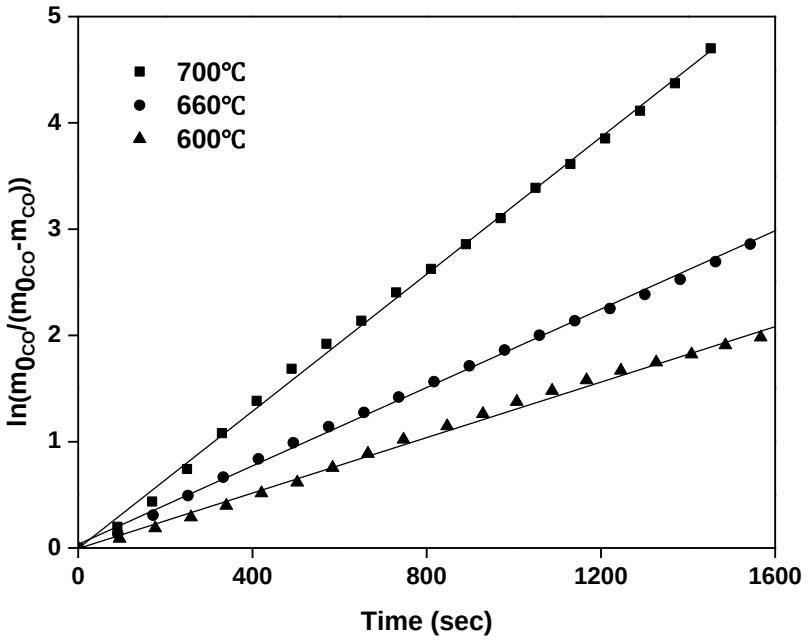

Figure 2.18 Plots of $ln(m_0/(m_0-m)$ versus time for CO formation at different temperatures. The solids lines are least squares analysis results.

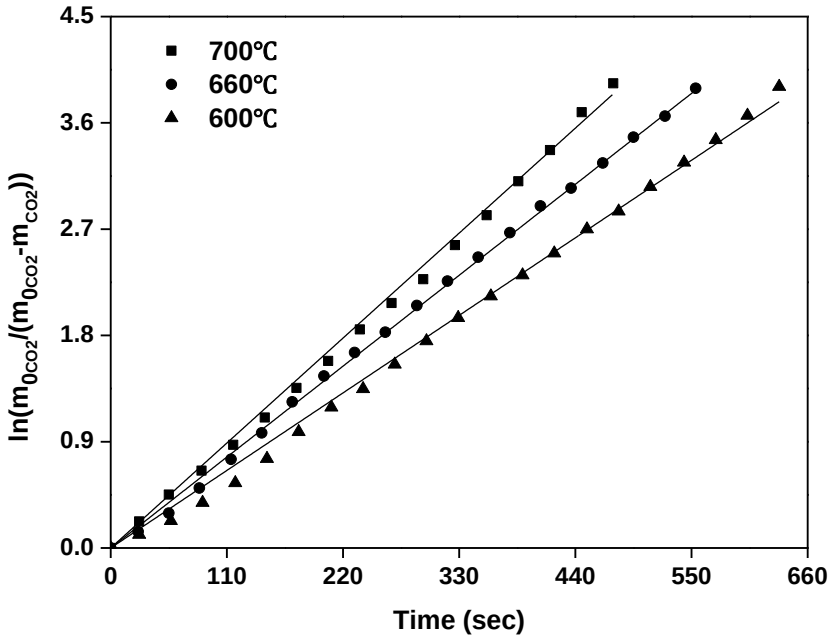

Figure 2.19 Plots of $ln(m_0/(m_0-m)$ versus time for CO_2 formation at different temperatures. The solids lines are least squares analysis results.

Figure 2.20 shows the effect of temperature on the rates of CH_4, CO and CO_2 formation. The specific rates (rate constant k) at different temperatures 600℃, 660℃ and 700℃ are listed in Table 2.3. As expected, the reaction temperature had remarkable influence on the rate of product gas formation in the steam hydrogasification. The specific rate of CH_4 formation almost doubled and the rate of CO formation increased nearly twice when the reaction temperature increased from 600℃ to 700℃. The temperature led to the enhancement in the rate of gas formation. This result indicated that the dominant reactions occurred in the steam hydrogasification were favored by the reaction temperature. The product gas CO_2 was generated at a very fast rate that was

much higher than that of CO and CH_4 regardless of the temperatures. It is inferred that the release of CO_2 completed fast at the initial gasification step.

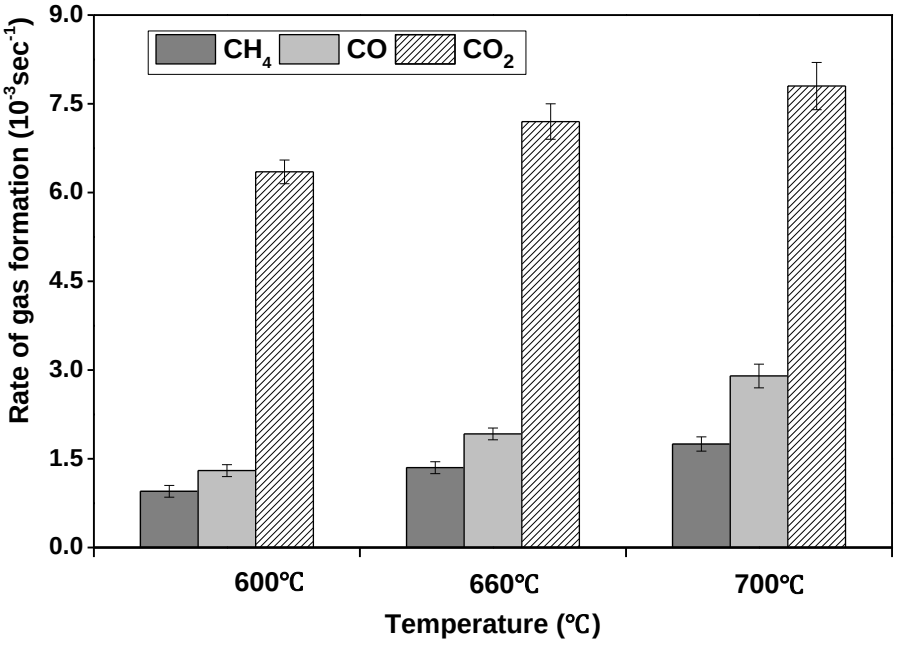

Figure 2.20 Effect of temperature on the rates of product gas formation

Table 2.3 Rate constants of CH_4, CO and CO_2 formation in the steam hydrogasification of pinewood at different temperatures

T (℃)	Rate constants ($10^{-3}sec^{-1}$)			Correlation coefficients		
	k_{CH_4}	k_{CO}	k_{CO_2}	$R^2_{CH_4}$	R^2_{CO}	$R^2_{CO_2}$
600	0.95	1.30	6.35	0.99	0.98	0.99
660	1.35	1.92	7.20	0.99	0.99	0.99
700	1.75	2.90	7.80	0.99	0.99	0.99

Activation Energies

Values of *k* can be expressed as an Arrhenius function of temperature given in the equation (2.7):

$$k = A\exp(-\frac{E_a}{RT}) \qquad \text{Equation (2.7)}$$

Where, A is Arrhenius pre-exponential factor or frequency factor (sec^{-1});

E is the activation energy (kJ $mole^{-1}$);

R is a gas constant (8.314J $mole^{-1}K^{-1}$);

T is the gasification temperature (K).

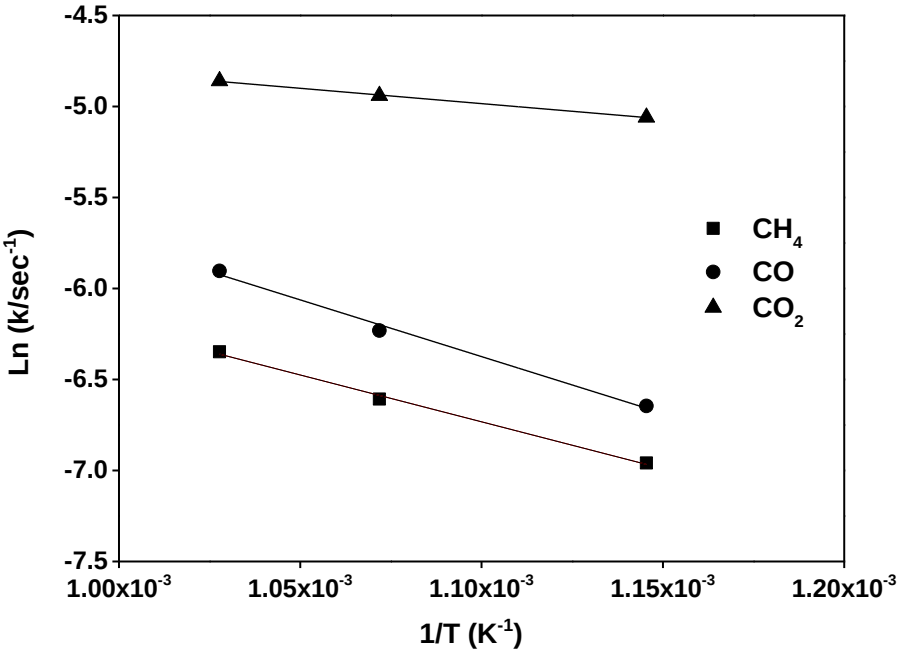

Figure 2.21 Arrhenius plots for CH_4, CO and CO_2 formation in the steam hydrogasification

The Arrhenius plots of CH_4, CO and CO_2 are shown in Figure 2.21. Table 2.5 lists the obtained activation energies of CH_4, CO and CO_2 formation and the Arrhenius pre-exponential factors and correlation coefficients in the steam hydrogasification of pinewood. The correlation coefficients up to 0.99 supported a good result of linear regression analysis for the Arrhenius equation. A comparison of the activation energies for CH_4 and CO formation in steam hydrogasification with other reported results under pyrolysis process [93, 94] are listed in Table 2.6. The dry pyrolysis experiments were conducted in an inert N_2 environment in a bench-scale reactor at high heating rate. It is indicated that the activation energies of individual product gas formation were strongly dependent on the feedstock materials. The steam hydrogasification has lower activation energy of CH_4 formation than that of pyrolysis due to the presence of steam and hydrogen.

Table 2.5 Activation energies, Arrhenius pre-exponential factors of CH_4, CO and CO_2 formation at the temperatures 600℃ to 700℃

Product gas	Activation energy	Arrhenius pre-exponential factors	Correlation coefficients
	E_a (kJ mole^{-1})	A (sec^{-1})	R^2
CH_4	42.8	0.24	0.99
CO	51.8	1.62	0.98
CO_2	14.0	0.04	0.99

Table 2.6 Activation energies for CH_4 and CO formation in this work and others

Biomass	Temperature (℃)	Activation Energy (kJ $mole^{-1}$)		Ref.
		CH_4	CO	
Pinewood	600-700	42.8	51.8	This work
Maize	400-700	76.7	18.9	[93]
Tobacco	400-700	80.2	23.1	[93]
Sunflower	400-700	61.6	19.6	[94]
Cherry stone	300-800	58.1	42.8	[94]

2.4 Conclusion

The steam hydrogasification of biomass pinewood was carried out at temperatures ranging from 600℃ to 700℃ with the H_2O to biomass ratio 1.2g/g. The inverted batch reactor was used to provide a high heating rate level of a few 10^2 K/s while the stirred batch reactor was used to perform a low heating rate level of a few 1 K/s. Effect of heating rate and temperature on the steam hydrogasification were determined. Kinetic parameters in the steam hydrogasification were obtained based on a first-order kinetic model. The results of this study have led to the following conclusions.

1. Heating rate is found to have a significant influence on the conversion efficiency in the steam hydrogasification. There was approximate 15% increase in carbon conversion when the heating rate was increased from less than 10 K/s to more than 10^2 K/s. A high heating rate in the steam hydrogasification led to a reduction in the char yield resulting in an increase of the carbon conversion.
2. Obvious changes of char morphologies at different heating rate were observed from SEM images. The chars produced at low heating rate had rough surface morphology with retained signs of the original cell structures. The de-volatilization of volatile matters occurred at low temperatures due to low heating rate that resulted in a porous network structure on the char surface. In contrast, high heating rate and high temperature led to thoroughly melting of particles, resulting in smooth surface morphology and large spherical cavities. It is concluded that heating rate had a remarkable impact on the char reactivity. The

de-volatilization, porosity evolution and melting phenomena are helpful to understand what happens during the steam hydrogasification.

3. The gasification temperature is a critical parameter to improve the steam hydrogasification efficiency. There was a 10% increase of carbon conversion in the steam hydrogasification of pinewood when the temperature was increased from 600℃ to 700℃. And the rate of CH_4 and CO formation had a dramatic increase at higher temperature 700℃. It is concluded that an increase of reaction temperature not only promoted the carbon conversion but also enhanced the gasification rates in the steam hydrogasification.
4. The inverted batch reactor is able to perform a realistic thermal condition for the kinetic measurement in lab-scale experiments, which is essential to determine the specific reaction rate at a particular temperature.
5. An approach for determination of kinetic parameters in the steam hydrogasification is established in this thesis. A simple first-order kinetic model is used to analyze the steam hydrogasification kinetics. The experimental results agreed well with the first-order kinetic rate. This simplified kinetic model was suitable for kinetic analysis in the steam hydrogasification. The gasification rate was governed by the rate of CH_4 and CO formation. The activation energies of CH_4 and CO formation in the steam hydrogasification of pinewood were 42.8 and 51.8 kJ/mole, respectively.

Chapter 3

Steam Hydrogasification of Co-mingled Biosolids with Biomass as the Feedstock

This chapter focuses on the co-utilization of biosolids and biomass in steam hydrogasification. It aims to investigate the effect of biosolids on the steam hydrogasification of biomass. The water content in the biosolids serves as the source of steam and the woody biomass supplies the main source for carbonaceous matters. The co-mingled feedstock of biomass and biosolids can achieve a desired carbon to water ratio. Steam hydrogasification of co-mingled feedstock were performed at 700℃ with a H_2O/C mole ratio 1.5:1. The effect of biosolids on steam hydrogasification was examined including carbon conversion, the reaction rate of CH_4 formation and CO formation. The metal elemental compositions in the biosolids were characterized by using ICP-AES and SEM- EDS. The possibility of biosolids integrated in the feedstock as in-situ catalyst to improve the steam hydrogasification efficiency was discussed in this chapter.

3.1 Introduction

Biosolids, sewage sludge from municipal wastewater treatment plants, contains nutrient-rich organic matter and high water content as well as high concentration of metal species. Biosolids has high ash content compared to cellulosic biomass. Major metal elements in the ash are Fe and Ca due to an addition of $FeCl_3$ or lime in the wastewater treatment processes [95]. Co-gasification of biosolids and biomass or coal has been extensively investigated [96-97]. Several researchers [98-101] have suggested that catalytic effects can occur in the co-gasification resulting in reduction of tars and increase of char reactivity due to the presence of Fe(III) and Ca in the biosolids ash. Based on literature review of catalysts, the metals in the biosolids have a potential for a catalytic effect. This study will investigate co-utilization of biosolids and biomass as the co-mingled in the steam hydrogasification, which is expected that the use of biosolids in the feedstock could improve steam hydrogasification efficiency. The main tasks in this chapter include evaluating the steam hydrogasification of co-mingled biosolids with biomass; determining how active and effective the biosolids affects the steam hydrogasification of biomass through a comparison of co-mingled feedstock with biosolids and biomass feedstock without biosolids; and investigating the impact of biosolids on char structure and elemental compositions by using SE- EDS and ICP-AES.

3.2 Experimental sections

3.2.1 Feedstock materials

Biomass The biomass feedstock used in this study is pinewood sawdust. The samples were dried at 105℃ for 2 hours and sieved to a particle size of 150-180um.

Biosolids Biosolids used in this study is supplied by the Riverside Regional Water Quality Treatment Plant located in the city of Riverside, California. The raw biosolids samples are obtained from the top level of Dissolved Air Floatation Thickener. For that, the biosolids samples are from the secondary treatment process without dewatering or digestion treatment. Raw biosolids samples were stored in sealed jar in refrigerator before tests in order to avoid moisture evaporation.

Table 3.1 Chemical compositions of the biosolids and pinewood samples

Composition (wt%)	pinewood	biosolids
Moisture	5.65	92.9
Volatile matter	81.52	4.9
Fixed carbon	12.58	0.6
Ash	0.25	1.6
Total	100	100
Moisture	5.65	92.9
C	44.87	2.90
H	5.95	0.44
N	0.05	0.53
O	43.22	1.64
Ash	0.25	1.59

Chemical compositions of biosolids and pinewood biomass used in this study are presented in Table 3.1. It is seen that the biosolids sample contains more than 90% moisture content and approximate 1.6% ash content while its carbon content is as low as 3%. For that, biosolids without dewatering process is not available to feed into a gasifier due to the high moisture content and low carbon level. But woody biomass contains high carbon content and lower ash content. Hence, the biosolids co-mingled with woody biomass as the feedstock for steam hydrogasification can achieve a desired carbon to water ratio by utilizing the water content of biosolids as the source of steam in the SHR and the biomass as the main source of carbonaceous matters.

Table 3.2 Analysis of inorganic elements in the biosolids and pinewood samples

Inorganic elements [a] (mg/g dry basis)	Biosolids [b]	Biomass [c]
Iron (Fe)	13.2	0.02
Calcium (Ca)	22.2	0.82
Aluminum (Al)	5.50	0.04
Magnesium (Mg)	4.30	0.20
Potassium(K)	5.10	0.61
Sodium (Na)	2.50	0.03
Titanium (Ti)	1.40	0.00
Phosphorous (P)	1.20	0.06
Sicilon (Si)	2.70	0.16

(a) measured on ash basis as equivalent oxides
(b) 17.98 wt% ash on dry basis
(c) 0.33wt% ash on dry basis

Biosolids and woody biomass not only show differences in organic matter but also in inorganic matter. Inductively coupled plasma-atomic emission spectroscopy (ICP-AES) is used to analyze the inorganic elements in biosolids and biomass ash. Ash samples were obtained on a dried sample basis after stage ashing to 750℃ and holding at temperature for 8 hours. The analysis results (received from Huffman Laboratories Inc.) are listed in Table 3.2. Biosolids contains high concentrations in metal elements including Fe, Ca, Al, Mg, K, Na compared to the pinewood biomass. Most of the main metal species in the biosolids comes from inorganic compounds added in the wastewater treatment plant, such as $FeCl_3$, lime (CaO), $CaCO_3$. $FeCl_3$ is dosed to the primary treatment process as a coagulant by Riverside Water Plant that results in the high concentration of iron in the biosolids.

Preparation of biomass feedstock and co-mingled feedstock

To prepare biomass and water mixture as biomass feedstock, 1g of pinewood was added with 1g of distilled water and mixed together.

Figure 3.1 Procedure for biomass mixed with biosolids as co-mingled feedstock

Table 3.3 Comparison of compositions of biomass and co-mingled feedstock

Compositions	Biomass Feedstock	Co-mingled Feedstock
Biomass	1.0 g	0.93 g
Biosolids	0.0 g	1.1 g
Biosolids loading	0 wt%	50 wt%
Total H_2O	1.0 g	1.0 g
Total Carbon	0.45 g	0.45 g
Ash	0.0025 g	0.02 g

The fresh biosolids mixed with the dry biomass is used as co-mingled feedstock (seen in Figure 3.1). The biosolids loading in the feedstock is defined as the amount of biosolids per the total amount of the feedstock (biomass and biosolids). The biosolids amount in the co-mingled feedstock is determined by a desired H_2O amount and the biomass amount is determined by the total carbon needed in the feed. The co-mingled feedstock should keep the same water and carbon amount as biomass feedstock in order to make a comparison. Approximate 1.1 g biosolids and 0.93g biomass were weighed respectively and then mixed together to achieve a total of 0.45 g carbon and 1g water in the feed. From Table 3.3, it can be seen that the biomass feedstock and co-mingled feedstock have the same amount of water, carbon, solids loading except for the ash content.

3.2.2 Experimental procedure

Lab scale experiments of steam hydrogasification were carried out in the inverted batch reactor. A schematic diagram of the experimental setup for steam hydrogasification of biomass feedstock and co-mingled feedstock is shown in Figure 3.2. The experimental conditions for biomass feedstock and co-mingled feedstock are listed in Table 3.4.

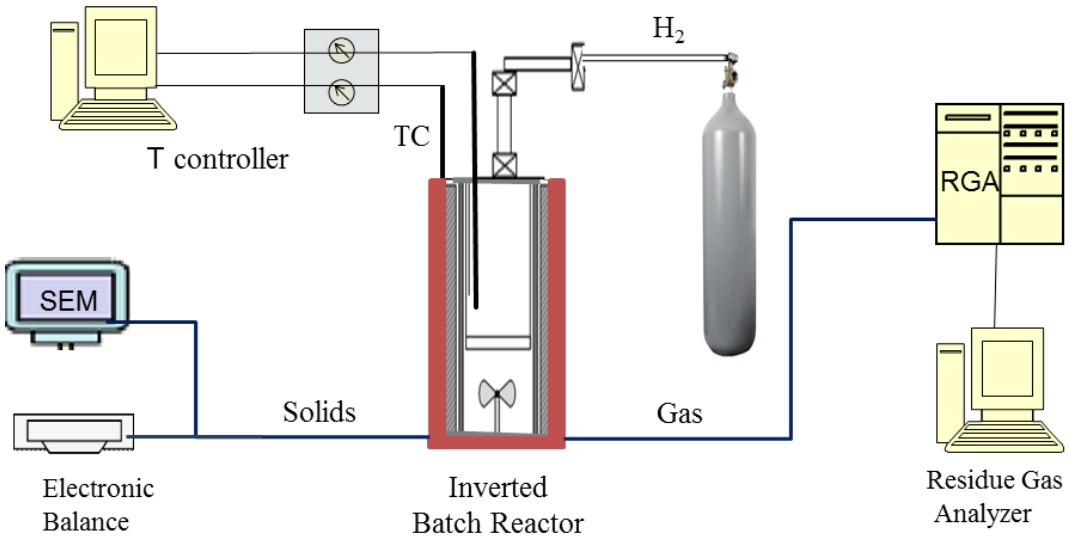

Figure 3.2 A schematic diagram of an experimental setup

Table 3.4 Experimental conditions for steam hydrogasification of biomass feedstock and co-mingled biosolids with biomass feedstock

Parameters	Biomass Feedstock	Co-mingled Feedstock
Feed materials	pinewood+H_2O	pinewood+biosolids
H_2O/carbon mole ratio	1.5:1	1.5:1
Biosolids loading (wt %)	0	50
Temperature (℃)	700	700
H_2 pressure (psi)	270	270

Steam hydrogasification of co-mingled feedstock were performed under the same conditions as those for biomass feedstock. For each test, the feedstock was loaded into the reactor only after the temperature in the reactor was reached 700℃. Each test took at least 30 minutes until no more product gases were released in the steam gasification. The char yield was measured directly by weighing the quartz tube before and after each test. And gaseous products were analyzed in a real-time using RGA to determine the gas evolutions.

3.2.3 Analysis methods

In this study, the steam hydrogasification performances are evaluated including carbon conversion efficiency and the rates of energetic product gas CH_4 and CO formation. The carbon conversion is determined based on the weight of chars that is described in section 2.2.3. The rates of product gas are determined based on a first-order kinetic model. It is proven that this kinetic model is fit for analysis of kinetics in the steam hydrogasification. Hence, the kinetic rate expression for CH_4 and CO formation can be described as follows:

$$\ln \frac{m_0}{m_0 - m} = kt$$

Where, m is moles of a gas species generated at a given time t; m_0 is the total moles of a gas species generated in the gasification process; k is the rate constant of gas formation. A plot of the left side of equation versus time should yield a straight line with the slope for k.

Scanning Electron Microscopy (SEM) is used to analyze surface morphology and Energy Dispersive X-ray Spectroscopy (EDS) is used for the elemental analysis and chemical characteristics of a char sample after the steam hydrogasification. An EDS equipped with a XL30-FEG SEM is utilized in this study to investigate the representative char samples with and without biosolids. The chars with biosolids were collected from co-mingled feedstock and the chars without biosolids were obtained from biomass feedstock after the steam hydrogasification.

3.3 Results and Discussion

3.3.1 Effect of biosolids on reaction rates

Steam hydrogasification of co-mingled biosolids with biomass as the feedstock were carried out at 700℃ with a H_2O/C mole ratio 1.5:1.The steam hydrogasification of biomass feedstock were performed under the same reaction conditions as blank tests in this study. A comparison can allow the assessment of biosolids influence on the steam hydrogasification.

A kinetic study of steam hydrogasification was discussed in the previous section 2.3.3. The experimental results provide an evident support for the first-order kinetic model based on the rate of gas formation. According to the previous study, it assumes that the global reaction kinetics is controlled mainly by the chemical reactions and the internal mass and heater transfer limitation can be negligible. CO_2 is released fast in the gasification process, yielding a high formation rate compared with the energetic product gases CH_4 and CO. Hence, the reaction rates in the steam hydrogasification are governed by the rates of CH_4 and CO formation.

Verification of kinetic plots for CH_4 formation using biomass feedstock and co-mingled feedstock are shown in Figure 3.3. It can be seen that the $\ln(m_0/(m_0-m)$ versus time yielded a straight line with correlation coefficients of up to 0.99 for least squares analysis. It is proven that the experimental data was good fit to the first-order kinetic rate. Moreover, it is found that the slope of the straight line for co-mingled feedstock is higher than that for biomass feedstock. The value of the slope stands for the specific reaction rate. It means that co-mingled feedstock has a higher rate of CH_4 formation compared to

the biomass feedstock. Plots of CO formation in Figure 3.4 show the similar results as that observed in Figure 3.3.

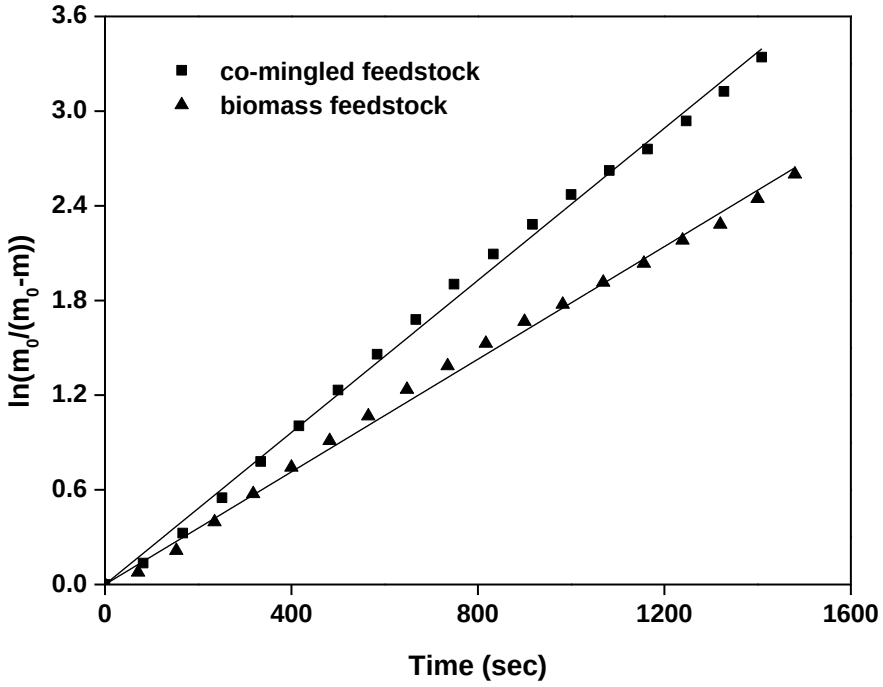

Figure 3.3 Kinetic plots for CH_4 formation using co-mingled feedstock and biomass feedstock. The solids lines are least squares analysis results.

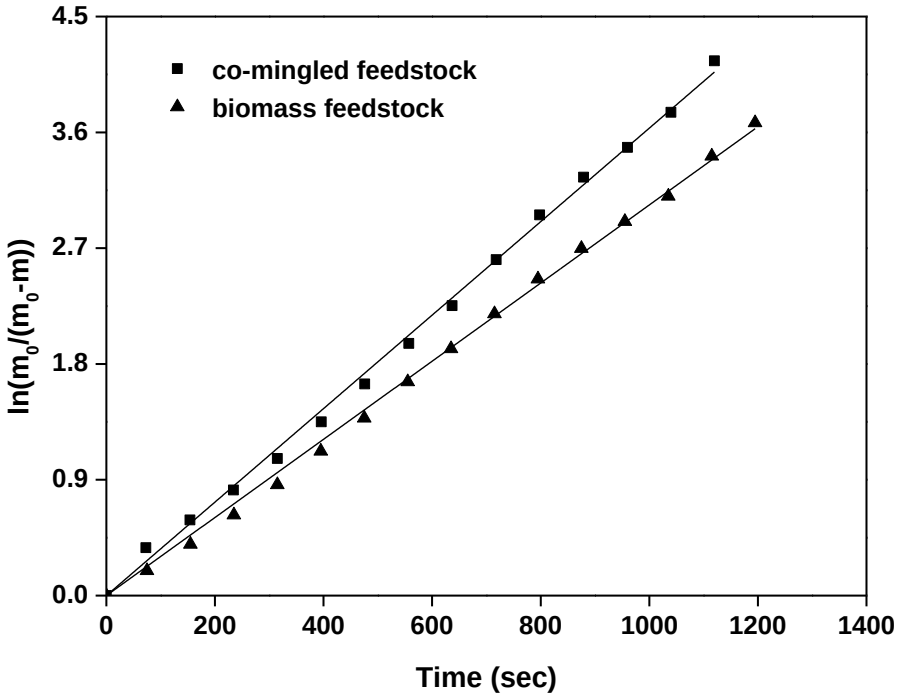

Figure 3.4 Kinetic plots for CO formation using co-mingled feedstock and biomass feedstock. The solids lines are least squares analysis results.

The rates of CH_4 and CO formation were obtained from the slopes in kinetic plots. The experiments were repeated at least four times to obtain an average value and error bars. The results are presented in Figure 3.5. It is found that the steam hydrogasification with 50wt% biosolids in the feed had a higher rate of CH_4 formation than that with no biosolids. An increased rate of CO formation was also observed when using co-mingled feedstock with biosolids. The biosolids loading in the feed promoted the reaction rate of CH_4 and CO formation. As previous discussion, the steam gasification rate is controlled based on the rate of product gas CH_4 and CO formation. Hence, it is referred that the

biosolids integrated in the feed resulted in a positive influence on the reaction rate in the steam hydrogasification.

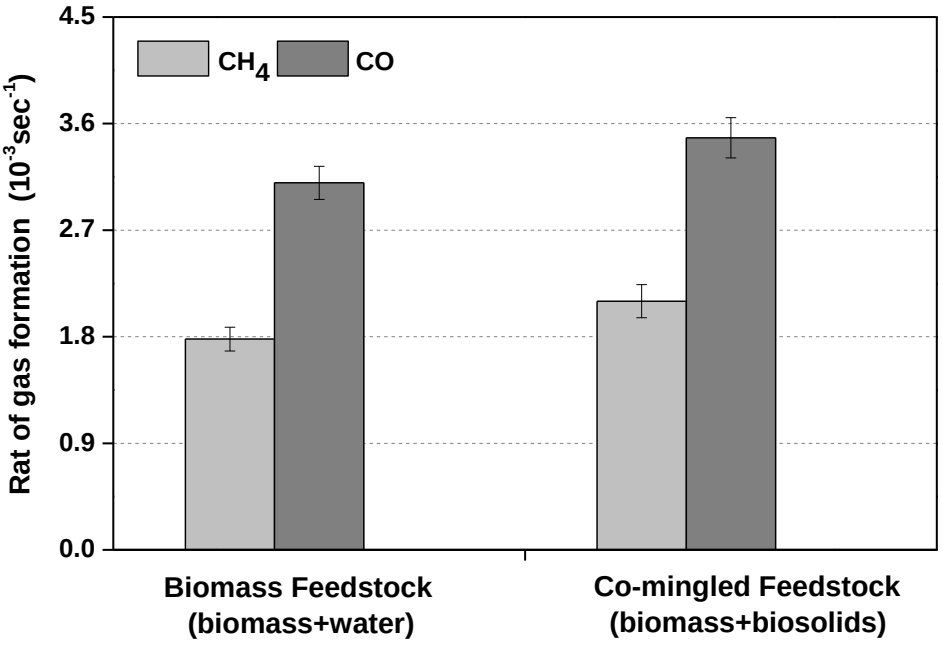

Figure 3.5 Effect of biosolids on the rates of CH_4 and CO formation in the steam hydrogasification of biomass at 700℃

3.3.2 Effect of biosolids on the carbon conversion

Figure 3.6 shows the effect of biosolids on carbon conversion in the steam hydrogasification. More than 70% conversion efficiency was achieved in the steam hydrogasification of co-mingled feedstock of biomass and biosolids, which was a 6% higher conversion than using only biomass feedstock. It is found that the biosolids integrated in the biomass feedstock led to an increase of carbon conversion.

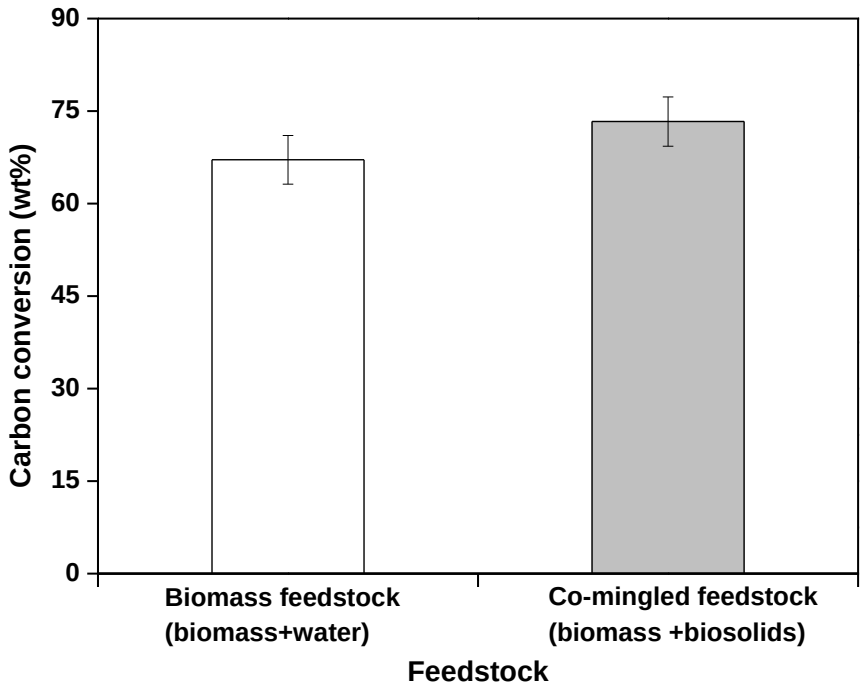

Figure 3.6 Effect of biosolids on carbon conversion in the steam hydrogasification of biomass at 700℃

For a comparison, the results from steam hydrogasification of co-mingled feedstock and biomass feedstock are presented in Table 3.5. The carbon conversion was increased from 67% to 73% when the biosolids was loaded by 50wt% in the feed. In addition, the co-mingled feedstock with 50wt% biosolids yielded an approximate 18% increase in the rate of CH_4 formation and a 12% increase in the rate of CO formation. These results demonstrated that the utilization of biosolids in the steam hydrogasification not only could enhance the gasification rate but also could improve the carbon conversion efficiency.

Table 3.5 Experimental comparison of biomass feedstock and co-mingled feedstock

	Biomass Feedstock[b]	Co-mingled Feedstock[b]
Biosolids loading (wt%)	0%	50%
H_2O/carbon mole ratio	1.5:1	1.5:1
Temperature (℃)	700	700
CH_4 formation k [a] ($10^{-3}sec^{-1}$)	1.78 +/- 0.14	2.10 +/- 0.15
CO formation k [a] ($10^{-3}sec^{-1}$)	3.10 +/- 0.19	3.48 +/- 0.18
Carbon conversion [a] (wt %)	67.1 +/- 3.95	73.3+/- 3.99

a. Data (+/-) represents 95% confidence intervals.

b. Differences are statistically significant.

From Table 3.3, it is seen that the only difference from biomass feedstock and co-mingled feedstock is the ash content in the feed. The biosolids contain higher ash content than woody biomass. That results in the more ash in the co-mingled feedstock. From the

ash analysis in Table 3.2, it is found that biosolids contains high concentrations of metal species, especially in potentially catalytic metal elements such as Fe, Ca, Mg, K, Na. The iron compounds, alkali salts and alkaline earth oxides have been extensively used as the gasification catalysts [68, 69]. It is considered that the enhanced conversion and rate may be the result of a catalytic effect caused by the metal species in the biosolids. Some researchers [98-100] found the biosolids had influence on the gas fuel composition in the pyrolysis/gasification and suggested that the improved results were as the consequences of catalytic actions from the inorganic matters in the biosolids. Saw W. et al. [101] studied the influence of biosolids blended in wood pellets on the steam gasification in a fluidized bed gasifier and found that biosolids had a significant influence on the syngas composition. The presence of Fe, Ca and other alkali metal K and Na in the biosolids ash were considered to contribute to the catalytic effect in this literature [99]. Manya J.J. et al. [100] investigated air gasification of dried biosolids and suggested that the reduction of tars was due to the catalytic effect of ash in the biosolids. However, more evidences are needed to confirm the catalytic effect of biosolids and to suggest that ash-rich biosolids could serve as an in-situ catalyst. In the following studies, the catalytic steam hydrogasification using different catalysts will be performed to investigate the effect of different catalytic additives on steam hydrogasification such as compounds of iron, alkali or alkaline earth metals.

3.3.3 Characterization of co-mingled chars

The experimental results found that the co-mingled feedstock improved steam hydrogasification efficiency. The ICP-AES analysis shows that biosoloids samples contain high concentrations in metals of Fe, Ca, Ka, Na and Mg. It is expected to find the evident differences between the feedstock with and without biosolids. Therefore, scanning electron microscopy (SEM) and energy dispersive X-ray spectrometry (EDS) are used in this study to characterize the physical morphology and determine the elemental compositions of co-mingled chars and biomass chars without biosolids.

Figures 3.8 and 3.9 show the SEM images of chars from biomass feedstock and co-mingled feedstock after the steam hydrogasification. It is observed from Figure 3.8 that biomass chars had melting morphology with smooth surface. As expected, the SEM results were consistent with that in the previous study (seen in 2.3.1). SEM images in Figure 3.9 show surface morphology of the co-mingled chars. It is clearly observed that co-mingled chars presented inter-mixing of biomass and biosolids residue. The melting structures with smooth surface were from biomass chars while the micro particles with rough morphology were residues from biosolids. It can be seen that the biosolids residues are highly dispersed within the surface of biomass chars. This co-structure observed in biomass-biosolids char has a similar formation with the structure of catalytic active sites and the solid phases [102]. Hence, the morphological analysis of biomass-biosolids chars indicates that biosolids residue could serve as active sites on woody biomass for catalytic performances.

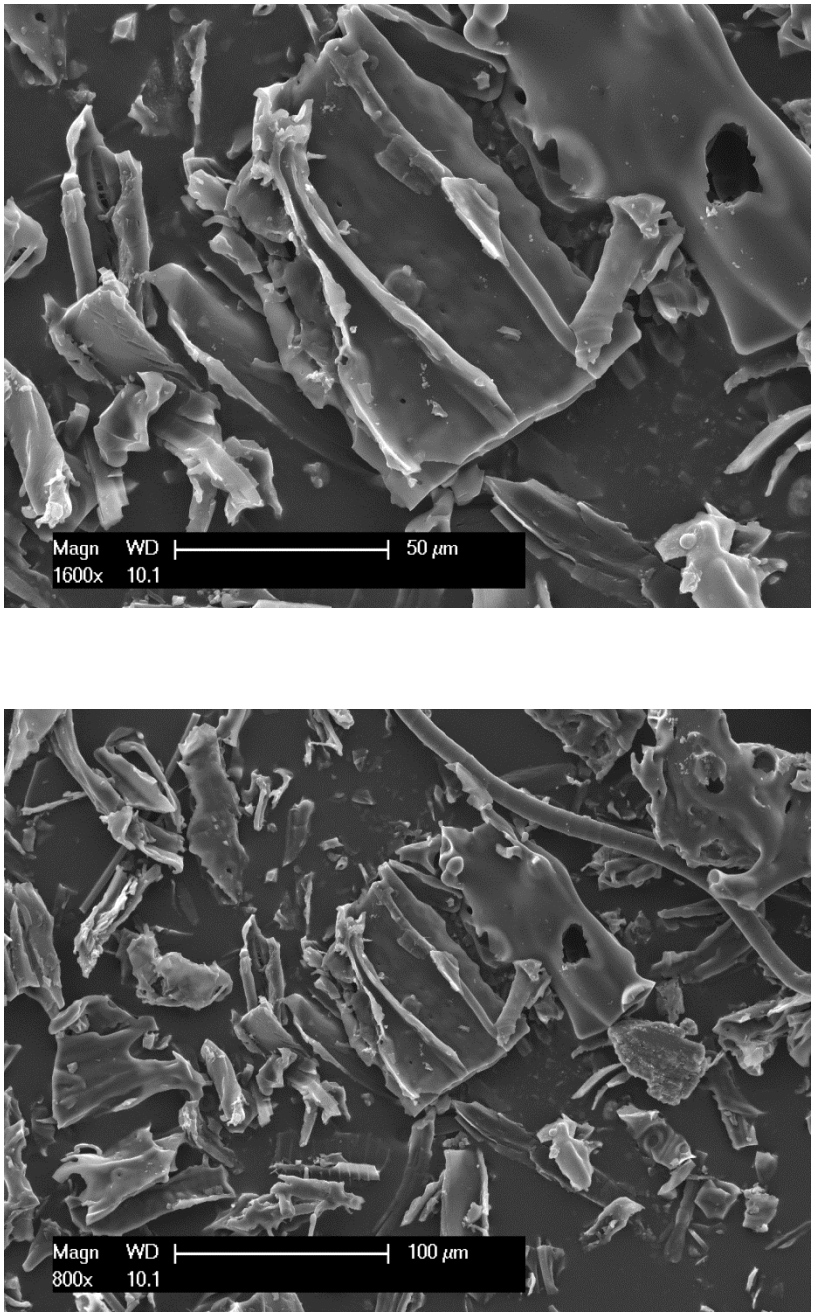

Figure 3.7 SEM images of chars from the biomass feedstock

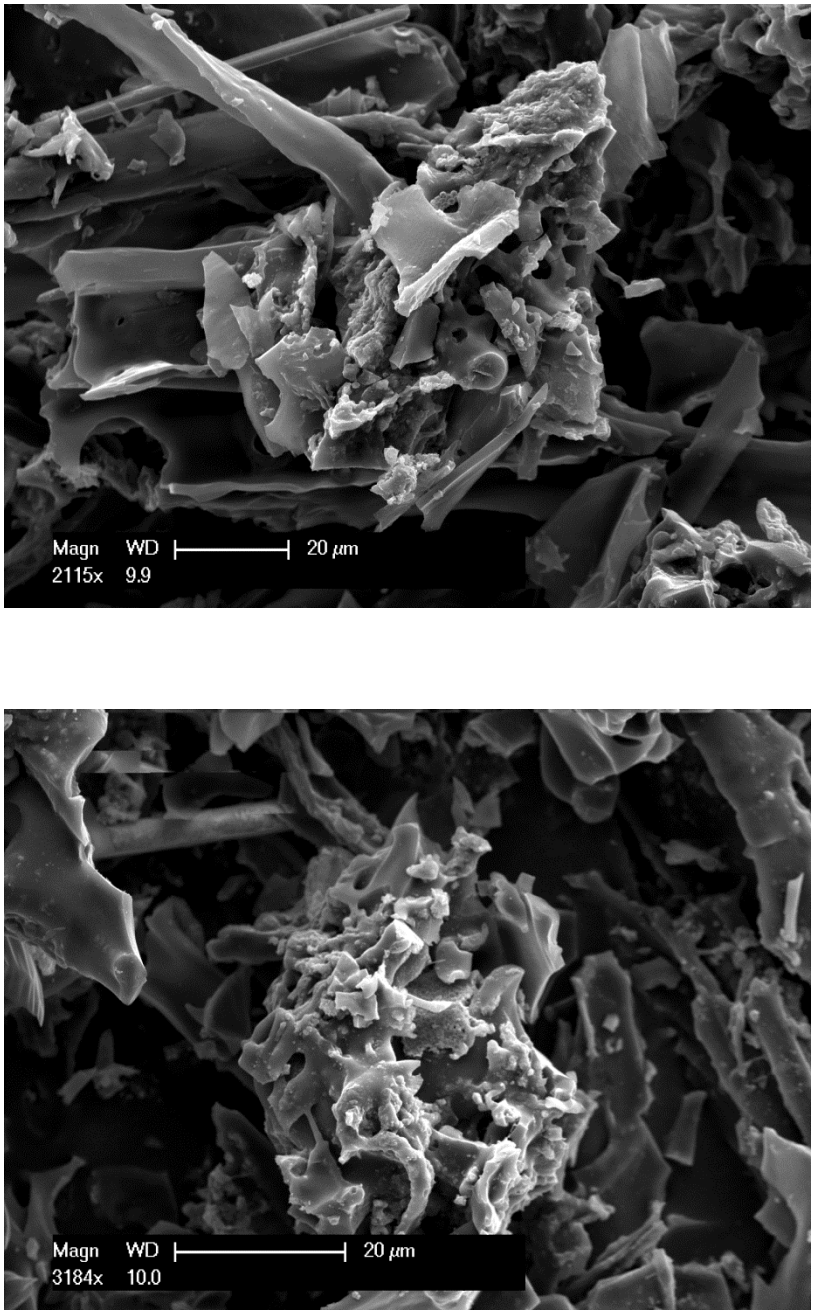

Figure 3.8 SEM images of chars from the co-mingled feedstock

SEM-EDS analysis is widely used to detect elemental compositions in microstructure areas. Results of energy-dispersive X-rays EDS can be visualized to provide elemental composition information.

The spectra analysis of biomass chars and co-mingled chars are shown in Figures 3.9 (a) and (b). The relatively weak signal intensities in the X-ray spectra indicate much lower concentrations of these elements in the particles. The EDS results reveal a large difference in chemical compositions between the chars with and without biosolids. Biomass char is elementally composed of a strong concentration of carbon, with lighter amount of oxygen. The char with biosolids is elementally composed of a high concentration of carbon, with lower level of oxygen and lower amount of inorganic elements of P, Na, Al, Si, P, K, Mg, Ca and Fe. The detected inorganic elements are originally from the biosolids. The ICP-AES analysis in Figure 3.2 shows that iron and calcium have the top two highest concentrations in biosolids ash. The quantitative data in EDS is consistent with the elemental compositions determined by ICP-AES. SEM-EDS analysis found a fact that the chars with biosolids were rich in Ca, Fe, Na and K. These results provided a good evidence for the presence of potentially catalytic substances in the steam hydrogasification due to the use of biosolids in the feed. It is referred that the effect of biosolids on the steam hydrogasification efficiency may be the consequences of catalytic effect of the metal species in the biosolids.

(a)

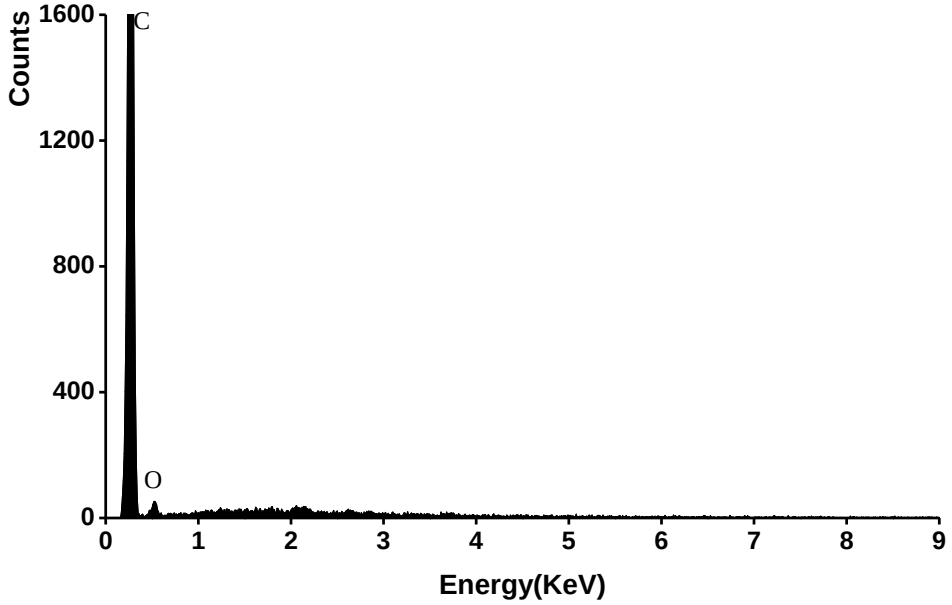

(b)

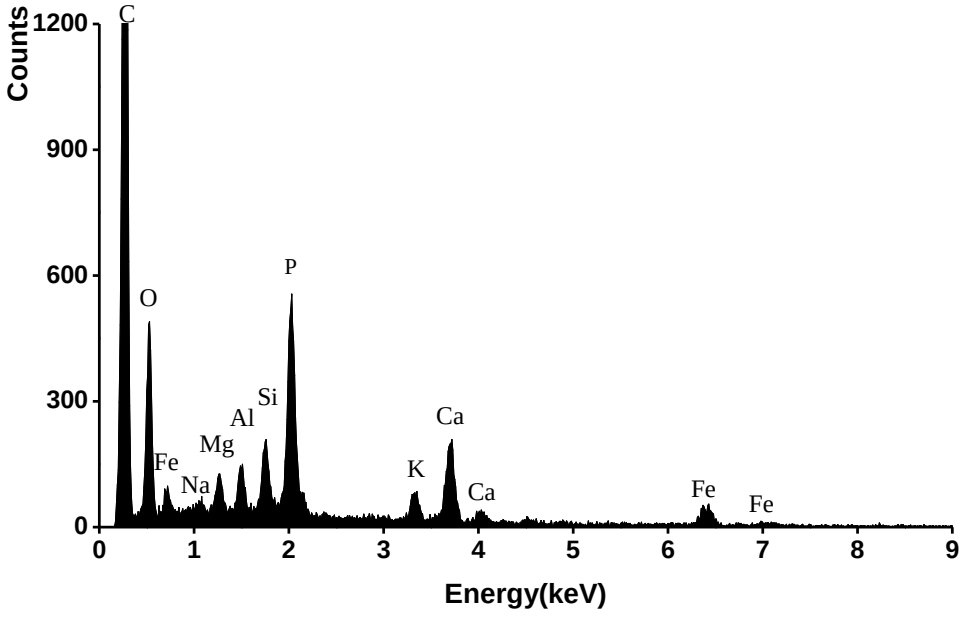

Figure 3.9 SEM-EDS of chars

(a) chars from biomass feedstock (b) chars from co-mingled feedstock

3.4 Conclusion

Steam hydrogasification of co-mingled biosolids and biomass as the feedstock were investigated in the inverted stirred batch reactor at 700℃ with a H_2O/C mole ratio 1.5:1. Steam hydrogasification of biomass were also carried out under the same conditions for a comparison. The effect of biosolids on steam hydrogasification was experimentally examined including reaction rate and carbon conversion. ICP-AES and SEM-EDS techniques were used to analyze the elemental compositions and char structures of co-mingled feedstock. The results are concluded as follows.

1. Co-utilization of biomass and biosolids as co-mingled feedstock yielded more than 70% carbon conversion under the appreciated reaction conditions. More than 90% water content in the biosolids is directly utilized as the source of steam instead of adding external water in the steam hydrogasification. Biosolids loading in the feed is depended on a desired H_2O/C ratio. It is experimentally demonstrated that steam hydrogasification has an important advantage on biosolids energy recovery by directly utilizing the raw biosolids which eliminates the cost on biosolids dewatering and drying. Steam hydrogasification provides an alternative for biosolids beneficial use in a potentially cost-efficient manner.
2. A comparison of the experimental results between the biomass feedstock and co-mingled feedstock was very impressive. It is found that biosolids in the co-mingled feedstock contributed to improve the steam hydrogasification efficiency. There was nearly 6% increase in the carbon conversion when the biosolids was loaded to 50wt% in the feed. The use of biosolids led to an increase in the rates of

CH_4 and CO formation. It is found that biosolids had significantly positive influence on the steam hydrogasification.

3. The ICP-AES analysis found that the biosolids samples had high contents in metal elements, in particular of iron (Fe) and calcium (Ca). The SEM micrographs of co-mingled chars showed that biosolids residues were highly dispersed on the surface of biomass chars. The structure of biosolids residue presented in SEM is considered to serve as activation sites on the surface of chars. A distinguish in the elemental compositions of chars with and without biosolids were found. As determined by EDS, the Na, Al, K, Mg, Ca and Fe were detected in the chars with biosolids while none of them were presented in the biomass chars without biosolids. The results revealed that co-mingled chars with the biosolids were rich in metal species including Fe, Ca, Na, K and Mg. And it is indicated that the improved efficiency may be attributed to the catalytic effect of biosolids on the steam hydrogasification due to the presence of iron, calcium compounds and other alkali metals Na, K in the biosolids.

In summary, the utilization of biosolids in the feedstock promoted the steam hydrogasification in carbon conversion and reaction rates. There was significant evidence in elemental compositions of chars to suggest that biosolids could serve as in-situ gasification catalyst due to the presence of metals Fe, Ca and other alkali metals. However, more evidences are needed to confirm the catalytic effect of biosolids. It is important to investigate the effect of catalytic materials on the steam hydrogasification which are Fe, Ca, Mg, Na and K based catalysts.

Chapter 4

Catalytic Steam Hydrogasification of Biomass with Catalysts

This chapter investigates catalytic steam hydrogasification of biomass using different catalysts to identify the catalytic activity of biosolids. It will contribute to understand the catalytic effect of biosolids on the steam hydrogasification. The tested catalysts in this study include alkali metal salts, mineral dolomite and transition metal iron. These catalysts are added to the biomass feedstock by physical mixing method. Series of experiments with the added catalysts were carried out under the same conditions as those in chapter three. Catalytic effects of the tested catalysts were evaluated and the catalytic activity was determined. A comparison of steam hydrogasification of biomass with non-catalysts, in-situ biosolids and the added catalysts were discussed in this chapter to verify the catalytic activity of biosolids as an effective, in-situ catalyst.

4.1 Introduction

4.1.1 Selection of catalytic materials

As introduced in the section 1.3, the catalysts for gasification can be generally classified into alkali metal salts, alkaline earth metal oxides and salts, minerals, transition metal based catalysts such as iron and nickel. Catalysts have been widely used in gasification of biomass or coal to improve quality of syngas and reduce tar formation. Although there have been extensive researches on catalytic gasification with agents of CO_2, steam or air, no research has been done on the catalytic steam hydrogasification. Therefore, this study aims to investigate the catalytic effect of catalysts on the steam hydrogasification by using different metal-based catalytic compounds. Selection of appropriate catalysts is the initial task before experimental tests. Alkali (K and Na), alkaline earth (Ca and Mg), and transition metal Fe are most commonly used catalysts and widely reported in the literature [67-69]. Furthermore, they are the major metal elements contained in the biosolids. The selection of tested catalysts in this study is based on the metals of K, Na, Ca, Mg and Fe.

Iron catalysts

Iron-based catalysts are nontoxic, cheaper and easy to prepare than other transition metal catalysts such as Ni, Rh. Single Fe(III) salts $FeCl_3$, $Fe_2(SO_4)_3$ and $Fe(NO_3)_3$ as iron catalyst precursor and iron oxides as additives in gasification are listed in Table 4.1. $FeCl_3$ is almost inactive to catalyze the gasification while conversion of $FeCl_3$ to Cl^- free can make active iron dispersed on the feedstock for iron-catalyzed gasification. Some researchers used the $FeCl_3$ solution as precursor salts to prepare

chlorine-free iron catalyst by using $Ca(OH)_2$ or NH_3 [103, 104]. However, the presence of chloride and sulfate not only causes serious corrosion during the gasification but also produces contamination needed for gas cleaning [105]. And also $FeCl_3$ and $Fe_2(SO_4)_3$ showed ineffective in hydrogasification [106]. It was found that $Fe(NO_3)_3$ had high catalytic activities on the gasification with gasifying agents such as steam, H_2 or air and CO_2[107-109]. Therefore, $Fe(NO_3)_3$ is selected as tested catalyst in the steam hydrogasification system because of its Cl^{-1} and S^{-1} free and high reactivity. In addition, iron oxides such as Fe_2O_3 and Fe_3O_4 have been demonstrated to be effective for reduction of C_2-C_3 emission in steam gasification of woody biomass [110, 111]. In this study, Fe_2O_3 is selected as a tested catalyst of iron oxides considering its activity in the presence of hydrogen and steam.

Table 4.1 Selection of Fe (III) salts and oxides as tested catalysts (Y- sample tested; N- no sample tested)

$FeCl_3$	$Fe_2(SO_4)_3$	$Fe(NO_3)_3$	Fe_2O_3	Fe_3O_4
N	N	Y	Y	N

Alkali metal salts

Alkali metal salts are well-known catalysts on the gasification. Among the alkali metals, Na and K metal salts are investigated in this study not only because they are cheaper than Li and Cs salts but also because Na and K are major metal elements in the biosolids. Single Na and K salts are listed in Table 4.2. Alkali metal chlorides are found

to be ineffective or less effective compared to the carbonates, sulfates and nitrates [112-114]. Among these salts, carbonates (K_2CO_3, Na_2CO_3) are the most common, high activity catalysts that can be added to biomass by dry mixing or wet impregnation in the steam gasification of biomass. It is found that the carbon conversion to gas products was increased using alkali carbonate catalysts due to the reduction of tars [115-117]. And the order of catalytic activities is $K_2CO_3 > Na_2CO_3$. In addition, binary eutectic catalyst of Na_2CO_3-K_2CO_3 was found to increase the gasification rate in the presence of hydrogen [118]. Therefore, Na_2CO_3 and K_2CO_3 salts are selected as tested catalysts for the steam hydrogasification due to high activity in the presence of steam and H_2.

Table 4.2 Selection of Na and K salts as tested catalysts (Y- sample tested; N-no sample tested)

	CO_3^{2-}	NO_3^-	SO_4^{2-}	Cl^-
Na^+	Y	N	N	N
K^+	Y	N	N	N

Alkaline earth metal catalysts

Alkaline earth metal catalysts include CaO, MgO or $CaCO_3$ and $MgCO_3$. In the gasification process, alkaline earth metal carbonates are transferred to the active form in alkaline earth metal oxide. Hence, their metal oxides have higher activity than their metal carbonates. Dolomite, a calcium magnesium ore with the general chemical formula $Ca{\cdot}Mg(CO_3)_2$, is a most common catalyst in biomass gasification [119, 120]. The advantages of these natural occurring catalysts are relatively inexpensive and abundant.

However, dolomites in their naturally occurring form are not nearly active as catalysts until they are calcined. The calcined dolomite is an attractive primary catalyst as bed material in the fluidized beds since it is highly effective to reduce the tar content in the product gas from a gasifier. Calcined dolomite contains alkaline earth metal oxides (CaO and MgO). The chemical name and formula of calcined dolomite is calcium magnesium oxide (CaO·MgO). In this study, calcined dolomite is investigated in the steam hydrogasification of biomass as a tested catalyst.

4.1.2 Catalyst loading methods

Two methods are applied for addition of catalysts to biomass in the gasification process. One method is dry mixing method also called physical mixing and the other method is wet impregnation method. Dry mixing is to directly add the catalyst material to biomass by physical mixture. This method is widely used for the catalysts as additives in a gasifier. For example, natural occurring minerals such as limestone, dolomite, iron ores can be mixed with the biomass as a primary catalyst as well as bed materials in the fluidized beds [67, 108]. In addition, it is available for alkali salts such as K_2CO_3, Na_2CO_3 [120]. In contrast, wet impregnation is multi-step method for catalyst preparation compared to dry mixing. A general wet impregnation process is described in brief as follows. Some amount of a catalyst precursor salt is dissolved in the distilled water or methanol and then the solution is added to biomass based on a catalyst loading. The wet mixture is agitated and the suspension is subject to evaporation for removal of water or methanol. After that, the impregnated biomass with the catalyst is dried at 105^{o}C for 24h

before use. It is widely used for catalysts supported by material Al_2O_3 such as Ni-based catalysts. And it is the most common method for catalyst preparations with the precursor salts, such as iron salts and alkali metal salts. Some researcher found that catalyst impregnation techniques improved catalyst dispersion on the feedstock [106, 108, 120]. $Fe(NO_3)_3$, K_2CO_3 and Na_2CO_3 can be either impregnated or dry mixed with the biomass.

All the tested catalysts in this study are able to be physical mixing with the biomass feedstock. Therefore, the physical mixing of catalyst with the biomass feedstock is chosen as catalyst addition method for all the tested catalysts due to its availability and simplicity. Importantly, the method can be compared with the physical mixture method of co-mingled feedstock.

4.2 Experimental Sections

4.2.1 Materials

Feedstock materials The biomass feedstock used in this study is pinewood sawdust. The samples were dried at 105℃ for 2 hours and sieved to a particle size of 150-180um. The composition analysis of pinewood is presented in Table 2.3.

Catalyst materials The five catalysts to be tested in the steam hydrogasification of biomass are $Fe(NO_3)_3$, Fe_2O_3, Na_2CO_3, K_2CO_3 and calcined dolomite ($CaO{\cdot}MgO$).

Fe_2O_3 (CAS number 1309-37-1) is purchased from Alfa Aesar Reagent Company. The chemical name is Iron (III) oxide and purity is 99.998% (metals basis).

$Fe(NO_3)_3{\cdot}9H_2O$ is used for Fe(III) nitrates. The chemical name of $Fe(NO_3)_3{\cdot}9H_2O$ (CAS number 7782-61-8) is ferric nitrate nonahydrate. This reagent (assay ≥98% purity) is purchased from Sigma Aldrich Corporation.

The alkali metal salts Na_2CO_3 and K_2CO_3 purchased from Sigma Aldrich Chemical Company are analytical reagent grade (≥99.9%)

Calcined dolomite samples used in this study are purchased from Chemical Lime Corporation (Fort Worth, TX). The chemical name and formula for calcined dolomite is calcium magnesium oxide ($CaO{\cdot}MgO$). Calcined dolomite samples are grounded and sieved to the particle size 75-120um before experimental tests. The chemical compositions of calcined dolomite are identified by inductively coupled plasma emission spectroscopy (ICP-ES). The oxide compositions of the calcined dolomite sample are presented in Table 4.3. And X-ray Diffraction (XRD) pattern of calcined dolomite sample is shown in Figure 4.1.

Table 4.3 Chemical compositions of calcined dolomite sample *(wt%)*

Catalyst	CaO	MgO	SiO_2	Fe_2O_3	Al_2O_3
Calcined dolomite	56%	43%	0.53%	0.34%	0.13%

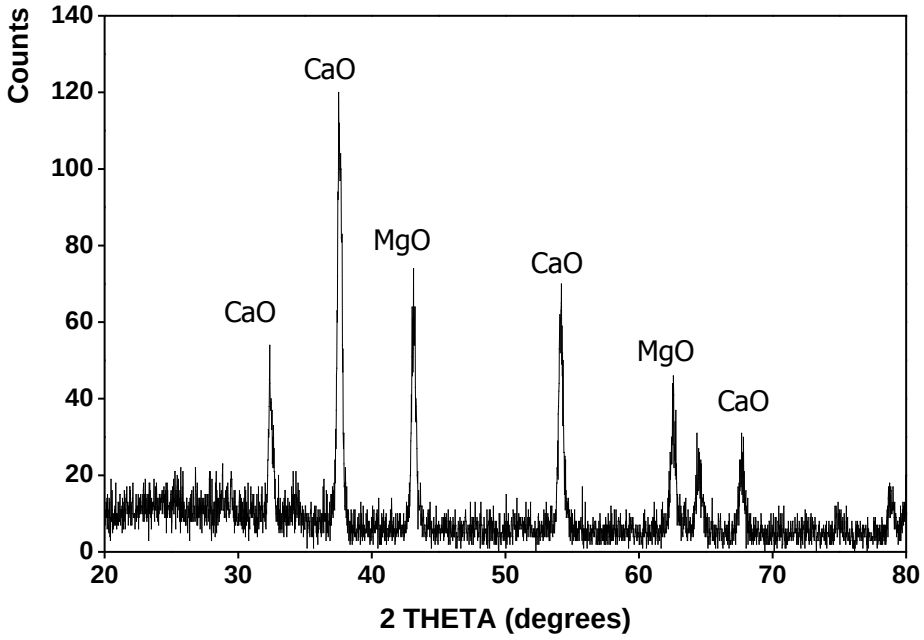

Figure 4.1 X-ray diffraction patterns for calcined dolomite sample

4.2.2 Addition of catalysts

Physical mixing method is used for preparation the mixture sample of biomass added with catalyst as follows. The prepared mixture sample is added with 1.0g amount of distilled water to achieve a biomass to H_2O ratio 1:1(g/g).

Preparation of Fe_2O_3 and biomass mixture

The catalyst Fe_2O_3 loading (wt%) is defined as the mass of metal Fe in the catalyst per mass of biomass. Fe (III) oxide contains 69.9 wt% Fe. To obtain a 7 wt% Fe loading on 1g of biomass, 0.1g amount of Fe_2O_3 was weighed. To prepare biomass mixed with Fe_2O_3 catalyst, the weighed Fe_2O_3 fine powder was added to 1.0g biomass manually in a flask. And the mixture was then stirred physically for a sufficient time in order to obtain a better homogeneity of the mixture sample. Finally, 1.0 g of distilled water was added to the prepared Fe_2O_3 and biomass mixture ready for the experimental test.

Preparation of $Fe(NO_3)_3$ and biomass mixture

The reagent $Fe(NO_3)_3 \cdot 9H_2O$ was firstly prepared for fine powder by grounding in a agate mortar. The ferric nitrate compound $Fe(NO_3)_3 \cdot 9H_2O$ contains 13.8 wt% Fe. To obtain approximate 6 wt% Fe loading of 1g of biomass, 0.43g amount of $Fe(NO_3)_3 \cdot 9H_2O$ was weighed. The weighed $Fe(NO_3)_3 \cdot 9H_2O$ was added to 1.0 g biomass physically to yield a mixture sample. After the addition of catalyst to biomass, 0.17g H_2O had been contained in the mixture sample due to 40.1 wt% H_2O composition of $Fe(NO_3)_3 \cdot 9H_2O$. For that, less than 1.0 g water was added for the mixture to achieve biomass to H_2O mass ratio 1g/1g.

Preparation of Na_2CO_3 or K_2CO_3 and biomass mixture

The reagent Na_2CO_3 contains 43.4 wt% Na and the reagent K_2CO_3 contains 56.6 wt% K. To achieve 7% K and 7% Na loading of 1g of biomass, the weighed amount of K_2CO_3 and Na_2CO_3 are 0.1g and 0.16 g, respectively. The weighed K_2CO_3 or Na_2CO_3 was directly added to 1.0 g amount of biomass and then the mixture was stirred manually to obtain a good dispersion of the catalyst.

Preparation of calcined dolomite and biomass mixture

The calcined dolomite contains mainly CaO and MgO. The catalyst loading (%wt/wt) is defined as the mass of calcined dolomite per unit the mass of biomass. In this study, 0.1g amount of calcined dolomite was used to mix with 1.0 g of biomass by physical mixing. In this study, the calcined dolomite loading is 10 wt%.

4.2.3 Experimental procedure

The experimental conditions in this study are listed in Table 4.4. Five different substances based on metal of Fe, K, Na, Ca, Mg are examined as catalysts for steam hydrogasification of biomass. The prepared mixture samples (biomass + catalyst mixture) are performed in the steam hydrogasification under the same reaction conditions as those for SHR with non-catalysts. Steam hydrogasification with catalysts were carried out using the inverted batch reactor. The inverted batch reactor was described in the section 2.2 and experimental procedures were presented in the section 3.2. Only a brief description is given as follows.

For each test, 1.0g pinewood biomass with catalyst and 1.0g water was held in the feeder tube of the reactor and then fed into the reactor when the reactor reached the gasification temperature 700℃. The gas flow passed through the capillary line to be injected into RGA and the gas products were on-line analyzed using RGA.

Effect of catalysts on the steam hydrogasification is evaluated in the rates of CH_4 and CO formation. The catalytic activity of catalysts is determined based on their influence on the reaction rate.

Table 4.4 Experimental conditions for steam hydrogasification of biomass with catalysts

Run No.	Catalyst (%wt)	Temperature (℃)	Biomass/H_2O (g/g)	Pressure (psi)
1	None catalyst	700	1:1	270
2	+ $Fe(NO_3)_3$	700	1:1	270
3	+ Fe_2O_3	700	1:1	270
4	+ Na_2CO_3	700	1:1	270
5	+ K_2CO_3	700	1:1	270
6	+ calcined dolomite	700	1:1	270

4.3 Results and Discussion

4.3.1 Catalytic effect of catalysts

The catalytic compounds including iron compounds ($Fe(NO_3)_3$, Fe_2O_3), alkali carbonate salts (Na_2CO_3, K_2CO_3) and calcined dolomite ($CaO{\cdot}MgO$) were physically mixed with the biomass feedstock and tested in the steam hydrogasification at 700℃ with a H_2O to biomass mass ratio 1:1. The effects of different catalysts on the steam hydrogasification of biomass were examined.

The catalysts have influence on the reactivity of chars in the catalytic gasification process. A first-order kinetic model based on the rate of gas formation is employed for kinetic measurements in the steam hydrogasification. In this study, the kinetic rate expression for catalytic steam hydrogasification coincides with that for non-catalytic case but taking into account the presence of catalyst. After separation and integration with details in section 2.3.3, the catalytic kinetic equation [121] in a batch reactor can be expressed as

$$\ln \frac{m_0}{m_0 - m} = k_c t \qquad \text{Equation (4.1)}$$

Where, m is moles of a gas species generated at a given time;

m_0 is the total moles of a gas species generated in the gasification process;

k_c is the specific rate of a gas formation for a given catalyst. It is noted that k_c, different from k with non-catalyst, is corresponded to temperature, catalyst type and concentration.

From equation 4.1, there should be a linearity of its left side versus time. Value of k_c is obtained from the least squares analysis results. Figure 4.2 shows kinetic plots of for

CH_4 and CO formations in the steam hydrogasification with $Fe(NO_3)_3$. Linear fits are obtained for CH_4 formation and CO formation in case of $Fe(NO_3)_3$ catalyst. The experimental data fit to the first-order kinetic rate is very acceptable due to the correlation coefficients up to 0.99. Similar plots for Fe_2O_3, K_2CO_3, Na_2CO_3 and calcined dolomite catalysts are shown in Figures 4.2-4.6. All these plots with different catalysts support for the first-order kinetic rate in catalytic steam hydrogasification.

Values of k_c at different temperatures allow one to determine the activation energies of CH_4 and CO formation. It will be future work to obtain activation energies in catalytic steam hydrogasification. It is expected that the activation energies of catalyzed process with catalysts are less than those for non-catalytic process [121-123].

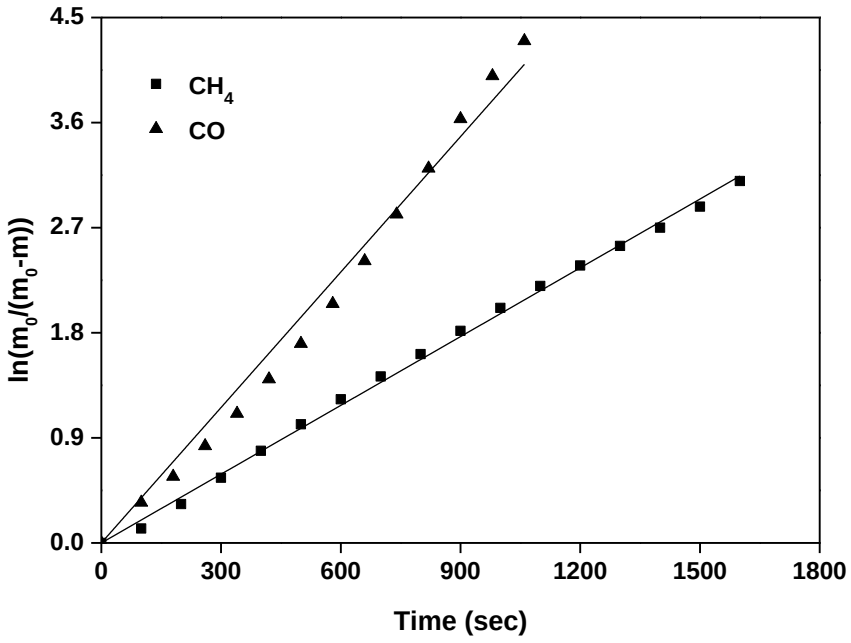

Figure 4.2 Kinetic plots of $ln(m_0/(m_0-m)$ versus time for CH_4 and CO formation with $Fe(NO_3)_3$catalyst. The solids lines are least squares analysis results.

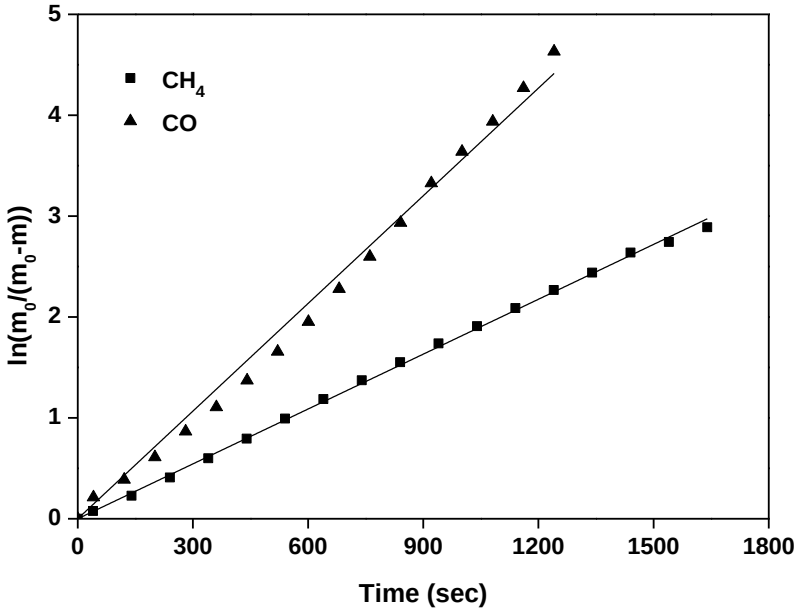

Figure 4.3 Kinetic plots of $ln(m_0/(m_0-m)$ versus time for CH_4 and CO formation with Fe_2O_3catalyst. The solids lines are least squares analysis results.

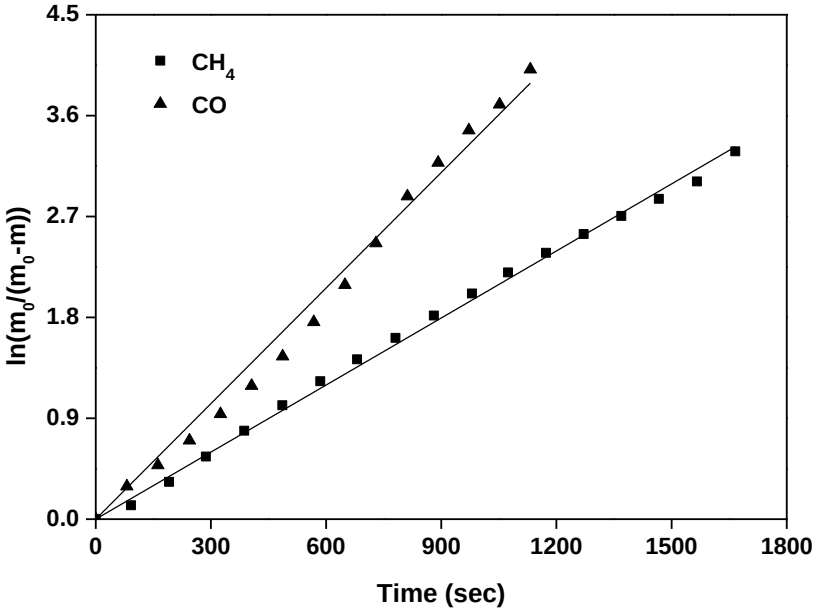

Figure 4.4 Kinetic plots of $ln(m_0/(m_0-m)$ versus time for CH_4 and CO formation with K_2CO_3 catalyst. The solids lines are least squares analysis results.

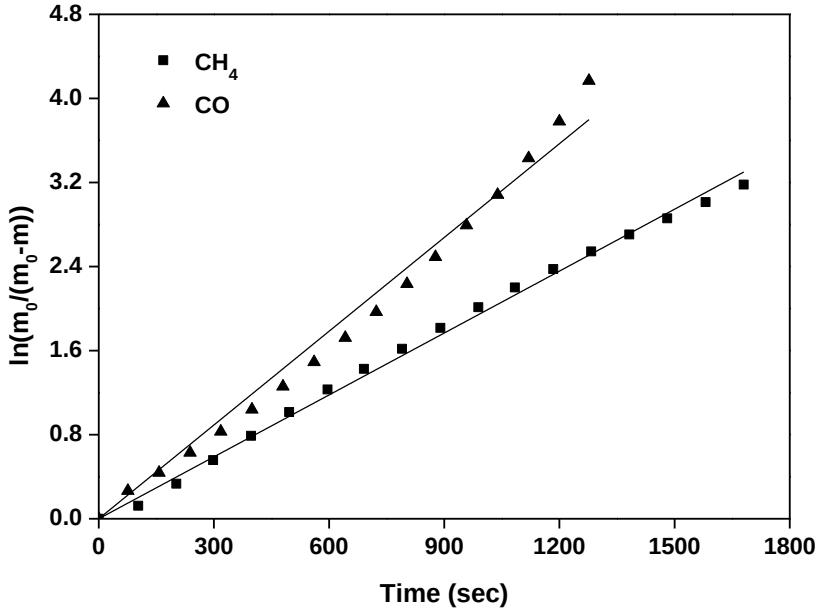

Figure 4.5 Kinetic plots of $ln(m_0/(m_0-m)$ versus time for CH_4 and CO formation with Na_2CO_3 catalyst. The solids lines are least squares analysis results.

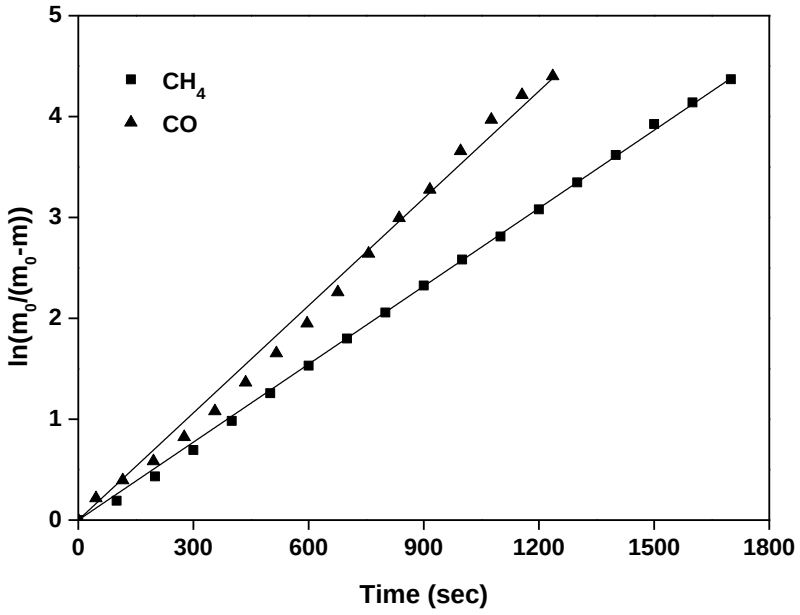

Figure 4.6 Kinetic plots of $ln(m_0/(m_0-m)$ versus time for CH_4 and CO formation with calcined dolomite. The solids lines are least squares analysis results.

According to the kinetic analysis, the specific rates of the CH_4 and CO formation for different catalysts were obtained. For a comparison, the steam hydrogasification of biomass with non-catalysts is also included. The experimental results are presented in Figures 4.7-4.8 and Table 4.5.

Figure 4.7 shows the rates of CH_4 formation in the steam hydrogasification of biomass without catalysts and with different added catalysts. Compared with un-catalytic steam hydrogasification, the added catalysts improved the reaction rate, respectively. Steam hydrogasification with calcined dolomite showed the highest rate of CH_4 formation among all the tested catalysts, yielding 45% higher rate than that of un-catalytic SHR. As observed, iron salt $Fe(NO_3)_3$ slightly increased the specific rate of CH_4 formation while the iron oxide Fe_2O_3 exerted no influence on that. As iron group catalysts, iron salt is more active than iron oxide. Both alkali salts K_2CO_3 and Na_2CO_3 led to a higher rate of CH_4 formation but K_2CO_3 is better than Na_2CO_3. From the comparable results in Table 4.5, it is demonstrated that calcined dolomite was the most effective catalyst to catalyze the steam hydrogasification for an increased rate of CH_4 formation. The results from the catalysts based on different metals also indicate that the catalytic effect followed the sequence of Ca-Mg > K > Na > Fe.

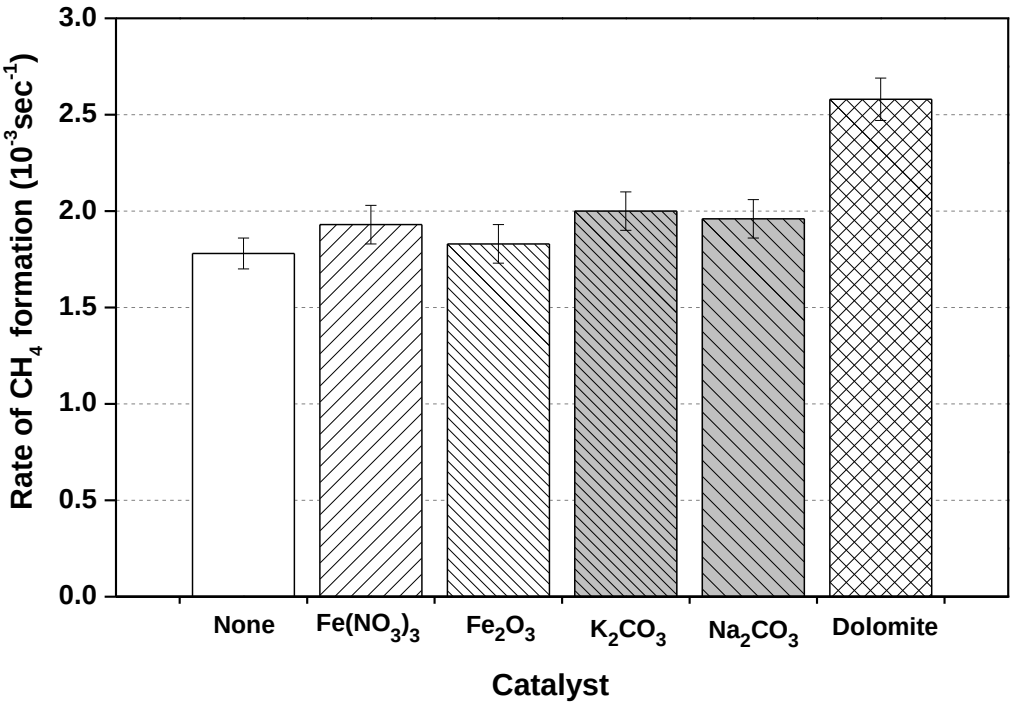

Figure 4.7 Effect of different catalysts on the rate of CH_4 formation

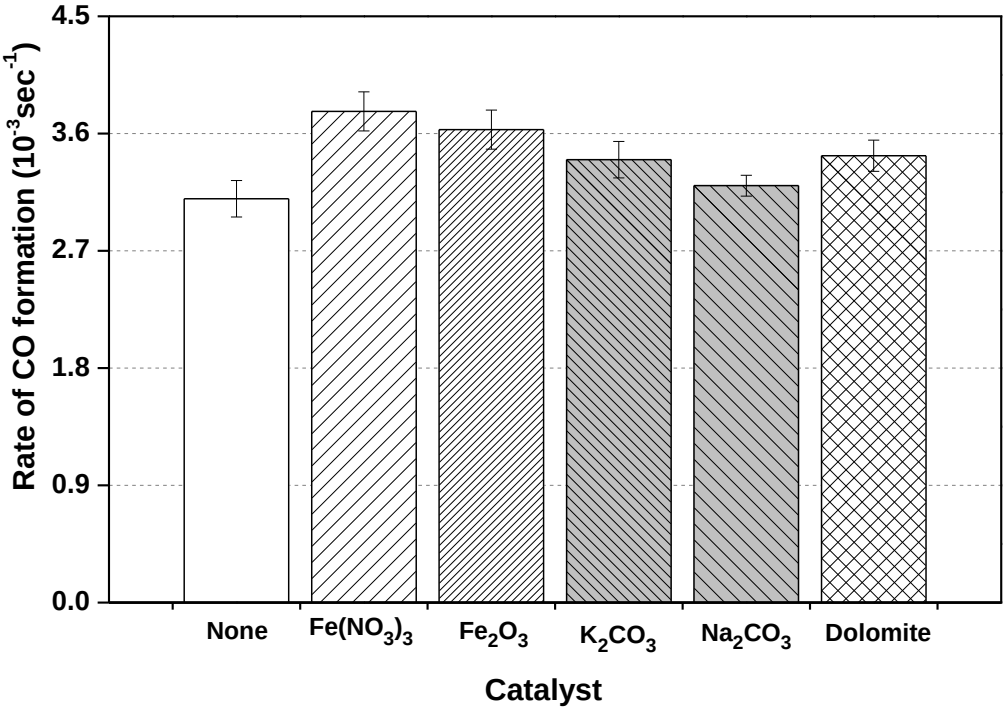

Figure 4.8 Effect of different catalysts on the rate of CO formation

Figure 4.8 shows a comparison of the rates of CO formation in the steam hydrogasification with various types of catalysts and without catalysts. It is found that iron catalysts had a strong influence on the CO formation rate and iron salt $Fe(NO_3)_3$ is more active than Fe_2O_3. Among all the tested catalysts, $Fe(NO_3)_3$ is highly active to catalyze the steam gasification, resulting in an approximate 22% higher rate of CO formation than that of un-catalytic SHR. The catalytic effect of alkali metal catalysts on CO formation is less than that of Fe(III) catalysts. For alkali metals, K_2CO_3 led to a higher rate of CO formation but Na_2CO_3 had little influence on that. The addition of calcined dolomite resulted in a similar catalytic effect with K_2CO_3 on the rate of CO

formation in the steam hydrogasification. The results in Figure 4.8 indicated that the metals of Fe, K, Ca and Mg are active for a catalytic effect on CO formation in the steam hydrogasification with the sequence of Fe > Ca-Mg > K. And it is also revealed that the iron catalysts were the most effective catalyst to catalyze the steam hydrogasification for an increase in the rate of CO formation.

Table 4.5 The rates of CH_4 and CO formation in the steam hydrogasification with non-catalysts and different catalysts

Temperature (℃)	Feedstock-catalyst (wt%)	CH_4 [a] ($10^{-3}sec^{-1}$)	CO [a] ($10^{-3}sec^{-1}$)
700	Biomass (None)	1.78 +/- 0.14	3.10 +/- 0.15
700	Biomass+$Fe(NO_3)_3$ [b]	1.92 +/- 0.11	3.77 +/- 0.16
700	Biomass+ Fe_2O_3 [c]	1.80 +/- 0.10	3.63 +/- 0.15
700	Biomass+ K_2CO_3 [b]	2.00 +/- 0.13	3.40 +/- 0.17
700	Biomass+ Na_2CO_3 [c]	1.96 +/- 0.15	3.20 +/- 0.14
700	Biomass+calcined dolomite [b]	2.58 +/- 0.13	3.43 +/- 0.16

a. Data (+/-) represents 95% confidence intervals.
b. Differences are statistically significant for both CH_4 and CO.
c. Differences are statistically significant for CO of Fe_2O_3 and CH_4 of Na_2CO_3.

4.3.2 Catalytic activity and mechanisms

From above discussion, the effectiveness of different catalytic materials in the steam hydrogasification depends on the type of catalyst. To assess the catalysts for catalytic steam hydrogasification, it is necessary to determine the catalytic activity of a catalyst. In this study, catalytic activities of different catalysts are evaluated based on their catalytic effect on the steam hydrogasification. A new parameter is defined to represent the catalytic activity [107] which is the ratio of specific rate with catalyst and without catalyst under any given conditions, expressed as k_c/k_{non}. The value of k_c/k_{non} is taken to evaluate the catalytic activity of a catalyst. k_{non} is the value for steam hydrogasification of biomass with none catalyst added. It is noted that k_{non} is 0.00178 sec^{-1} for CH_4 formation and 0.00310 sec^{-1} for CO formation and $k/k_{non}=1.0$ for un-catalytic steam hydrogasification of biomass at 700℃.

Table 4.6 Catalytic activities of catalysts in the steam hydrogasification at 700℃

Run No.	Catalyst	CH_4 k_c/k_{non}	CO k_c/k_{non}
1	None	1.00	1.00
2	$Fe(NO_3)_3$	1.08	1.22
3	Fe_2O_3	1.00	1.17
4	K_2CO_3	1.12	1.10
5	Na_2CO_3	1.10	1.00
6	Calcined dolomite	1.45	1.11

The catalytic activities of the tested catalysts used are presented in Table 4.6. The catalytic activities of the tested catalysts in the steam hydrogasification for CH_4 formation were in the order of calcined dolomite > $K_2CO_3 \approx Na_2CO_3 > Fe(NO_3)_3$ and their catalytic activities for CO formation followed the order of $Fe(NO_3)_3 > Fe_2O_3 >$ calcined dolomite ≈ K_2CO_3.

Calcined dolomite composed of CaO and MgO was an very effective catalyst to catalyze the steam hydrogasification which was not only highly active for CH_4 formation but also for CO formation. It is indicated that calcined dolomite can be used as bed materials as well as a catalyst in the fluidized bed gasifier of demonstration scale unit.

Iron catalysts were highly active for CO formation but a very minor effect on CH_4 formation. The iron in Fe^{3+} had stronger catalytic effect than iron in oxide. This may be attributed to improved iron dispersion on the surface of biomass chars [103, 106].

For alkali metals of K and Na, the catalytic activity in the steam hydrogasification followed the sequence of K > Na. That activity order has also been reported in the literature [114, 118].

The activities of catalysts based on metal of Fe, Ca, Mg, K and Na indicate that alkali (K and Na), alkaline earth (Ca and Mg) and transition (Fe) metals have different catalytic effects on the steam hydrogasification. Ca-Mg had the most catalytic effect in the steam hydrogasification. And iron salt catalyst had the highest catalytic activity for CO formation.

Proposed Mechanisms

The overall reaction for non-catalytic steam hydrogasification can be expressed as the equation 4.2

$$C + H_2O + H_2 \rightarrow CO + CH_4 + H_2 \qquad \text{Equation (4.2)}$$

The gasification in the presence of steam and hydrogen is very complex and it involves many possible reactions, for example:

$C + 2H_2 \rightarrow CH_4$ (Methanation/hydrogasification reaction)

$C + CO_2 \leftrightarrow 2CO$ (Boudouard reaction)

$C + H_2O \rightarrow CO + H_2$ (Water-gas/steam gasification reaction)

$CO + H_2O \leftrightarrow CO_2 + H_2$ (Water-gas shift reaction)

$CH_4 + H_2O \leftrightarrow 3H_2 + CO$ (Reforming reaction)

It would be difficult to understand the catalytic steam hydrogasification and explain the mechanisms for the catalytic activity if all the complex reactions are considered. Hydrogasification reaction and steam gasification reaction are two main reactions in the steam hydrogasification reactions. In this study, the catalytic action of catalysts in the gasification with H_2O and H_2 is explained through the separation mechanism of steam gasification and hydrogasification. It is proposed for CH_4 and CO formation in the steam hydrogasification that direct hydrogasification is the predominant mode of methane formation and steam gasification reaction is the rate determining step of the CO formation.

The catalytic activity of iron, alkali salts and alkaline earth metals in steam gasification have been explained with this oxygen exchange mechanism [103, 104, 124].

It is suggested for a best explanation of the catalytic action in steam hydrogasification for CO formation.

The proposed mechanism of catalytic steam hydrogasification for CO formation is described as

$$M + H_2O \rightarrow M(O) + H_2 \qquad \text{Equation (4.3)}$$

$$M(O) + C \rightarrow M + C(O) \qquad \text{Equation (4.4)}$$

$$C(O) \rightarrow CO \qquad \text{Equation (4.5)}$$

Where, M represents a given catalyst; M(O) and C(O) represents the intermediates. From equations 4.3-4.5, it is given the equation 4.6.

$$C + H_2O \rightarrow CO + H_2 \qquad \text{Equation (4.6)}$$

The catalytic action in hydrogasification can be explained by hydrogen adsorption mechanism involving solid-gas and solid-solid reactions [125, 126]. The proposed mechanism of catalytic steam hydrogasification for CH_4 formation is described as

$$N + H_2 \leftrightarrow N(H_2) \qquad \text{Equation (4.7)}$$

$$N(H_2) + C \rightarrow C(H_2) \qquad \text{Equation (4.8)}$$

$$C(H_2) + H_2 \rightarrow CH_4 \qquad \text{Equation (4.9)}$$

Where, N stands for the active sites on the catalyst surface. From the equations 4.7-4.9, it is given the equation 4.10.

$$C + 2H_2 \rightarrow CH_4 \qquad \text{Equation (4.10)}$$

This mechanism is suggested for an explanation of the catalytic activity of catalysts for CH_4 formation in the presence of hydrogen. The combination of equations 4.6 and 4.10 is the overall reaction of steam hydrogasification in the equation 4.2.

4.3.3 Catalytic effect of in-situ biosolids

The effect of biosolids on the steam hydrogasification has been discussed in chapter 3. Biosolids, in-situ within the steam hydrogasification, promoted the gasification rates and carbon conversion. In this chapter, it is demonstrated that metal catalysts have catalytic effect on the steam hydrogasification. Fe, Ca, Mg, Na and K are the major metal elements contained in the biosolids. Therefore, a comparison of steam hydrogasification with non-catalysts, in-situ biosolids and different catalysts are summarized in Figure 4.9 and Table 4.7 in order to determine catalytic effect of biosolids as in-situ catalyst for the steam hydrogasification.

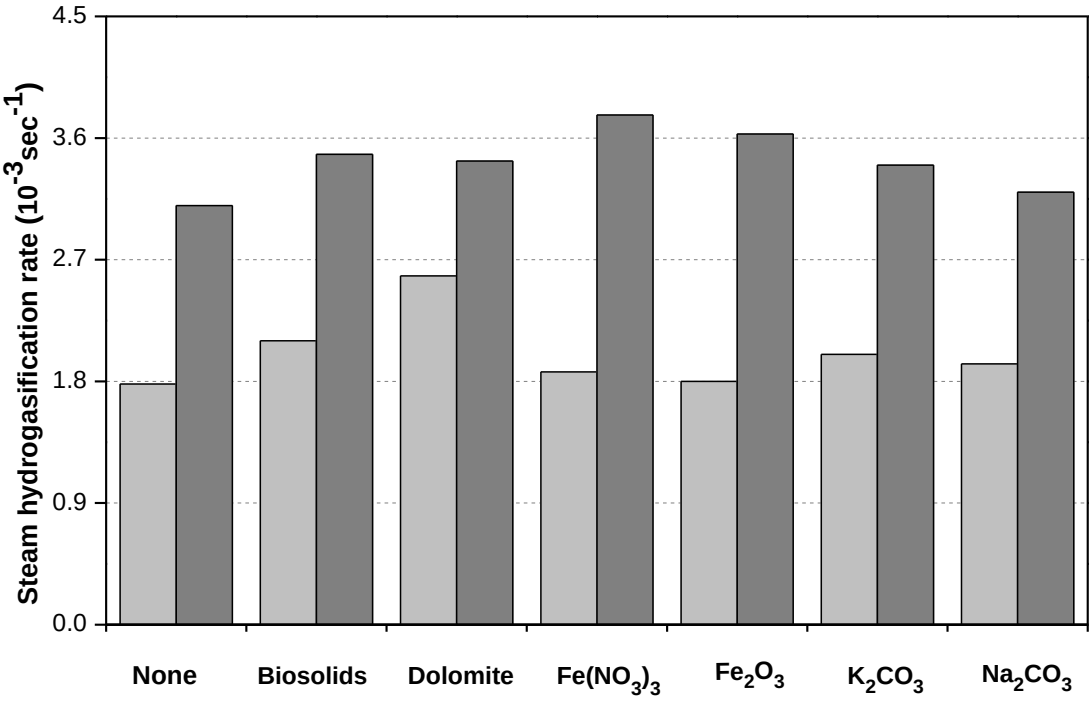

Figure 4.9 The gasification rates of steam hydrogasification of biomass with non-catalysts, in-situ biosolids and different catalysts

Figure 4.9 shows the rates of CH_4 and CO formation with non-catalysts, biosolids and different catalysts. The steam hydrogasification rates are governed by CO and CH_4 formation rates. It is found that biosolids had a dramatic catalytic effect on the steam hydrogasification for both CH_4 and CO formation compared with other tested catalysts. This evident fact confirmed that biosolids, integrated in the co-mingled feedstock could be an effective in-situ catalyst for the steam hydrogasification.

Table 4.7 Experimental conditions for un-catalytic and catalytic steam hydrogasification of biomass and catalytic activities of different catalysts

Catalyst	Temperature (◦C)	H_2O/C (mole)	Catalytic Activity	
			CH_4	CO
None	700	1.5:1	1.0	1.0
Biosolids	700	1.5:1	1.2	1.1
Calcined dolomite	700	1.5:1	1.4	1.1
$Fe(NO_3)_3$	700	1.5:1	1.1	1.2
Fe_2O_3	700	1.5:1	1.0	1.2
K_2CO_3	700	1.5:1	1.1	1.1
Na_2CO_3	700	1.5:1	1.1	1.0

Steam hydrogasification of biomass with non-catalysts, in-situ biosolids and added catalysts were carried out under the same conditions. The addition of a catalyst is physical mixing with the biomass feedstock which is the same method used for the mixture of biosolids and biomass as the co-mingled feedstock.

It can be seen from Table 4.7 that the biosolids could be a highly active catalyst to be in-situ with the steam hydrogasification. The catalytic activity of biosolids on CH_4 formation is higher than other tested catalysts except for calcined dolomite. The catalytic activity of biosolids on CO formation is similar with calcined dolomite. A fact is found that biosolids as in-situ catalyst had a good catalytic activity not only on CO formation but also on CH_4 formation.

Biosolids samples used in this study are rich in iron and calcium. Catalytic effects of different metal catalyst (Fe, Ca, Mg, K, Na) on the steam hydrogasification have been evaluated. The results indicate that the iron group catalyst is the most active to catalyze CO formation in the steam hydrogasification while calcium based catalyst is the most active to catalyze CH_4 formation in the steam hydrogasification. There are also significant evidences in the literatures for the enhancement of catalytic activity by mixture of catalysts [127, 128]. It is suggested that the good catalytic action of biosolids could be understood by synergistic effects of metals in the biosolids, in particular of Fe and Ca. The iron in the biosolids is important to affect the CO formation and calcium and other alkali metal species in the biosolids contribute to catalytic effect on the CH_4 formation in the steam hydrogasification. More research works will be taken in the future to propose explanations and mechanisms for the catalytic action of biosolids.

4.4 Conclusion

Catalytic steam hydrogasification of biomass with different catalysts were performed in the inverted batch reactor at 700℃ with a biomass to H_2O ratio 1:1 g/g. The tested catalysts included $Fe(NO_3)_3$, Fe_2O_3, K_2CO_3, Na_2CO_3 and calcined dolomite ($CaO \cdot MgO$). Catalytic effect of catalysts on the steam hydrogasification was evaluated and the catalytic activity was determined. Steam hydrogasification with non-catalysts, in-situ biosolids and the added catalysts were compared to determine the catalytic activity of biosolids as in-situ catalyst. The results are concluded as follows.

1. The reaction rates in catalytic steam hydrogasification were obtained using the same kinetic measurement approach for un-catalytic SHR. The experimental data with different catalysts was fit to the first-order kinetic rate expression.
2. The tested catalysts of iron compounds ($Fe(NO_3)_3$, Fe_2O_3), alkali carbonate salts (Na_2CO_3, K_2CO_3) and calcined dolomite ($CaO \cdot MgO$) were found to be active to catalyze the steam hydrogasification. The rates of CH_4 formation and CO formation were increased with the addition of catalysts in the steam hydrogasification. Iron catalysts were the most active to catalyze CO formation in the steam hydrogasification in the sequence of $Fe(NO_3)_3 > Fe_2O_3$. Among the tested catalysts, the calcined dolomite was the most effective catalyst in the steam hydrogasification, which not only enhance the rate of CH_4 formation but also improved the rate of CO formation. Alkali salts also had catalytic effect on steam hydrogasification in the order of $K_2CO_3 > Na_2CO_3$. The results indicate that the

metals of alkali (K and Na), alkaline earth (Ca and Mg) and transition (Fe) have different catalytic effects on the steam hydrogasification of biomass.

3. It is revealed that the physical mixing is an effective method for addition of catalyst addition to the feedstock. Effect of catalyst addition method and catalyst loading on catalytic steam hydrogasification will be studied in the future.
4. A defined parameter k_c/k_{non} is used to evaluate the catalytic activity of a catalyst. The metal catalysts have the catalytic activities in the order Ca-Mg > K≈ Na > Fe for CH_4 formation in the steam hydrogasification while their catalytic activities for CO formation follow the order of Fe > Ca-Mg ≈ K > Na. It is identified that iron and calcium catalysts have the best activity to catalyze the steam hydrogasification. The catalytic effect of catalysts in the steam hydrogasification could be explained by the oxygen exchange mechanism for the CO formation and hydrogen adsorption mechanism for the CH_4 formation.
5. Steam hydrogasification with non-catalysts, in-situ biosolids and the added catalysts were evaluated. Catalytic effect of biosolids on the steam hydrogasification was found to be evident. It is confirmed that biosolids, integrated in the biomass feedstock could serve as an effective in-situ catalyst in the steam hydrogasification. The ranking of the catalytic activity of catalysts for CH_4 formation in the steam hydrogasification at 700℃ is calcined dolomite > biosolids > alkali carbonate salts of K and Na > iron catalysts. The ranking of the catalytic activity for CO formation in the steam hydrogasification at 700^{o}C is iron catalyst > biosolids > other tested catalysts. A high catalytic activity of biosolids in

the steam hydrogasification was identified. It is inferred that biosolids could be innovatively utilized as in-expensive and in-situ catalyst in the scaling-up steam hydrogasification gasifier.

6. Catalytic steam hydrogasification with different catalysts in this chapter assisted in understanding the catalytic behaviors of biosolids on the steam hydrogasification. The biosolids has high contents in metals of Fe, Ca, Mg, K and Na, in particular of Fe and Ca. The catalytic activity of biosolids in the steam hydrogasification may be attributed to the synergistic effects of iron, calcium and other alkali metal species in the biosolids. The presence of iron and calcium in the biosolids is important for the catalytic effect of biosolids on the steam hydrogasification.

Chapter 5

Conclusions and Future Work

5.1 Conclusions

This chapter summarizes the experimental results and conclusions in this thesis and suggests some research works in the future. This thesis has investigated the use of biosolids integrated in biomass feedstock as in-situ catalyst for improving the steam hydrogasification efficiency. It is demonstrated that the biosolids has a good catalytic activity in the steam hydrogasification. The main tasks completed in three chapters are concluded as follows.

1. In chapter two, characteristics and kinetics of steam hydrogasification of biomass were evaluated including carbon conversion, char morphology, product gas formation and kinetic parameters. A series of experiments were performed with a H_2O to biomass pinewood ratio 1.2:1 g/g at temperatures ranging from 600-700℃.
   (1) Temperature and heating rate have significant influence on the steam hydrogasification process. Approximately 15% increase in carbon conversion was found when the heating rate was elevated from several K/s to a few 10^2 K/s. It is indicated that a high heating rate has a remarkable impact on the char reactivity. There was about 10% increase in the carbon conversion with the temperature increasing from 600 ℃ to 700℃. A high temperature not only promoted the carbon conversion but also enhanced the rates of product gas formation in the steam hydrogasification.

(2) It is proven in this thesis that the newly-designed lab-scale inverted batch reactor succeeded performing the desired realistic thermal conditions more closely to a fluidized type gasifier. This reactor is able to allow for kinetic measurements in the steam hydrogasification under catalytic or non-catalytic conditions.

(3) A kinetic measurement approach is established in this thesis by employing a simplified first-order kinetic model. The steam hydrogasification rate is governed by the rates of CH_4 and CO formation. The activation energies of CH_4 and CO formation in the steam hydrogasification of pinewood were 42.8kJ/mole and 51.8kJ/mole.

2. In chapter three, the effect of biosolids on steam hydrogasification of biomass was investigated. Steam hydrogasification of co-mingled biosolids with biomass as the feedstock were carried out at 700℃ with a H_2O/C mole ratio 1.5:1. A comparison of experimental results between the steam hydrogasification of co-mingled feedstock and biomass feedstock was discussed.

   (1) It is experimentally demonstrated that steam hydrogasification has an important advantage on biosolids energy recovery by directly utilizing the raw biosolids integrated with woody biomass in the feed. Steam hydrogasification technology can provide an alternative pathway for beneficial use of biosolids in a potentially cost-efficient manner which eliminates the cost and energy loss on biosolids dewatering and drying.

(2) It is concluded that the addition of biosolids in the feed dramatically improved the steam hydrogasification efficiency not only in the carbon conversion but also in the reaction rate. The steam hydrogasification with 50wt% biosolids in the feed yielded more than 70% carbon conversion under the appreciated reaction conditions that was an approximately 6% higher yield compared to that without biosolids loading. Furthermore, the CH_4 and CO formation rates were enhanced when using the co-mingled feedstock with biosolids.

(3) SEM-EDS and ICP analysis reveals that biosolids are rich in the metal elements of Fe, Ca, Mg, K, Na and Al. There was a significant evidence for the presence of Fe, Ca, Mg, K and Na in co-mingled chars due to the biosolids in-situ in the feedstock.

3. In chapter four, catalytic steam hydrogasification of biomass using different catalysts was investigated. The tested catalysts included $Fe(NO_3)_3$, Fe_2O_3, K_2CO_3, Na_2CO_3 and calcined dolomite ($CaO{\cdot}MgO$). Catalytic effect of catalysts on the steam hydrogasification was evaluated and the catalytic activity was determined. A comparison of steam hydrogasification of biomass with non-catalysts, in-situ biosolids and the added catalysts were discussed.

(1) The tested catalysts were demonstrated to have catalytic effects on the steam hydrogasification. Iron catalyst is the most active to catalyze the CO formation. Calcined dolomite composed of CaO and MgO is the most effective catalyst in the steam hydrogasification which is not only highly active for CH_4 formation but also effective for CO formation. It means that

calcined dolomite can be used as a catalyst bed material in the fluidized bed gasifier for demonstration scale steam hydrogasification.

(2) The catalytic activity of catalysts in the steam hydrogasification for CH_4 formation was found to be in the order of calcined dolomite > K_2CO_3 ≈ Na_2CO_3 > $Fe(NO_3)_3$ and their catalytic activity for CO formation followed the order of $Fe(NO_3)_3$ > Fe_2O_3 > calcined dolomite ≈ K_2CO_3. The oxygen exchange mechanism and hydrogen adsorption mechanism were proposed to assist in explaining the catalytic action of catalysts in the steam hydrogasification.

(3) Biosolids was found to have a high catalytic activity in the steam hydrogasification not only for CH_4 formation but also for CO formation compared to the tested catalysts. It is verified that biosolids integrated in biomass feedstock could serve as an effective, in-expensive, in-situ catalyst to improve the steam hydrogasification efficiency. The catalytic action of biosolids in the steam hydrogasification may be attributed to synergistic effect of iron, calcium and alkali metals in the biosolids, in particular of Fe and Ca.

5.2 Future Work

For a demonstration scale steam hydrogasification process, the pretreated feedstock of biomass and biosolids in form of slurries will be pumped into the fluidized bed gasifier. In that case, biosolids can be performed in-situ within the steam hydrogasification. The following tasks will be needed in the future to further investigate the performances of steam hydrogasification of biomass with the biosolids and develop the utilization of biosolids as in-situ catalyst in the fluidized bed gasifier.

1. Investigate the effect of biosolids on gas product yield and composition on the steam hydrogasification using co-mingled feedstock
2. Investigate the effect of biosolids loading on the steam hydrogasification of biomass by varying the biosolids loading in the feedstock
3. Investigate the catalytic effect of iron-calcium catalysts and compare the binary or ternary catalysts with the single catalysts. It will help to get a better understanding of catalytic behaviors of the biosolids due to the presence of a mixture of Fe, Ca and other metals.
4. Develop the utilization of biomass-biosolids chars as bed materials in the fluidized bed gasifier as well as in-situ catalyst and compare the biosolids with other additives such as silica sand and minerals.

References

1. Chum, H.L., Overend, R.P., Biomass and renewable fuels, Fuel Processing Technology, 2001, 71, 187-195.

2. Hoogwijk, M., et al., Exploration of the ranges of the global potential of biomass for energy, Biomass and Bioenergy, 2003, 25, 119-133.

3. Cantrell K.B., Ducey T., Ro S.K., Hunt G. P., Livestock waste-to-bioenergy generation opportunities, Bioresource Technology, 2008, 99, 7941-7953.

4. Dewulf, J., Langenhove H.V., Renewables-based technology: Sustainability assessment, Wiley, 2006.

5. Pellegrini, L.F., Junior, S.O., Combined production of sugar, ethanol and electricity thermoeconomic and environmental analysis and optimization, Energy, 2011, 36, 3704-3715.

6. McKendry, P., Energy production from biomass (part 1): Overview of biomass, Bioresource Technology, 2002, 83, 37-46.

7. Advancing Security and Sustainability through Collaboration and Diversification, America Biofuels Council, http://www.americanbiofuelscouncil.com.

8. Perlack, R.D., Stokes, B.J., Billion-ton update: Biomass supply for a bioenergy and bioproducts industry, U.S. Department of Energy, ORNL/TM-2011/224, 2011.

9. Perlack, R.D., et al., Biomass as feedstock for a bioenergy and bioproducts industry: the Technical feasibility of a billion-ton annual supply, U.S. Department of Energy, U.S. Department of Agriculture, ORNL/TM-2005/66, 2005.

10. Jenkins, B.M., Tiangco, V., Krebs, M., A Preliminary Roadmap for the Development of Biomass in California, CEC-500-2006-095-D, 2006.

11. Gildart, M.C., et al., An assessment of biomass resources in California. California Biomass Collaborative, California Energy Commission, Sacramento, CA, Contract 500-01-016, 2006.

12. U.S. Environmental Protection Agency, EPA Lifecycle Analysis of Greenhouse Gas Emissions from Renewable Fuels, EPA-420-F-09-024, 2009.

13. Escobar, J.C., et al., Biofuels: Environment, technology and food security, Renewable and Sustainable Energy Reviews, 2009, 13, 1275-1287.

14. Demirbas, A., Biofuels sources, biofuel policy, biofuel economy and global biofuel projections, Energy Conversion and Management, 2008, 49, 2106-2116.

15. U.S. Department of Energy, Roadmap for Agriculture Biomass Feedstock Supply in the United States, DOE/NE-ID-11129, 2003.

16. McLauglin, S.B., et al., High-value renewable energy from prairie grasses, Environmental Science and Technology, 2002, 36, 2122-2199.

17. Parikka, M., Global biomass fuel resources, Biomass and Bioenergy, 2004, 27, 613-620.

18. Sims, R.E.H., et al., An overview of second generation biofuel technologies, Bioresource Technology, 2010,101, 1570-1580.

19. Naik, S.N., Goud, V.V., Rout, P.K., Dalai, A.K., Production of first and second generation biofuels: A comprehensive review, Renewable and Sustainable Energy Reviews, 2010, 14, 578-597.

20. Wyman, C.E., Ethanol from lignocellulosic biomass: Technology, economics, and opportunities, Bioresource Technology, 1994, 50, 3-15.

21. Kumar, S., Singh, S.P., Mishra, I.M., Adhikari, D.K., Recent advances in production of bioethanol from lignocellulosic biomass, Chemical Engineering & Technology, 2009, 32, 517-526.

22. Kazi, F.K., et al., Techno-economic comparison of process technologies for biochemical ethanol production from corn stover, Fuel, 2010, 89, 20-28.

23. Bridgwater, A.V., Renewable fuels and chemicals by thermal processing of biomass, Chemical Engineering Journal, 2003, 91, 87-102.

24. Demirbas, A., Mechanisms of liquefaction and pyrolysis reactions of biomass, Energy Conversion and Management, 2000, 41, 633- 646.

25. McKendry, P., Energy production from biomass (part 2): Conversion technologies, Bioresource Technology, 2002, 83, 47-54.

26. Elliott, D.C., et al., Developments in direct thermochemical liquefaction of biomass: 1983-1990, Energy & Fuels, 1991, 5, 399-410.

27. Demirbas, A., Arin, G., An overview of biomass pyrolysis, Energy Sources, 2002, 24,471-482.

28. Chen, G., Andries, J., Luo, Z., Spliethoff, H., Biomass pyrolysis/gasification for product gas production: the overall investigation of parametric effects, Energy Conversion and Management, 2003, 44, 1875-1884.

29. Son, Y., Yoon, S.J, Kim, Y.K., Lee, J.G., Gasification and power generation characteristics of woody biomass utilizing a down draft gasifier, Biomass and Bioenergy, 2011, 35, 4215-4220.

30. Pereira, E.G., et al., Sustainable energy: A review of gasification technologies, Renewable and Sustainable Energy Reviews, 2012, 16, 4753-4762.

31. McKendry, P., Energy production from biomass (part 3): Gasification technologies, Bioresource Technology, 2002, 83, 55-63.

32. Balat, M., Gasification of biomass to produce gaseous products, Energy Sources, Part A, 2009, 31, 516-526.

33. Kumar, A., Jones, D.D., Hanna, M.A., Thermochemical biomass gasification: A review of the current status of the technology, Energies, 2009, 2, 556-581.

34. Achary, B., Dutta, A., Basu, P., An investigation into steam gasification of biomass for hydrogen enriched gas production in presence of CaO, International Journal of Hydrogen Energy, 2010, 35, 1582-1589.

35. Wei, L., Xu, S., Steam gasification of biomass for hydrogen-rich gas in a free-fall reactor, International Journal of Hydrogen Energy, 2007, 32, 24-31.

36. Van Swaaij W.P.M., Gasification- the process and the technology, Resources and Conversion, 1981, 7, 337-349.

37. Warecke, R., Gasification of biomass: comparison of fixed bed and fluidized bed gasifier, Biomass and Bioenergy, 2000, 18, 489-497.

38. Beenackers, A.A.C.M., Biomass gasification in moving beds, a review of European technologies, Renewable Energy, 1996, 16, 1180-1186.

39. Bridgwater, A.V., The technical and economic feasibility of biomass gasification for power generation, Fuel, 1995, 14, 631-653.

40. Li, X.T., et al., Biomass gasification in a circulating fluidized bed, Biomass and Bioenergy, 2004, 26, 171-193.

41. Rapagna, S., Jand, N., Kiennemann, A., Foscolo, P.U., Steam-gasification of biomass in a fluidized-bed of olivine particles, Biomass and Bioenergy, 2000, 19, 187-197.

42. Beck, S. R., Wang, M. J., Wood gasification in a fluidized bed, Ind. Eng. Chem. Process Design and Development, 1980, 19, 312-317.

43. Corella, J., Orio, A., Aznar, P., Biomass gasification with air in fluidized bed: reforming of the bas composition with commercial steam reforming catalysts, Industrial & Engineering Chemistry Research, 1998, 37, 4617-4624.

44. Gil, J., et al., Biomass gasification in fluidized bed at pilot scale with steam-oxygen mixtures: Product distribution for very different operating conditions, Energy & Fuels, 1997, 11, 1109-1118.

45. Brown, A.L., et al., Design and characterization of an entrained flow reactor for the study of biomass pyrolysis chemistry at high heating rates, Energy & Fuels, 2001, 15, 1276-1285.

46. Kurkela, E., Stahlberg, P., Laatikainen, J., Simell, P., Development of simplified IGCC-processes for biofuels: supporting gasification research at VTT, Bioresource Technology, 1993, 46, 37-47.

47. Raju, A.S.K., Park, C.S., Norbeck, J.M., Synthesis gas production using steam hydrogasification and steam reforming, Fuel Processing Technology, 2009, 90, 330-336.

48. Jeon, S.K., Park, C.S., Hackett, C.E., Norbeck, J.M., Characteristics of steam hydrogasification of wood using a micro-batch reactor, Fuel, 2007, 86, 2817-2823.

49. He, W., Park, C.S., Norbeck, J.M., Rheological study of comingled biomass and coal slurries with hydrothermal pretreatment, Energy &Fuels, 23, 4763-4767, 2009.

50. Gray, D., et al., Increasing Security and Reducing Carbon Emissions of the U.S. Transportation Sector: A Transformational Role for Coal with Biomass, National Energy Technology Laboratory, 2007.

51. Walker P.L., Ruskino F., Austin, L.G., Gas reactions of carbon, Advances in Catalysis, 1959, 11, 133-221.

52. Suzuki, T., et al., Influence of calcium on the catalytic behavior of nickel in low temperature hydrogasification of wood char, Fuel, 1998, 77, 763-767.

53. Shetha, A.C., Catalytic gasification of coal using eutectic salts: reaction kinetics for hydrogasification using binary and ternary eutectic catalysts, Fuel, 2004, 83, 557-572.

54. Huang, B.S., et al., Hydrogen production by biomass gasification in a fluidized bed reactor promoted by a Fe/CaO catalyst, International Journal of Hydrogen Energy, 2012, 37, 6511-6518.

55. National Association of Clean Water Agencies (NACWA), Renewable Energy Resources: Banking on Biosolids, 2010.

56. Rulkens, W. H., Bien, J. D., Recovery of energy from sludge-Comparison of the various options. Water Science Technology, 2004, 50, 213-221.

57. U.S. Environmental Protection Agency, Biosolids generation, use, and disposal in the United States, EPA530-R-99-009, 1999.

58. U.S. Environmental Protection Agency, Emerging Technologies for Biosolids Management, EPA 832-R-06-005, 2006.

59. Claassen, P.A.M., et al., Utilization of biomass for the supply of energy carriers, Applied Microbiology Biotechnology, 1999, 52, 741-755.

60. Kearney, R., Bolin, K., The new SlurryCarb process under construction in Rialto, CA will convert biosolids to a renewable fuel, WEF Residuals and Biosolids Conference Proceedings, Philadelphia, PA, 2008.

61. Davis R., Slaughter, J., Biosolids Management: Options, Opportunities & Challenges, Related Practices, A NACWA Handbook, 2006.

62. Wim Rulkens, Sewage sludge as a biomass resource for the production of energy: Overview and assessment of the various options, Energy & Fuels, 2008, 22, 9-15.

63. Dowdy, R.H., Larson, W.E., Epstein, E., Sewage sludge and effluent use in agriculture, Land Application of Waste Materials, Soil Conservation Society of America, 1976, 138-153.

64. U.S. Environmental Protection Agency, Biosolids Recycling: Beneficial Technologies for a Better Environment, EPA 832-R-94-009, 1994.

65. Stolarek, P., Ledakowicz, S., Thermal processing of sewage sludge by drying, pyrolysis, gasification and combustion, Water Science Technology, 2001, 44, 333-340.

66. Svanstrom, M., Modell, M., Tester, J., Direct energy recovery from primary and secondary sludges by supercritical water oxidation, Water Science Technology, 2004, 49, 201-208.

67. Sutton, D., Kelleher, B., Ross, J.R.H., Review of literature on catalysts for biomass gasification, Fuel Processing Technology, 2001, 73, 155-173.

68. Bridgwater, A.V., Catalysts in thermal biomass conversion, Applied Catalysis A: General, 1994, 116, 5-47.

69. Abu El-Rub, Z., Bramer, E.A., Brem, G., A review of catalysts for tar elimination in biomass gasification processes, Industrial Engineering Chemistry Research, 2004, 43, 6911-6919.

70. Brown, R.C., Liu, Q., Norton, G., Catalytic effects observed during the co-gasification of coal and switchgrass, Biomass and Bioenergy, 2000, 18, 499-506.

71. Dogru, M., et al., Gasification of hazelnut hells in a downdraft gasifier, Energy, 2002, 27, 415-427.

72. Valkenburg, C., Products and reaction kinetics using steam hydrogasification of various carbonaceous feedstock, M. S. Thesis, Chemical & Environmental Engineering, University of California, Riverside, CA, 2006.

73. Raju, A.S.K., Park, C.S., Norbeck, J.M., Steam hydrogasification of coal-wood mixtures in a batch reactor, International Pittsburgh Coal Conference, Pittsburgh, PA, USA, 2008.

74. Ono, A., Kurita, M., Nagashima, T., Horio, M., Evaluation of waste pyrolysis characteristics in a pressurized fluidized bed reactor, Waste Management, 2001, 21, 451-456.

75. Kojima, T., Assavadakorn, P., Furusawa, T., Measurement and evaluation of gasification kinetics of sawdust char with steam in an experimental fluidized bed, Fuel Processing Technology, 1993, 36, 201-207.

76. Gadhe, J.B., Gupta, R.B., Hydrogen production by methanol reforming in supercritical water: Suppression of methane formation, Industrial &Engineering Chemistry Research, 2005, 44, 4577-4585.

77. Antal, M.J., et al., Biomass gasification in supercritical water, Industrial & Engineering Chemistry Research, 2000, 39, 4040-4053.

78. Scott, A., et al., Improving the detection limit of a quadrupole mass spectrometer, J. Vacuum Science & Technology, 2001, A19, 1032.

79. Singh, H., et al., Mass spectrometric detection of reactive neutral species: Beam-to-background ratio, Journal of Vacuum Science & Technology, 1999, A17, 2447.

80. Li, B., Mitchell, S.C., Snape, C.E., Effect of heating rate on normal and catalytic fixed-bed hydropyrolysis of coals, Fuel, 1996, 75, 1393-1396.

81. Fushimi, C., et al., Effect of heating rate on steam gasification of biomass. 1. Reactivity of Char, Industrial & Engineering Chemistry Research, 2003, 42, 3922-3928.

82. Xiu, S., Yi, W., Li, B., Flash pyrolysis of agricultural residues using a plasma heated laminar entrained flow reactor, Biomass and Bioenergy, 2005, 29, 135-141.

83. Zabaniotou, A., Ioannidou, O., Evaluation of utilization of corn stalks for energy and carbon material production by using rapid pyrolysis at high temperature, Fuel, 2008, 87, 834-843.

84. Zanzi, R., Sjöström K., Björnbom, E., Rapid high-temperature pyrolysis of biomass in a free-fall reactor, Fuel, 1996, 75, 545-550.

85. Fu, P., et al., Effect of pyrolysis temperature on characteristics of porosity in biomass chars, International Conference on Energy and Environmental Technology, 2009.

86. Cetin, E., Gupta, R., Moghtaderti, B., Effect of pyrolysis pressure and heating rate on radiata pine char structure and apparent gasification reactivity, Fuel, 2005, 84, 1328-1334.

87. Wang, X., et al., Properties of gas and char from microwave pyrolysis of pine sawdust, Bioresource Technology, 2009, 4, 946-959.

88. Kentaro, U., Yamamoto, K., High temperature steam-only gasification of woody biomass, Applied Energy, 2010, 87, 791-798.

89. Franco, C., et al., The study of reactions influencing the biomass steam gasification process, Fuel, 2003, 82, 835-842.

90. Dupont, C., Boissonnet, G., Study about the kinetic processes of biomass steam gasification, Fuel, 2007, 86, 32-40.

91. Orfao, J.J.M., Figueiredo, J.L., A simplified method for determination of lignocellulosic materials pyrolysis kinetics from isothermal thermogravimetric experiments, Termochimica Acta, 2001, 380, 67-78.

92. Shin, E.G., Nimlos, M.R., Evans, R.J., Kinetic analysis of the gas-phase pyrolysis of carbohydrates, Fuel, 2001, 80, 1697-1709.

93. Encinar, J.M., et al., Pyrolysis of maize, sunflower, grape and tobacco residues, Journal of Chemical Technology and Biotechnology, 1997, 70, 400-410.

94. Gonzalez, J.F., et al., Pyrolysis of cherry stones: energy uses of the different fractions and kinetic study, Journal of Analytical and Applied Pyrolysis, 2003, 67, 165-190.

95. Marrero, T.W., et al., Fate of heavy metals and radioactive metals in gasification of sewage sludge, Waste Management, 2004, 24, 193-198.

96. Folgueras, M.B., Diaz, R.M., Influence of $FeCl_3$ and lime added to sludge on sludge-coal pyrolysis, Energy, 2010, 35, 5250-5259

97. Gro, B., et al., Energy recovery from sewage sludge by means of fluidised bed gasification, Waste Management, 2008, 28, 1819-1826.

98. Midilli, A., Dogru, M., Akay, G., Howarth, C.R., Hydrogen production from sewage sludge via a fixed bed gasifier product gas, International Journal of Hydrogen Energy, 2002, 27, 1035-1041.

99. Nipattummaku, N., Ahmed, I.I., Kerdsuwan, S., Gupta, A.K., Hydrogen and syngas production from sewage sludge via steam gasification, International Journal of Hydrogen Energy, 2010, 35, 11738-11745.

100. Manya, J.J., et al., Influence of gas residence time and air ratio on the air gasification of dried sewage sludge in a bubbling fluidized bed, Fuel, 2006, 85, 2027-2033.

101. Saw, W., Mckinnon, H., Gilmour, I., Pang, S., Production of hydrogen-rich syngas from steam gasification of blend of biosolids and wood using a dual fluidized bed gasifer, Fuel, 2012, 93, 473-478.

102. Kutchko, B.G., Kim, A.G., Fly ash characterization by SEM-EDS, Fuel, 2006, 85, 2537-2544.

103. Asami, K., Sears, P., Furimsky, E., Ohtsuka, Y., Gasification of brown coal and char with carbon dioxide in the presence of finely dispersed iron catalysts, Fuel Processing Technology, 1996, 47, 139-151.

104. Yua, J., et al., Effect of iron on the gasification of Victorian brown coal with steam: enhancement of hydrogen production, Fuel, 2006, 85, 127-133

105. Ohtsuka, Y., Asami, K., Highly active catalysts from inexpensive raw materials for coal gasification, Catalysis today, 1997, 39, 111-125.

106. Ohtsuka, Y., Tamai, Y., Tomita, A., Iron-catalyzed gasification of brown coal at low temperatures, Energy & Fuels, 1987, 1, 32-36.

107. Song, B.H., Kim, S.D., Catalytic activity of alkali and iron salt mixtures for steam-char gasification, Fuel, 1993, 72, 797-803.

108. Hurley, S., Li, H., Xu, C., Effects of impregnated metal ions on air/CO_2-gasification of woody biomass, Bioresource Technology, 2010, 101, 9301-9307.

109. Chan, W.S., Baek, H., Jang, H.T., Hydrogasification of various carbonaceous sources using pressure change properties, Korean Journal of Chemical Engineering, 2007, 24, 532-536.

110. Ross, D., et al., Axial gas profiles in a bubbling fluidised bed biomass gasifier, Fuel, 2007, 86, 1417-1429.

111. Uddin, M.A., Tsuda, H., Wu, S., Sasaoka, E., Catalytic decomposition of biomass decomposition of biomass tars with iron oxide catalysts, Fuel, 2008, 87, 451-459.

112. Liu, Z., Zhu, H., Steam gasification of coal char using alkali and alkaline-earth metal catalysts, Fuel, 1986, 65, 1334-1338.

113. Shimada, N., Kawamoto, H., Saka, S., Different action of alkali/alkaline earth metal chlorides on cellulose pyrolysis, Journal of Analytical and Applied Pyrolysis, 2008, 81, 80-87.

114. Veraa, M.J., Bell, A.T., Effect of alkali metal catalysts on gasification of coal char, Fuel, 1978, 57, 194-200.

115. Hauserman, W.B., et al., High-yield hydrogen production by catalytic gasification of coal or biomass, International Journal of Hydrogen Energy, 1994, 19, 413-419.

116. Mudge, L.K., Baker, E.G, Mitchell, D.H., Brown, M.D., Investigations on catalyzed steam gasification of biomass, Journal of Solar Energy Engineering, 1985, 107, 89-92.

117. Wang Z., Wang, F., Cao, J., Wang, J., Pyrolysis of pine wood in a slowly heating fixed-bed reactor: Potassium carbonate versus calcium hydroxide as a catalyst, Fuel Processing Technology, 2010, 91, 942-952.

118. Sheth, A.C., Catalytic gasification of coal using eutectic salts: reaction kinetics for hydrogasification using binary and ternary eutectic catalysts, Fuel, 2004, 83, 557-582.

119. Weerachanchi, P., Horio, M., Tangsathitkulchai, C., Effects of gasifying conditions and bed materials on fluidized bed steam gasification of wood biomass, Bioresource Technology, 2009, 100, 1419-1427.

120. Elliot, D.C., Baker E.G., The effect of catalysis on wood gasification tar composition, Biomass, 1986, 9, 195-203.

121. Encinar, J.M., Beltran, F.J., Catalyzed pyrolysis of grape and olive bagasse. Influence of catalyst type and chemical treatment, Industrial &Engineering Chemistry Research, 1997, 36, 4176-4183.

122. Meijera, R., Kapteijn, F., Moulijn, J.A., Kinetics of the alkali-carbonate catalysed gasification of carbon: 3. H_2O gasification, Fuel, 1994, 73, 723-730.

123. Pande, A.R., et al., Catalytic gasification of active charcoal by carbon dioxide: influence of type of catalyst and carbon particle size, Fuel, 1992, 71, 1299-1306.

124. McKee, D.W., Chatterji D., The catalytic behavior of alkali metal carbonates and oxides in graphite oxidation reactions, Carbon, 1975, 13, 381-390.

125. Lussier, M.G., Zhang, Z., Miller, D.J., Characterizing rate inhibition in steam/hydrogen gasification via analysis of adsorbed hydrogen, Carbon, 1998, 36, 1361-1369.

126. Huttinger, K.J., et al., Mechanism of water vapor gasification at high hydrogen levels, Carbon, 1988, 26, 79-87.

127. T. Haga, Y. Nishiyama, Promotion of iron-group catalysts by a calcium salt in hydrogasification of coal chars, Industrial Engineering Chemistry Research, 1989, 28, 724-728.

128. Huang, Y., et al., Effects of metal catalysts on CO_2 gasification reactivity of biomass char, Biotechnology Advances, 2009, 27, 568-572.